LA-13066-MS

UC-802
Issued: January 1996

Preliminary LIBS Analysis of Yucca Mountain Manganese Oxide Minerals

J. Blacic
D. Pettit
D. Cremers

Los Alamos
NATIONAL LABORATORY
Los Alamos, New Mexico 87545

MASTER

DISTRIBUTION OF THIS DOCUMENT IS UNLIMITED

CONTENTS

PRELIMINARY LIBS ANALYSIS OF YUCCA MOUNTAIN MANGANESE OXIDE MINERALS

by

J. Blacic, D. Pettit, and D. Cremers

ABSTRACT

The licensing and performance of a potential repository at Yucca Mountain will require the characterization of radionuclide sorptive capacity of the host rock, which in turn calls for hundreds of analyses based on extensive sampling or in situ measurements. A rapid method specifically for characterizing the manganese oxide minerals occurring heterogeneously throughout the Yucca Mountain block as fracture surface coatings is needed. Our unique solution is a laser-induced breakdown spectroscopy (LIBS) surface-analysis technique that is usable in the field to produce high-resolution atomic emission spectra. In tests with manganese oxide minerals and fracture surface coatings from a few Yucca Mountain core samples, we used four spectral bands to show that qualitative measurement of all constituent elements except K and Na (in the presence of Mn) is possible with LIBS. Detailed calibration of final hardware will make the system quantitative.

INTRODUCTION

An important aspect of the licensing and performance of a potential repository at Yucca Mountain will be the characterization, quantification, and documentation of the radionuclide sorptive capacity of the host rock. A key element of this process will be the characterization of the fracture mineral fillings, particularly the manganese oxide minerals, that occur heterogeneously throughout the Yucca Mountain block. The manganese oxide minerals are important because of their potential to control or affect ground water redox reactions (Bish and Post, 1989) and to retard actinide mobility (Means, et al., 1978; Triay, 1991; Triay, et al., 1991); localization along fractures as coatings and fillings increases their importance because these fractures are likely to be the main pathways of chemical transport by way of ground water. Evaluation of the actinide retardation capacity of Mn-oxides is currently underway with mineral-specific and autoradiography experiments in progress (Vaniman, personal communication, 1995).

Up to this time, characterization of manganese minerals in the Yucca Mountain block has been done by time-consuming optical and scanning electron microscopy of a small number of samples returned to the laboratory, supported by laboratory analytical chemistry and x-ray diffraction analysis (Carlos, 1989, Carlos et al., 1990, Carlos et al., 1993). Complete fracture filling characterization at Yucca Mountain could be done with such methods, but manpower limits and access within the limited exposure time of the tunnel walls make such an approach difficult. Potentially thousands of analyses may be needed to fully characterize the distribution of sorbing minerals in the rock mass and along fracture surfaces in the vicinity of the repository. This means that extensive sampling or in situ measurements will have to be performed along the walls of much of the tunnel produced before wire and shotcrete support is put in place, fractures exposed in experiment alcoves need to be characterized, and core samples taken from below the repository horizon will have to be extensively characterized. It will be especially important to characterize the fractures below the potential repository horizon (e.g., in the Calico Hills tuffs) if excavations or core drilling are performed there since any lateral transport path will likely first pass through this region. We believe use of a LIBS (laser induced breakdown spectroscopy) instrument may be an optimum, perhaps unique, solution to this problem because of its capability for fine spatial resolution (point analysis) and rapid, near real-time analysis capability in the field (Blacic, et al., 1994).

We envision a portable LIBS unit with an analysis head that contains a laser source, optical fiber to convey the spark signal, optical aiming magnifier and reticule to fix the analysis point, and a photographic or video imaging element to document each analysis point. The head would be placed on the surface of a tunnel wall or core sample with a soft, conforming seal to safely enclose the laser beam. Such a device might be used as part of the tunnel wall characterization activities planned to be used at the gantry access of the tunnel boring machine (TBM). Point analyses along lines on the tunnel wall, obtained as the TBM advances, would, along with similar analyses of available core samples, allow construction of a fracture-filling data base. From such a data base a statistical estimate of, for example, the amount of sorptive manganese mineral fracture fillings within the repository block could be constructed. The *in situ* LIBS measurements would also be a useful guide to sample selection for more extensive laboratory characterization.

This report describes the results of an initial laboratory LIBS study of selected Yucca Mountain core samples containing manganese oxide fracture coatings that were previously analyzed by the geochemical methods described above, along with a LIBS analysis of a suite of standard manganese oxide minerals for comparison. We also describe progress in the development of a portable LIBS instrument to be tested at the Yucca Mountain Exploratory Studies Facility later this year.

EXPERIMENTAL METHOD

A laboratory-based LIBS system was used to analyze YMP samples for manganese minerals occurring as vein fillings and fracture coatings. A Laser Photonics Nd-YAG laser at 20 mj/pulse and 10 ns duration was used as the excitation source by focusing the 3 mm diameter beam into a spot less than a millimeter in diameter with a 50 mm focal length lens. The YMP samples consisting of fractured drill core were placed at the focal point. A 12.7 mm focal length by 6.35 mm diameter ultraviolet grade lens coupled the plasma emissions into a 1.25 mm diameter ultraviolet grade fiber-optic bundle. The fiber-optic bundle, with round to line cross section, directed the light through a 50 mm slit into a 0.5 m focal length, f6 Spex spectrograph with a 1200 groove/mm grating. A Photometrics model CE200 CCD camera recorded the spectra using a Tektronics thinned, back-illuminated, metachrome-coated, 1024 × 1024 chip. A Macintosh IIsi computer running Kestrelspec software reduced and archived the data. The instrument dispersion was 1.6 nm/mm, giving a spectral range of 40 nm with a resolution of 0.12 nm. The wavelength calibration was made using Hg and Ne lamps as well as Au, Al, Ti, and Pb standards. Spectra were taken centered at 272, 350, 400, and 655 nm which allowed for identification of the major and minor elements of interest. manganese mineral standards (>95% pure by x-ray diffraction) of Coronadite (Broken Hills, Australia), Hollandite (Socorro, NM), Manganite (#83837, Hartz Mountains, Germany), Romanechite (Casa Grande, AZ), Pyrolusite (#111929, Lake Valley, NM), and Todorokite (#106238, Santa Rita, Cuba) were analyzed using LIBS for comparison to YMP samples. Table 1 lists the chemical composition of the current set of standard manganese oxide minerals.

Table 1
Approximate Chemical Compositions of Mineral Standards

Mineral Standard	Coronadite $Pb(Ca,Al,Si)_xMn_8O_{16}0.3\text{-}0.8H_2O$ %	Hollandite $Ba(Ca,Li,Pb,Al)_xMn_8O_{16}0.3\text{-}0.8H_2O$	Manganite MnOOH	Romanechite $(Ba,Ca)(Li,Al,Mg)_xMn_8,O_{16}0.3\text{-}0.8H_2O$	Pyrolusite MnO_2	Todorokite $(Na,Ca,K,Ba,Sr)_{0.3\text{-}0.7}(Mn,Mg,Al)_6O_{12}$ $3.2\text{-}4.5H_2O$
MnO_2	61.7	76-873	75	79.5	100	55.8
Al_2O_3	--	0.4	--	0.2	--	--
SiO_2	0.2	0.1	--	0.9	--	--
CaO	0.02	0.1-0.2	--	0.5	--	1.5
BaO	0.02	13.4	--	12.8	--	0.1
MgO	--	0.1	--	0.1	--	3.0
PbO	30.6	2.6	--	0.3	--	--
SrO	--	0.2	--	2.2	--	0.1
Fe_2O_3	3.0	--	--	0.3	--	--
K_2O	--	0.6	--	0.2	--	0.1
Na_2O	--	--	--	0.1	--	2.6
ZnO	0.4	0.2	--	--	--	--
Cu	0.1	--	--	--	--	--
W	0.1	--	--	--	--	--

Ce and Li not analyzed or reported. -- indicates less than 0.1% or not analyzed.

There are three levels of calibration required for complete interpretation of the emission line spectra: (1) line wavelength for element identification, (2) line height (or area for emissions of extended width) for element concentration, and (3) comparison with standard mineral line emissions for deducing mineralogy. Of these calibrations, the wavelength and mineral standards are the most readily accomplished and independent of the particular LIBS system in use. Calibration of line height as a function of concentration is instrument specific. At the time of this writing, we have not completed the final hardware configuration for the YMP LIBS instrument to be used in conjunction with the tunnel boring operation, and therefore detailed calibrations for relating line height to concentration have not been done. However, the detection of manganese bearing minerals and deducing their mineralogy can be accomplished in some cases with the current level of calibration.

EXPERIMENTAL RESULTS

The fracture surface coatings of dark brown to blackish mineralization on YMP samples G4 2947.7-2947.9, GU3 752.2-752.8, and GU3 797.5-797.6 were analyzed using LIBS. The G4 sample is from the Tram Member of the Crater Flat Tuff and the GU3 sample is from the Topopah Spring Member of the Paintbrush Tuff. On the fracture surface of sample GU3 797, two distinctly different-looking micaceous coatings along with the host rock were also analyzed. A complete listing of these spectra as well as those of the manganese mineral standards are given in Appendix I.

After some adjustment, we settled on the four spectral bands, centered at 272, 350, 400, and 655 nm, to best characterize the major and minor element characteristics of the manganese oxide minerals. Examples of the spectra with labeled emission peaks are shown in Figures 1a-d and 2a-d for the Hollandite standard and the tuff sample GU3 797, respectively. Given the large amount of manganese in all of the samples, ranging from ~50 to ~90 at. % MnO_2, it is not surprising that the spectra are dominated by the many neutral and singly ionized lines for manganese. However in only one case did we find an interference between an important element and a manganese line for which we could not substitute another line in a clear part of the spectrum, and that was for potassium. The best line for potassium in the bands we used is the neutral doublet at 404.4 and 404.7 nm but these are masked by strong neutral manganese lines at 404.5 and 404.9 nm, respectively. For all of the other major element constituents of manganese oxide minerals, we were able to identify one or more isolated lines. These elements include Al, Ca, Si, Fe, Mg, Ba, Sr, Li, and Pb. In addition, there are a number of minor or trace-level elements exhibiting LIBS emission lines which appear to vary systematically among the manganese oxide minerals and which may prove useful for correlation purposes. These include Ti, Zn, W, Cu, Ni, and the rare earth element Ce. Cerium is particularly interesting in that it occurs as a major element in some of the standard manganese oxide minerals (e.g., Hollandite from Socorro, NM, Fig. 1c) and is widespread among host rock and manganese oxide minerals at Yucca Mountain (Broxton et al., 1989; Carlos et al., 1993), although work in progress indicates that positive Ce anomalies only occur in Mn-oxides above the static water level at Yucca Mountain (Vaniman, personal communication, 1995).

As noted above, absolute quantification of elemental concentrations from peak heights or areas is hardware-specific, and has not been performed for these preliminary LIBS analyses. However, relative comparisons and qualitative estimates of element variations can be obtained from the spectra by normalizing specific element peaks to a common element. For this purpose, element ratios for manganese

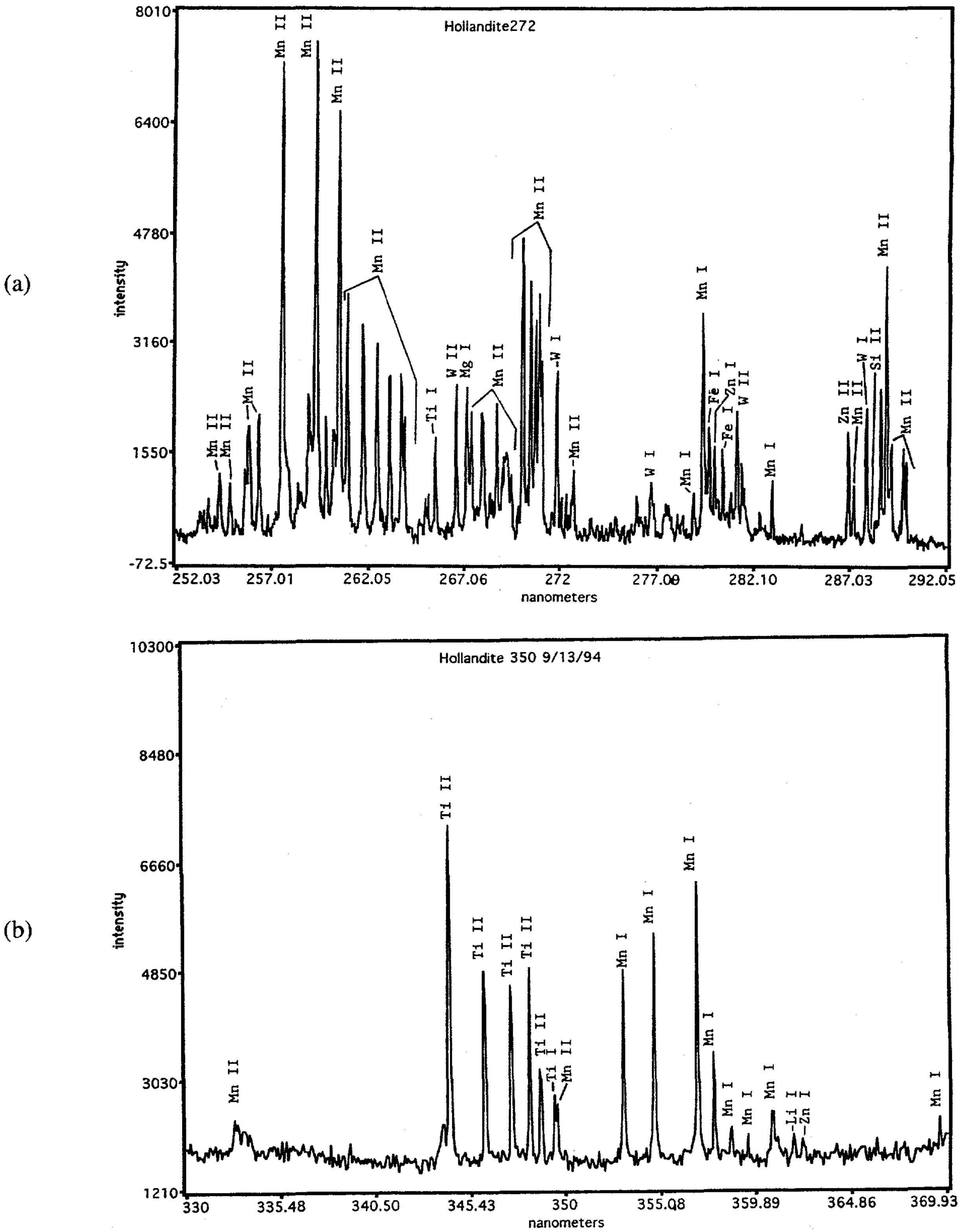

Fig. 1a-b. LIBS spectra of Hollandite mineral standard over four wavelength bands: (a) band from 252 to 292 nm, and (b) band from 330 to 370 nm. Emission lines for individual elements are identified with I indicating neutral and II indicating singly ionized species, respectively.

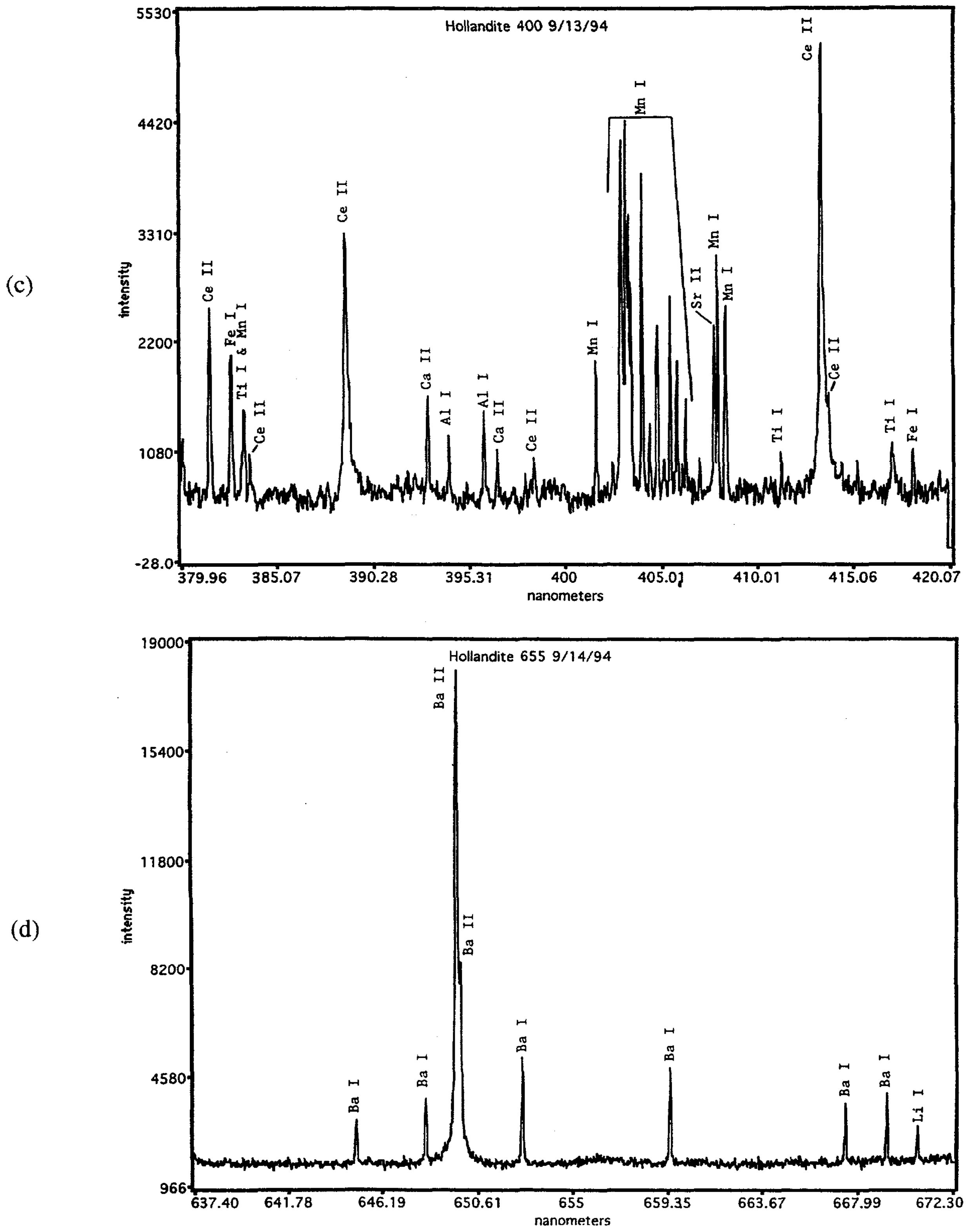

Fig. 1c-d. LIBS spectra of Hollandite mineral standard over four wavelength bands: (c) band from 380 to 420 nm and (d) band from 637 to 672 nm. Emission lines for individual elements are identified with I indicating neutral and II indicating singly ionized species, respectively.

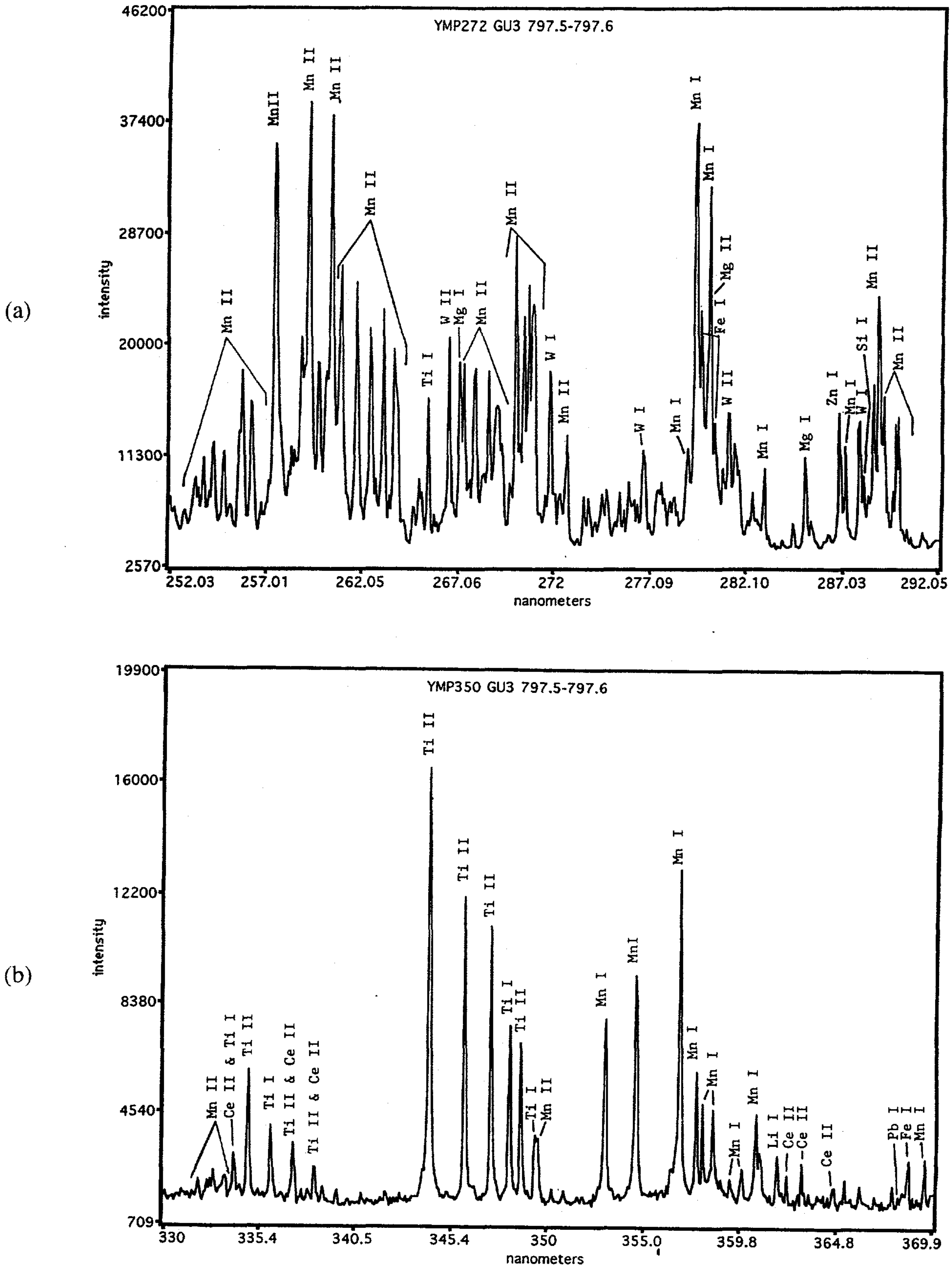

Fig. 2a-b. LIBS spectra of Yucca Mountain tuff sample GU3 797. Bands and notation are the same as in Figure 1a-b.

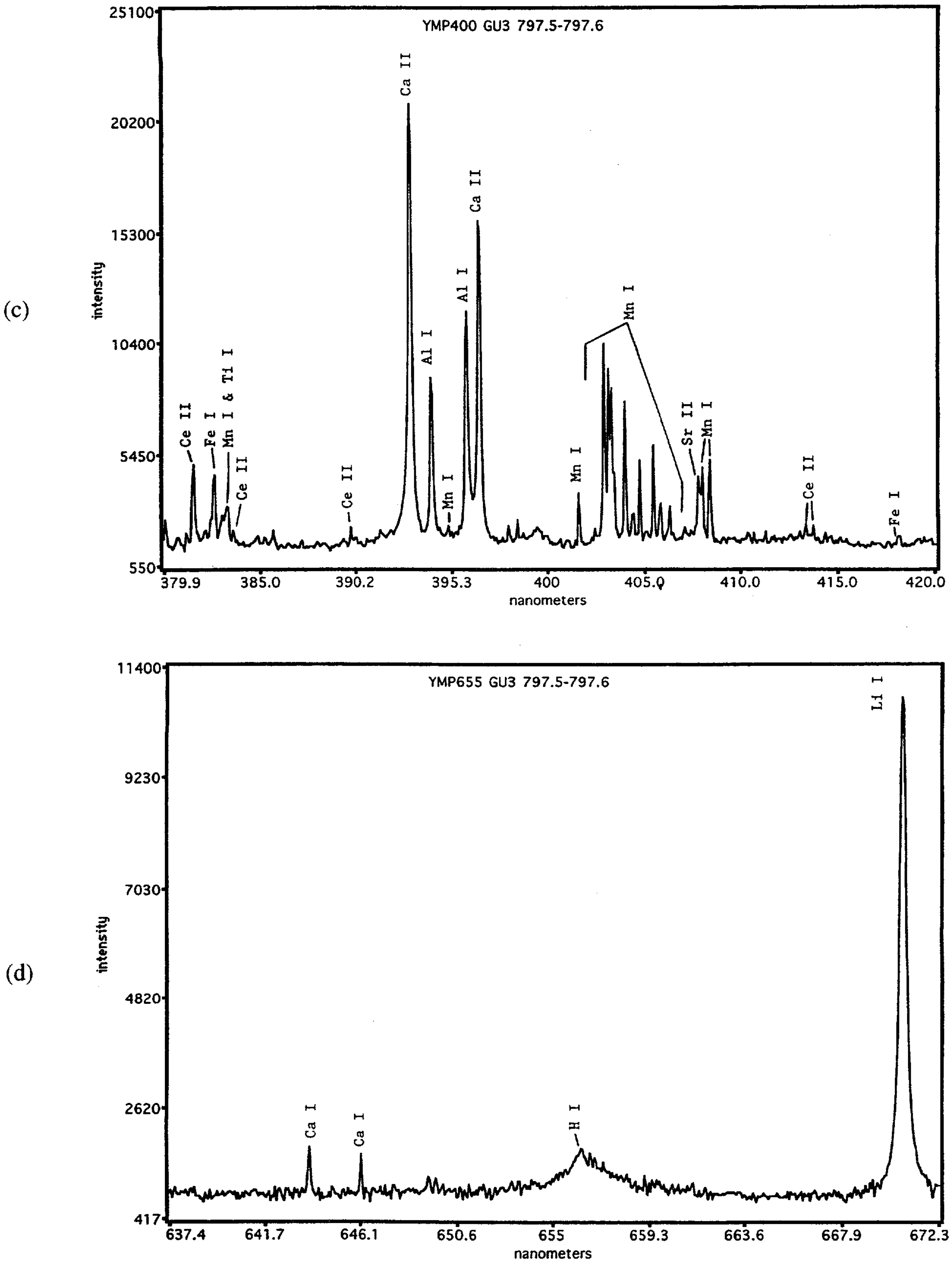

Fig. 2c-d. LIBS spectra of Yucca Mountain tuff sample GU3 797. Bands and notation are the same as in Figure 1c-d.

normalizing specific element peaks to a common element. For this purpose, element ratios for manganese oxide mineral standards and tuff samples were calculated for Mg/Mn, Si/Mn, Pb/Mn, Al/Mn, Ca/Mn, Ce/Mn, Li/Mn, and Ba/Mn, and are presented by the ratio of spectral line heights taken at 285.21 nm for Mg, 288.16 nm for Si, 368.35 nm for Pb, 396.15 nm for Al, 393.37 nm for Ca, 388.99 nm for Ce, 670.78 nm for Li, 669.38 nm for Ba, and 356.95 nm for Mn. These lines were chosen in part by signal strength and absence of interference with lines from other elements. A composite bar chart displays these ratios for the manganese oxide standards in Figure 3 and for the YMP samples in Figure 4; individual sample bar charts for all analyzed samples are presented in Appendix II.

Figures 3 and 4 show the potential of the LIBS method for analyzing fracture fillings at Yucca Mountain for relative proportions of manganese oxide minerals with a rapid, field-portable technique. Ultimately, the method could be made quantitative when the complete calibrations discussed above have been performed. There are distinct differences in major, minor and trace element ratios among the manganese oxide standards, allowing them to be distinguished from one another, and there are significant variations in the same element ratios among the few Yucca Mountain samples we have analyzed so far. For example the manganese-rich, dark brown coating on the fracture surface contained within sample G4 2947 exhibits a relatively large amount of Mg, moderate amounts of Al, Ca, and Li, small amounts of Ba and Ce, and the absence of Si and Pb suggesting that it consists of a mixture of Hollandite and Todorokite with minor amounts of Romanechite or Lithophorite, although the Li content could be explained entirely by Hollandite. Qualitative x-ray diffraction of Mn-Fe oxide fracture coatings from this depth by Carlos et al., 1990 notes major amounts of Hollandite (Cryptomelane-Hollandite group) with possible Pyrolusite and Todorokite; Todorokite is reported in minor amounts at a slightly greater depth (2954.8-2955.1). Thus, deductions from the LIBS analysis of this sample are in qualitative agreement with the x-ray diffraction results.

The GU3 samples from the Topopah Spring tuff show complex variations in chemistry based on the LIBS analyses. Sample GU3 797 exhibits two qualitatively different dark coatings - a blackish-brown Mn-rich coating exhibiting low Li and Pb with moderate amounts of Ca, Al, Si, and Mg and no detectable Ba, also with notable amounts of Zn, W, Ti, and Ce (Figure 2a-d); and a greenish-brown, platy coating exhibiting high Li, Ca, Al, Fe with moderate amounts of Mg, Si and low Pb and Ba. The former is consistent with a low-Ba Todorokite or, based on the composition reported by Carlos et al., (1993) Rancieite, $CaMn_4O_9.4H_2O$, which was reported to occur in drill hole GU3 at levels just below our sample. The greenish-brown, micaceous mineral would appear to be Lithophorite, $Li_2Al_8(Mn, Co, Ni)_2Mn_{10}O_{35}.14H_2O$, possibly mixed with Rancieite and Hematite(?) to account for the relatively high Ca and Fe relative to Mn. Lithiophorite is reported as the dominant Mn-oxide mineral in GU3 at levels just below our sample (Carlos et al., 1993).

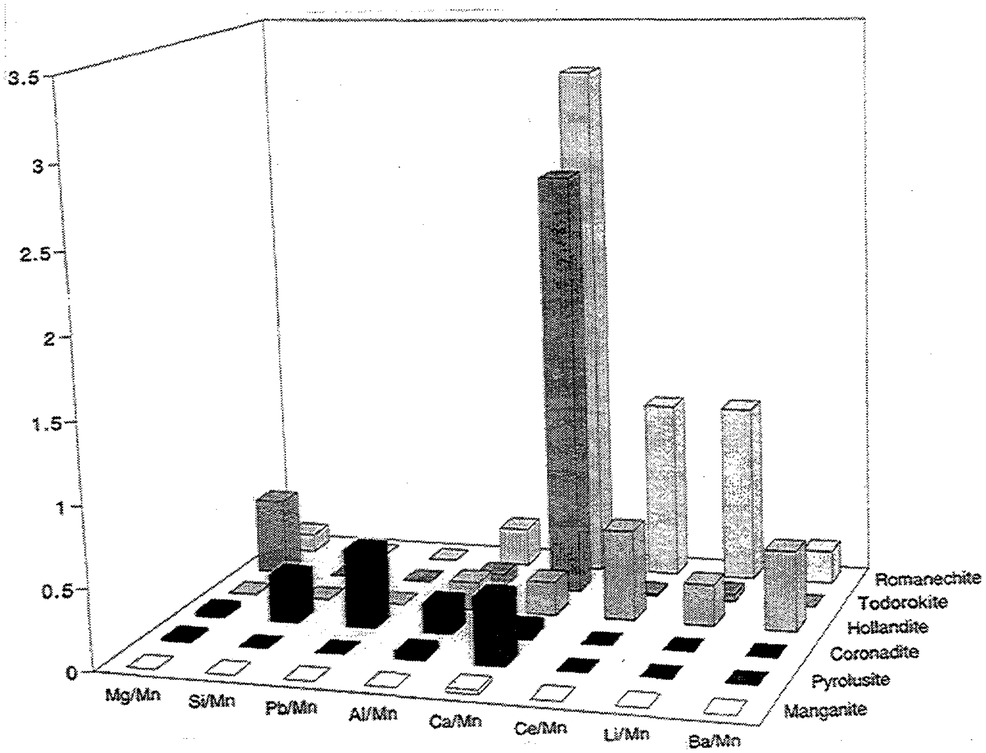

Fig. 3. Ratios of LIBS spectral line heights for selected elements from each manganese mineral standard. Individual lines are identified in the text.

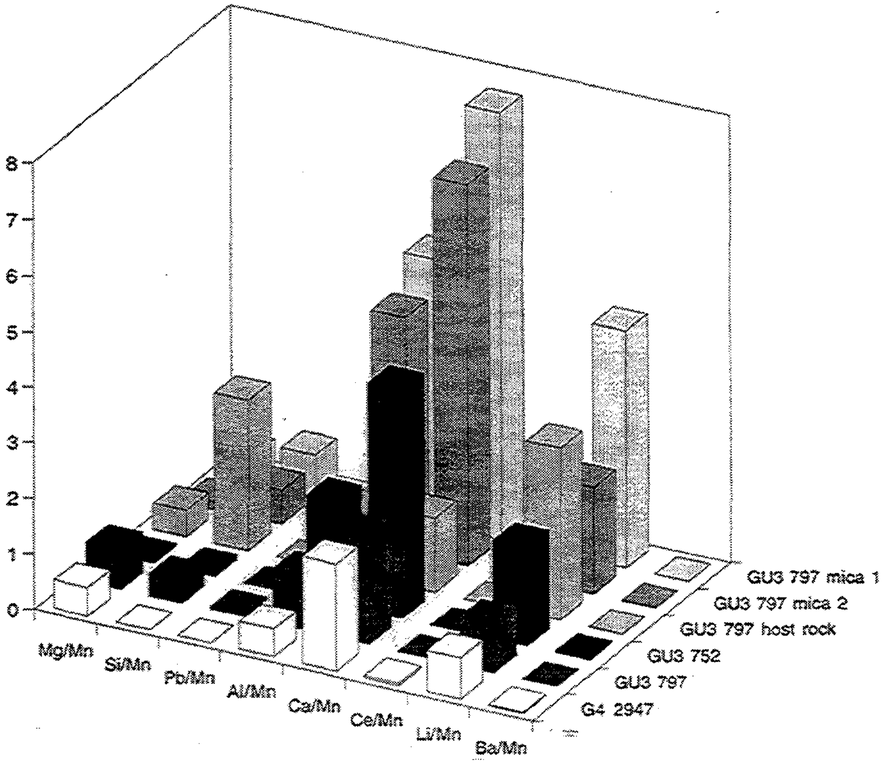

Fig. 4. Ratios of LIBS spectral line heights for selected elements from Yucca Mountain tuff samples. Individual lines are identified in the text.

A LIBS analysis of the host rock of sample GU3 797 was made on the same fracture surface away from the Mn-oxide coatings. It is notable for the strong Li line and a line identified as Ni (also present in the Lithiophorite spectra).

DISCUSSION

During the LIBS data collection, multiple laser pulses were found not to ablate through the thin coating of manganese oxide minerals. This is essential for spectral consistency since four separate laser pulses are needed at each analysis spot, one at each setting of the grating. Multiple spot analyses on the manganese oxide mineral coatings were found to show no significant elemental variation over a particular sample. Differentiation between manganese mineralization, host rock, and other vein/coating mineralization was readily apparent, as seen in the spectra and in the element ratios, particularly those involving Si, Ca, and Al. With additional data collection on standards and development of quantitative calibration curves for key elements, identification of manganese oxide minerals with the LIBS method should improve and become definitive.

CURRENT STATE OF THE FIELD LIBS INSTRUMENTATION

The LIBS instrumentation is evolving into a design for surface analysis of vein filling manganese oxide or other mineralization, either from the tunnel surface in the wake of the TBM or from drill core. The prototype hardware has a Laser Photonics 20 mj pulsed Nd-YAG laser built into an eye safe, hand held probe (see Fig. 5) which is pressed against the surface to be analyzed. A rubber boot prevents light leakage from around the probe. A cylinder adapter is used for drill core. A 20X Edmund Scientific binocular microscope is built into the probe so that the reticule cross hairs intersect at the YAG spark location. A pressure sensitive interlock prevents the laser from firing when not against a solid surface; thus, the laser beam is completely enclosed and eye safe. A 5 meter-long, ultraviolet grade fiber-optic bundle directs the emission light into a sealed instrument case enclosing a 1/3 m spectrograph and CCD with detector. A laptop computer operates the CCD detector and stores the spectra. This hardware is slated to be tested at the Yucca Mountain Exploratory Studies Facility later this year.

CONCLUSIONS AND RECOMMENDATIONS

We have demonstrated that the laser-induced breakdown spectroscopy (LIBS) surface analysis technique is capable of producing high resolution atomic emission spectra in a configuration amenable to field operation. Analysis of manganese oxide mineral samples and fracture surface coatings from a few Yucca Mountain core samples indicates that qualitative measurement of all constituent elements except K and Na (in the presence of Mn) is possible with LIBS. We have identified four spectral bands which will cover all of the key elements for the manganese oxide minerals. Further work including detailed calibration of final hardware will be needed to make the system quantitative. The LIBS analyses should allow at least approximate estimates to be made of the relative proportions of specific manganese oxide minerals based on their distinctive element ratios and concentrations.

We will shortly field-test a first prototype LIBS instrument at the Yucca Mountain Exploratory Studies Facility. Once the design of this device is stable, quantitative calibration curves for about a dozen key elements should be developed, and additional mineral standards analyzed along with further comparisons to Yucca Mountain samples analyzed by other methods. With these data in hand and development of an improved prototype instrument, systematic measurements can begin in the Exploratory Facility and on core samples.

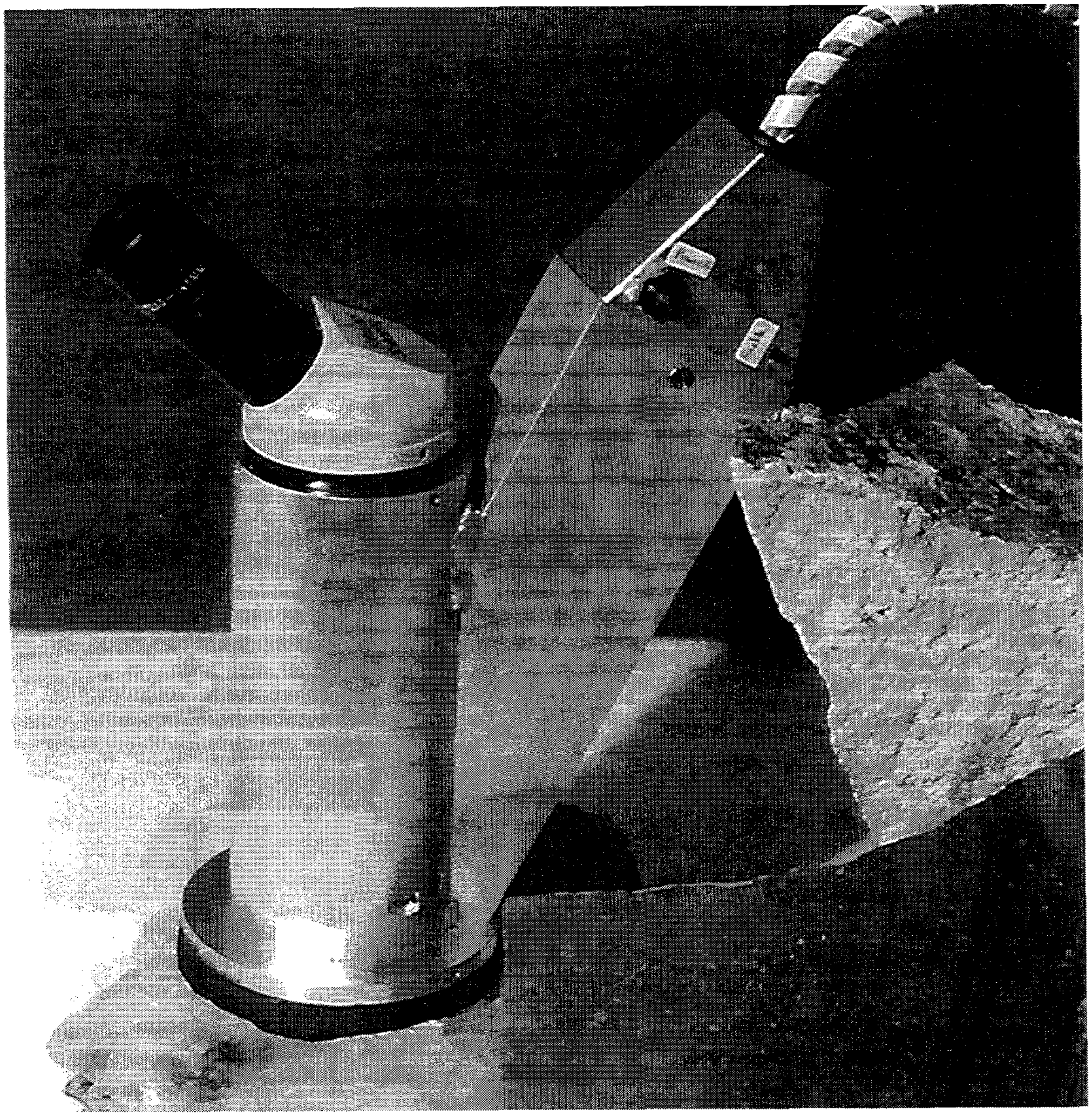

Fig. 5. Prototype analysis head of field-portable LIBS instrument. The eye piece shown to the top-left is used to accurately position the laser spark on the sample to be analyzed (e.g., a narrow filled fracture). The laser head and fiber optic light-return cable are shown at the right.

ACKNOWLEDGMENTS

Steve Chipera supplied the manganese oxide mineral samples and collected what analytical data were available for them. Monty Ferris was helpful in developing the design approach for the prototype field LIBS analysis head and performed the initial construction. Barbara Carlos provided analyzed samples from Yucca Mountain, and aided us in understanding the occurrence of manganese oxide minerals at Yucca Mountain. Dave Vaniman and Ines Triay provided useful discussions of the potential sorptive capacity of manganese oxides and their importance at Yucca Mountain.

This work was supported by the Yucca Mountain Site Characterization Office as part of the Civilian Radioactive Waste Management Program. This project is managed by the U.S. Department of Energy, Yucca Mountain Site Characterization Project.

REFERENCES

Bish, D. L. and J. E. Post, Thermal behavior of complex, tunnel-structure manganese oxides, Amer. Mineral., 74, 177-186, 1989.

Blacic, J., D. Pettit, and D. Cremers, Field deployment test of LIBS technology at the Yucca Mountain Exploratory Studies Facility, test alcove #1, March 2-9, 1994, Los Alamos Nat. Lab. Rept., LA-13043-MS, 1995.

Broxton, D. E., R. W. Warren, and F. M. Byers, Chemical and mineralogic trends within the Timber Mountain-Oasis Valley caldera complex, Nevada: Evidence for multiple cycles of chemical evolution in a long-lived silicic magma system, J. Geophys. Res., 94, 5961-5985, 1989.

Carlos, B., Fracture-coating minerals in the Topopah Spring Member and Upper Tuff of Calico Hills from Drill Hole J-13, Los Alamos Nat. Lab. Rept. LA-11504-MS, 20 pp., 1989.

Carlos, B. A., D. L. Bish, and S. J. Chipera, manganese-oxide minerals in fractures of the Crater Flat tuff in drill Core USW G-4, Yucca Mountain, Nevada, Los Alamos Nat. Lab. Rept. LA-11787-MS, 61 pp., 1990.

Carlos, B. A., S. J. Chipera, D. L. Bish, and S. J. Craven, Fracture-lining manganese oxide minerals in silicic tuff, Yucca Mountain, Nevada, U.S.A., Chem. Geol., 107, 47-69, 1993.

Means, J. L., D. A. Crerar, M. P. Borcsik, and J. O. Duguid, Adsorption of Co and selected actinides by Mn and Fe oxides in soils and sediments, Geochim. Cosmochim. Acta, 42, 1763-1273, 1978.

Triay, I. R., Radionuclide migration as a function of mineralogy, oral presentation at 2nd annual High-Level Radioactive Waste Management Conf., Las Vegas, Nev., 1991.

Triay, I. R., A. J. Mitchell, and M. A. Ott, Radionuclide migration as a function of mineralogy, Proc. at 2nd annual High-Level Radioactive Waste Management Conf., Las Vegas, Nev., 494-498, 1991.

Vaniman, D. personal communication, June, 1995.

APPENDIX I: LIBS EMISSION SPECTRA

This appendix contains LIBS emission spectra for all mineral standards and Yucca Mountain samples analyzed.

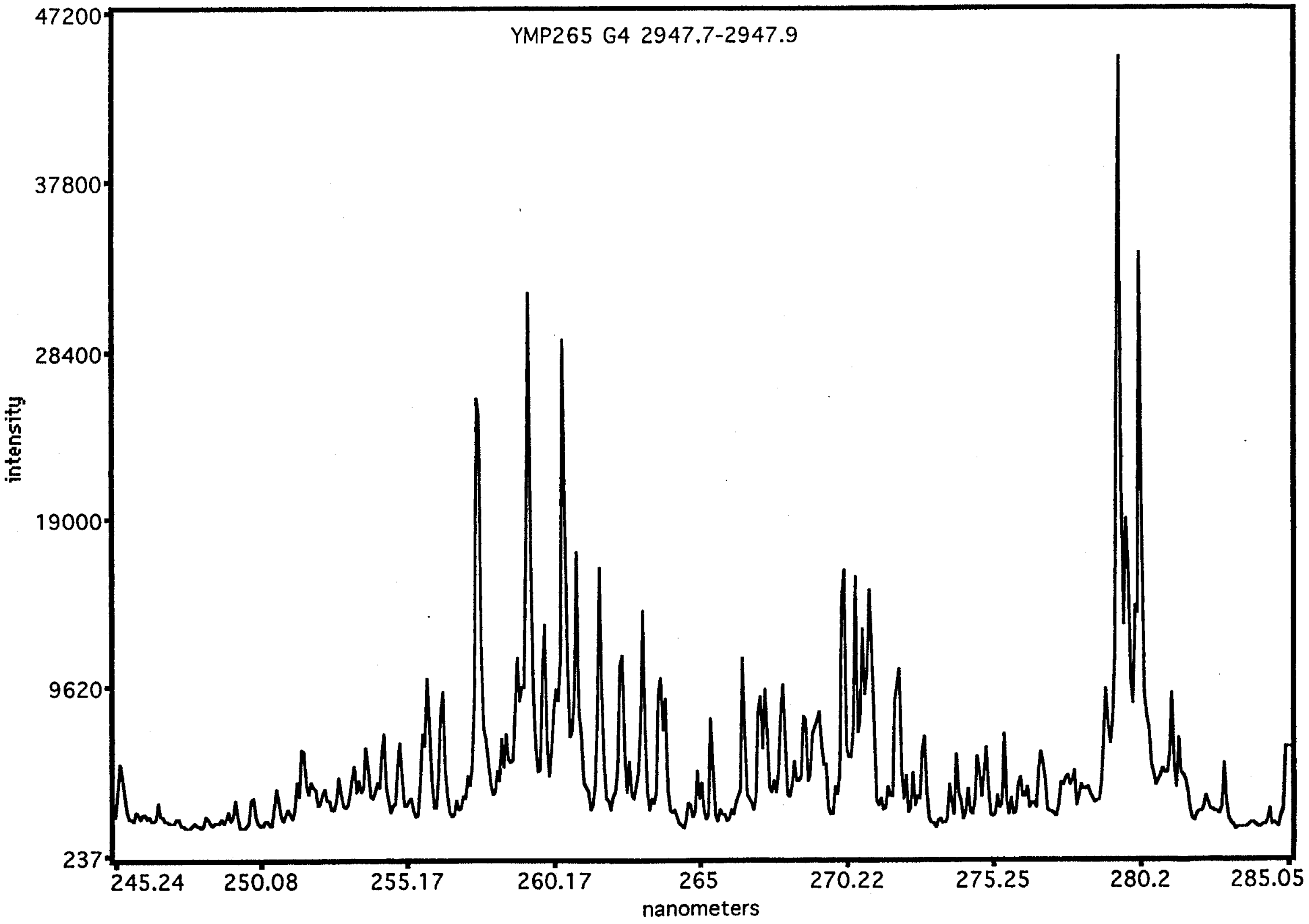
YMP265 G4 2947.7-2947.9
intensity
47200
37800
28400
19000
9620
237
245.24
250.08
255.17
260.17
265
270.22
275.25
280.2
285.05
nanometers

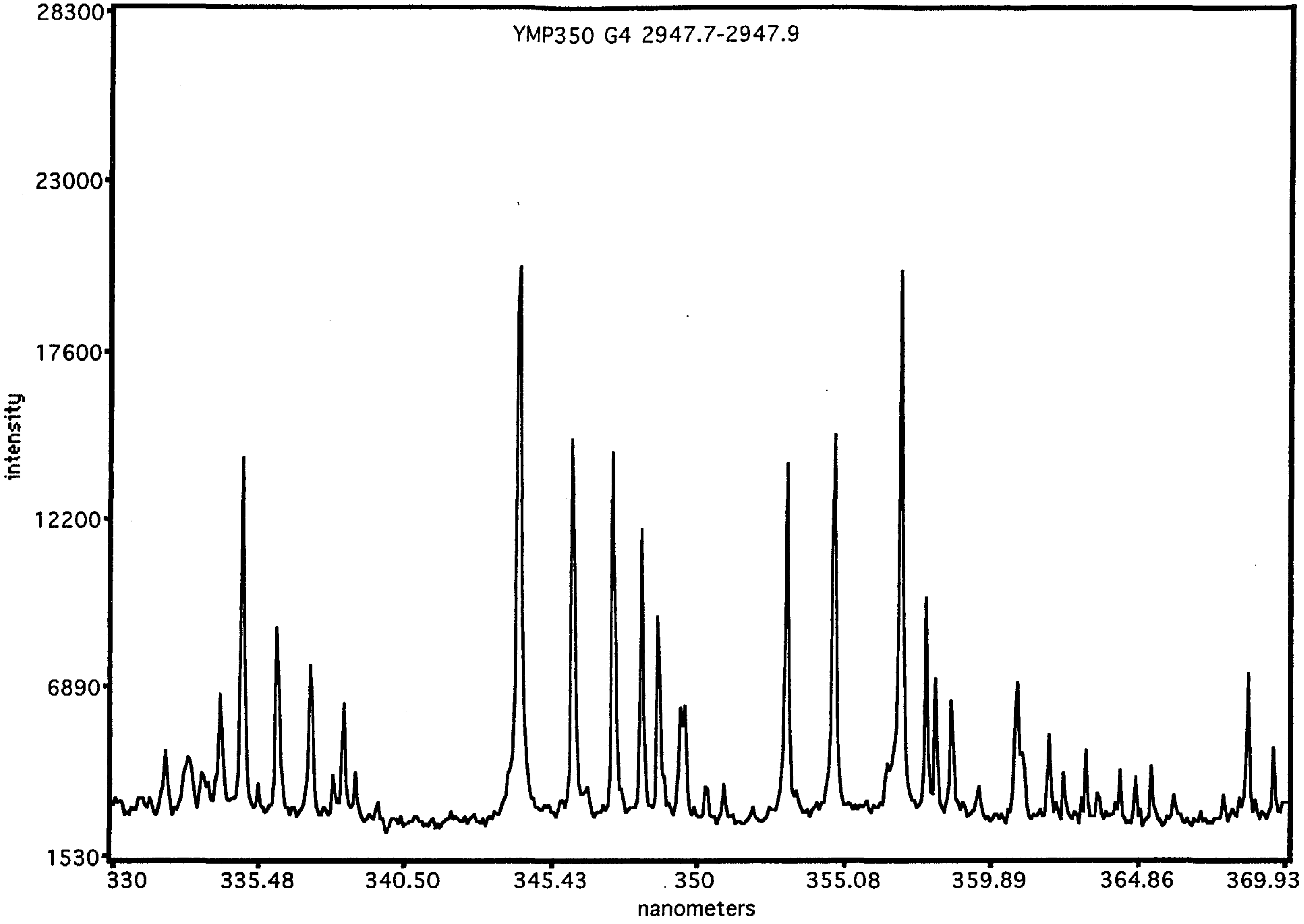
YMP350 G4 2947.7-2947.9
intensity
28300
23000
17600
12200
6890
1530
330
335.48
340.50
345.43
350
355.08
359.89
364.86
369.93
nanometers

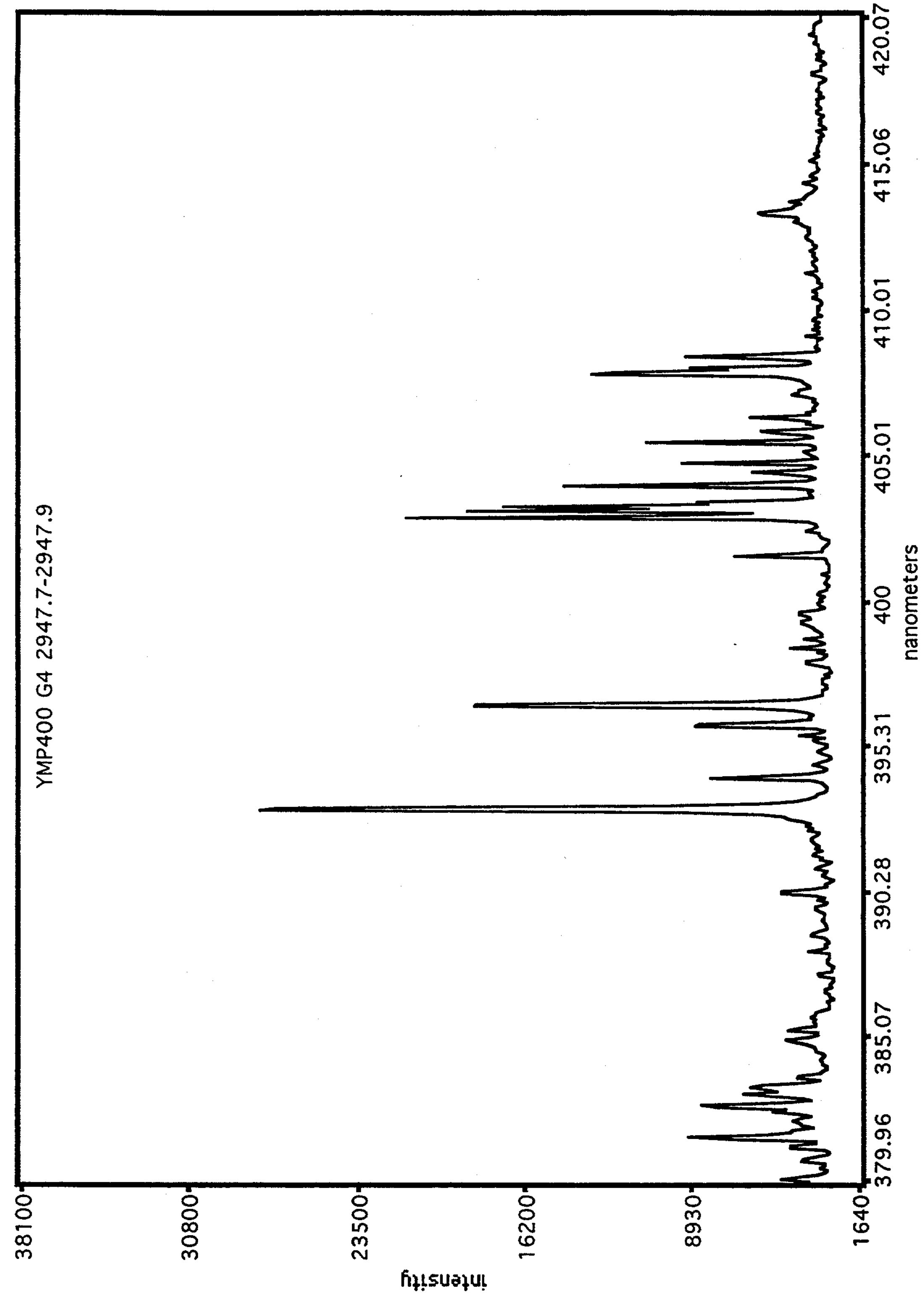
YMP400 G4 2947.7-2947.9
intensity
38100
30800
23500
16200
8930
1640
nanometers
379.96
385.07
390.28
395.31
400
405.01
410.01
415.06
420.07

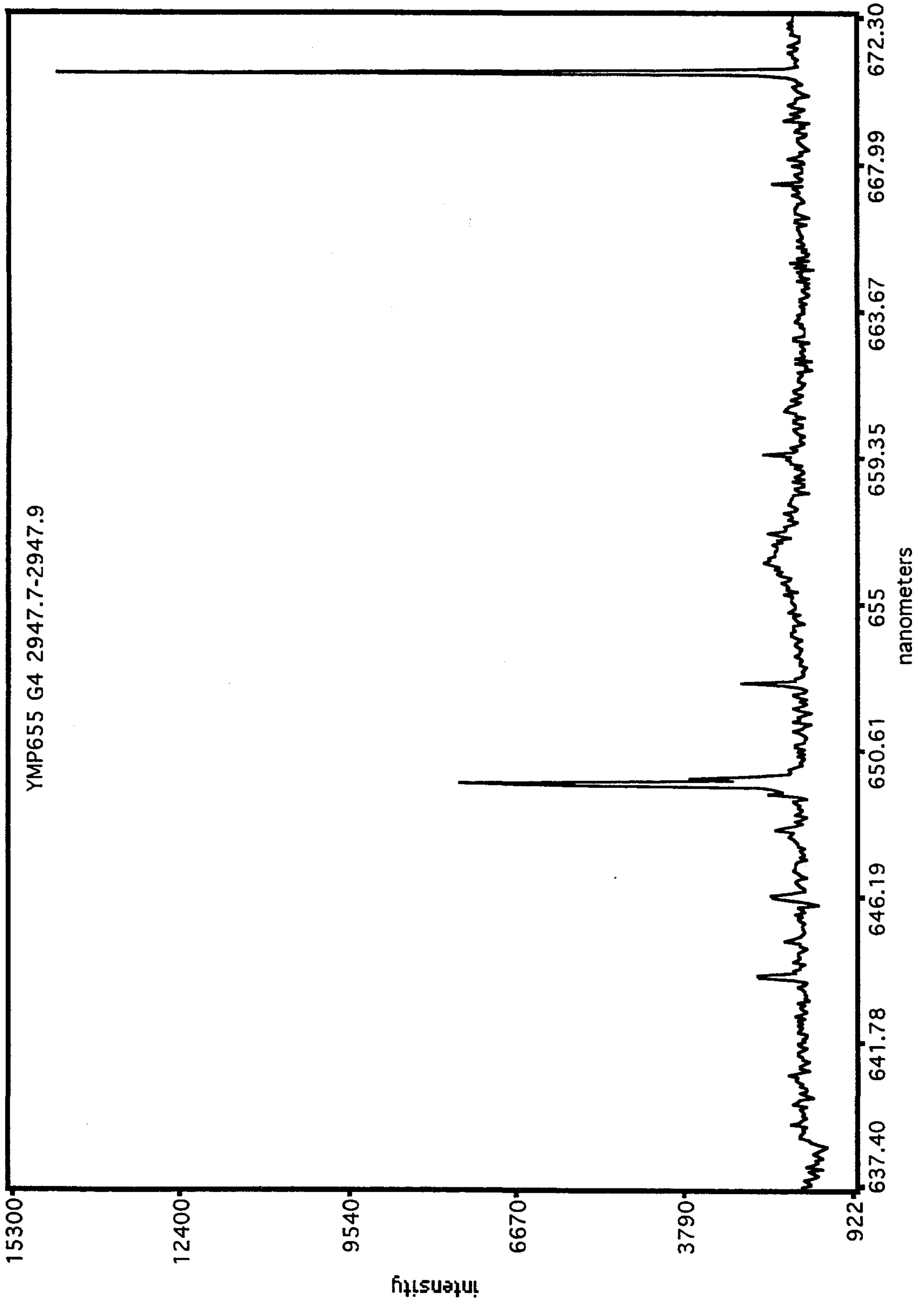
YMP655 G4 2947.7-2947.9
intensity
15300
12400
9540
6670
3790
922
nanometers
637.40
641.78
646.19
650.61
655
659.35
663.67
667.99
672.30

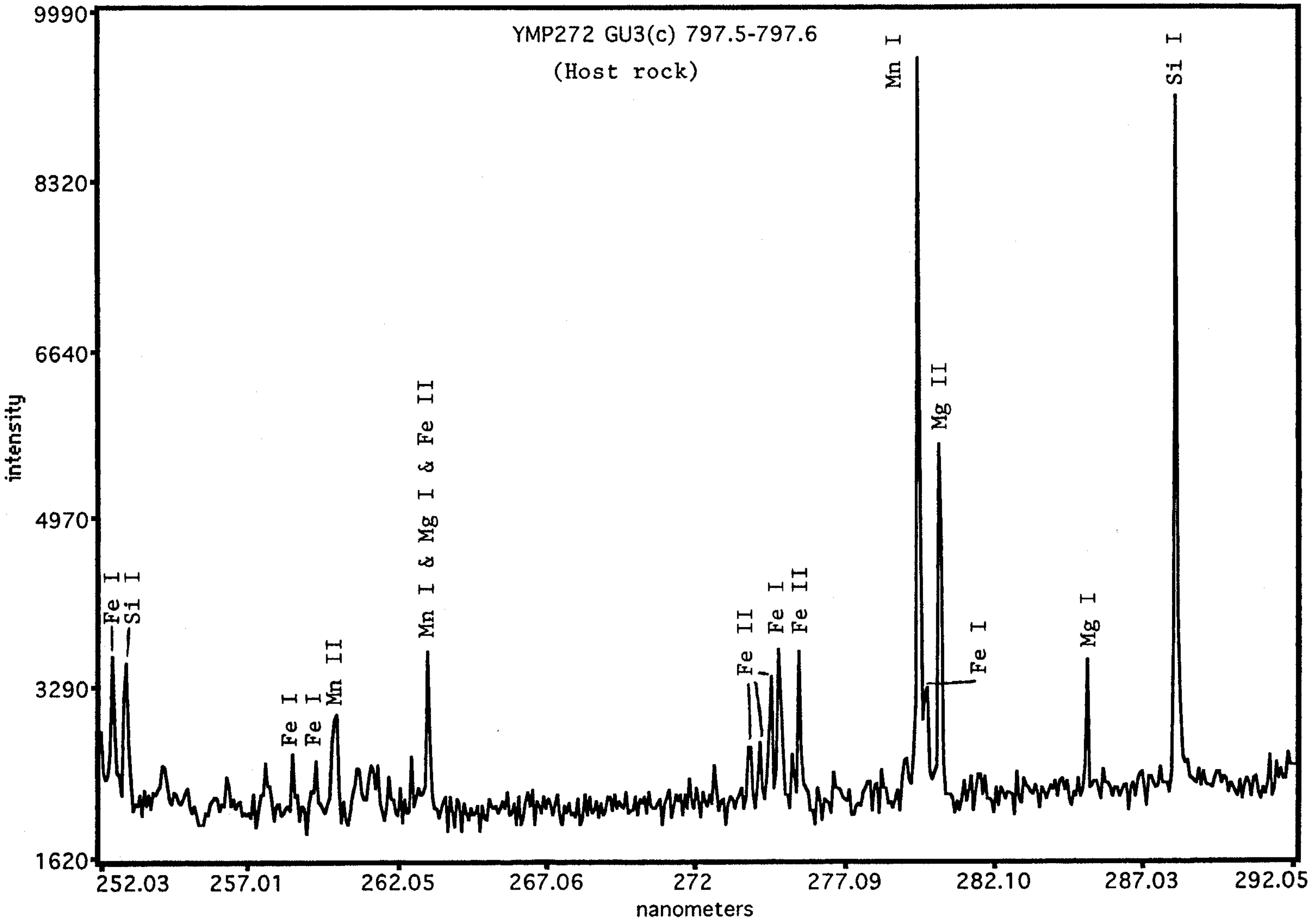
YMP272 GU3(c) 797.5-797.6
(Host rock)
intensity
9990
8320
6640
4970
3290
1620
nanometers
252.03
257.01
262.05
267.06
272
277.09
282.10
287.03
292.05
Fe I
Si I
Fe I
Fe I
Mn II
Mn I & Mg I & Fe II
Fe II
Fe I
Fe II
Mn I
Mg II
Fe I
Mg I
Si I

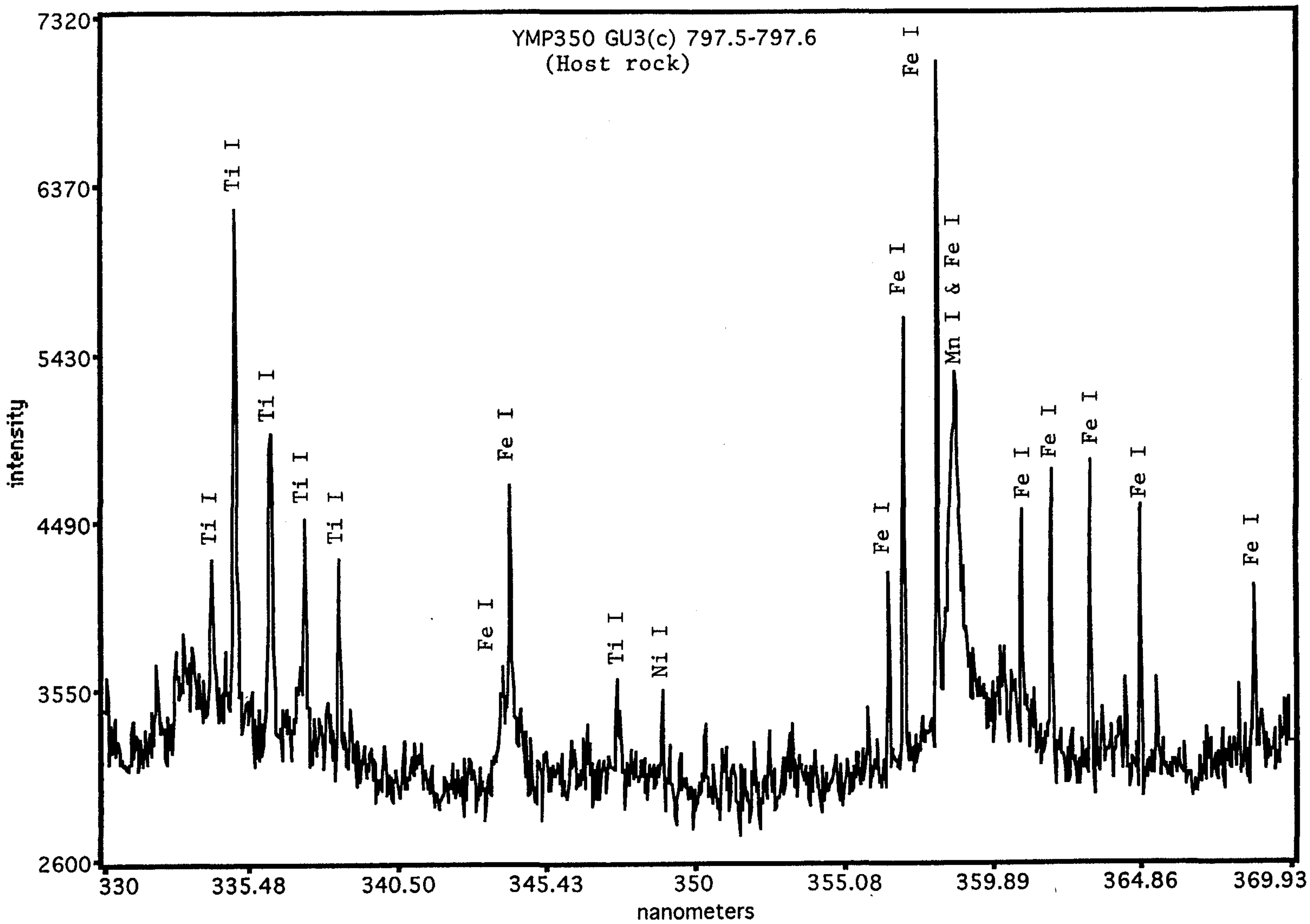
YMP350 GU3(c) 797.5-797.6
(Host rock)
intensity
7320
6370
5430
4490
3550
2600
330
335.48
340.50
345.43
350
355.08
359.89
364.86
369.93
nanometers
Ti I
Ti I
Ti I
Ti I
Ti I
Fe I
Fe I
Ti I
Ni I
Fe I
Fe I
Fe I
Mn I & Fe I
Fe I
Fe I
Fe I
Fe I
Fe I

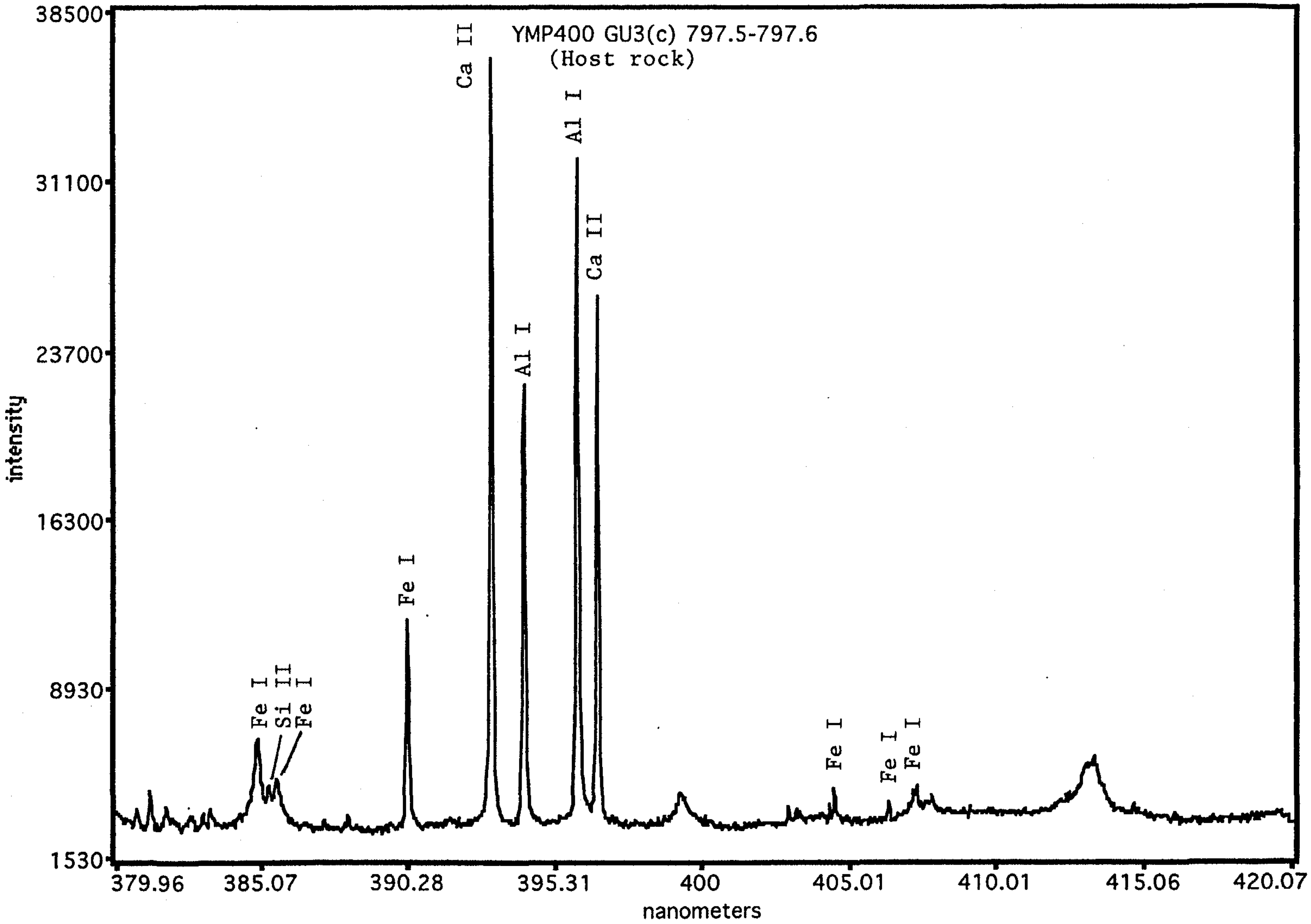
YMP400 GU3(c) 797.5-797.6
(Host rock)
intensity
38500
31100
23700
16300
8930
1530
379.96
385.07
390.28
395.31
400
405.01
410.01
415.06
420.07
nanometers
Fe I
Si II
Fe I
Fe I
Ca II
Al I
Al I
Ca II
Fe I
Fe I
Fe I

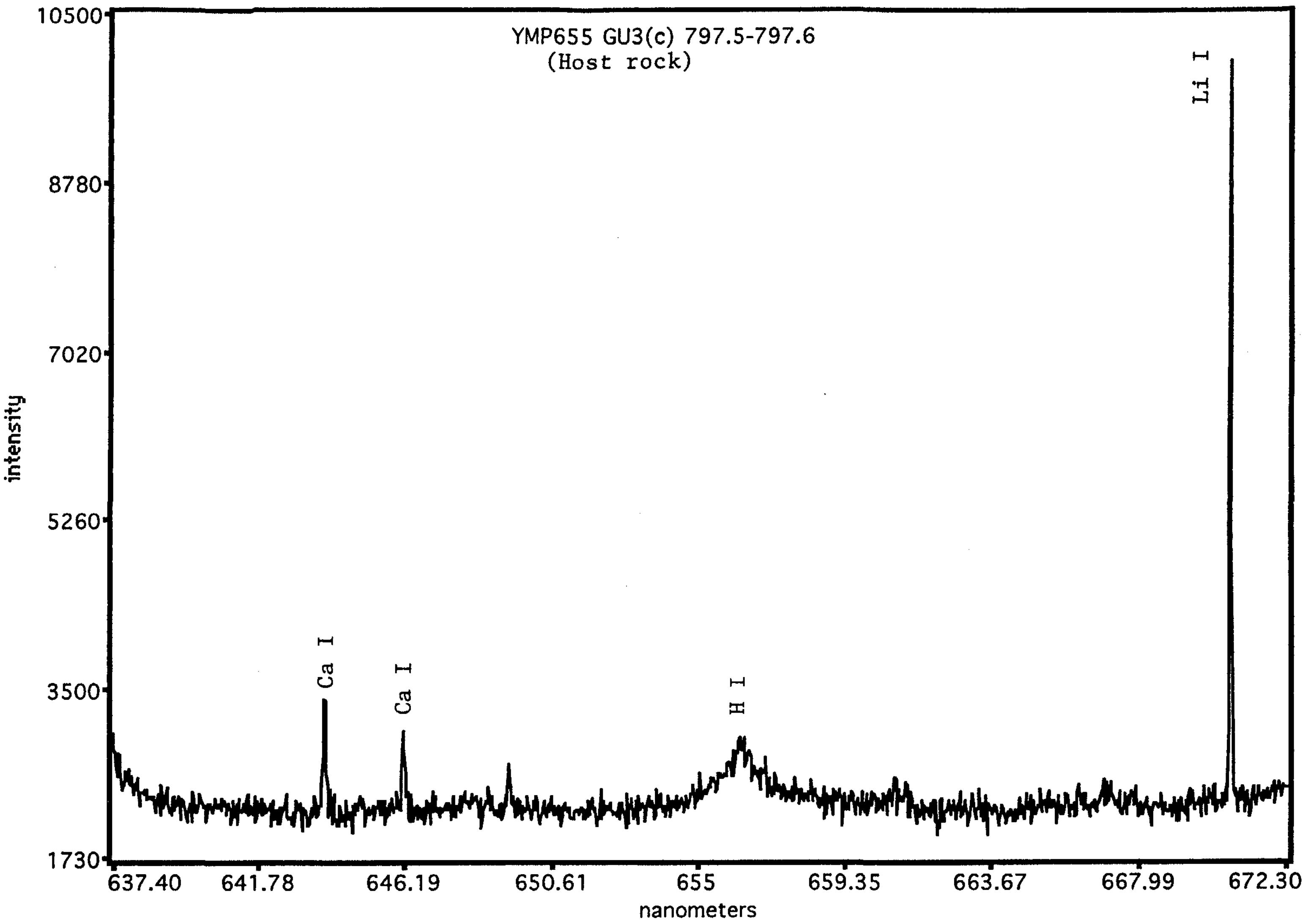
YMP655 GU3(c) 797.5-797.6
(Host rock)
Li I
Ca I
Ca I
H I
intensity
10500
8780
7020
5260
3500
1730
637.40
641.78
646.19
650.61
655
659.35
663.67
667.99
672.30
nanometers

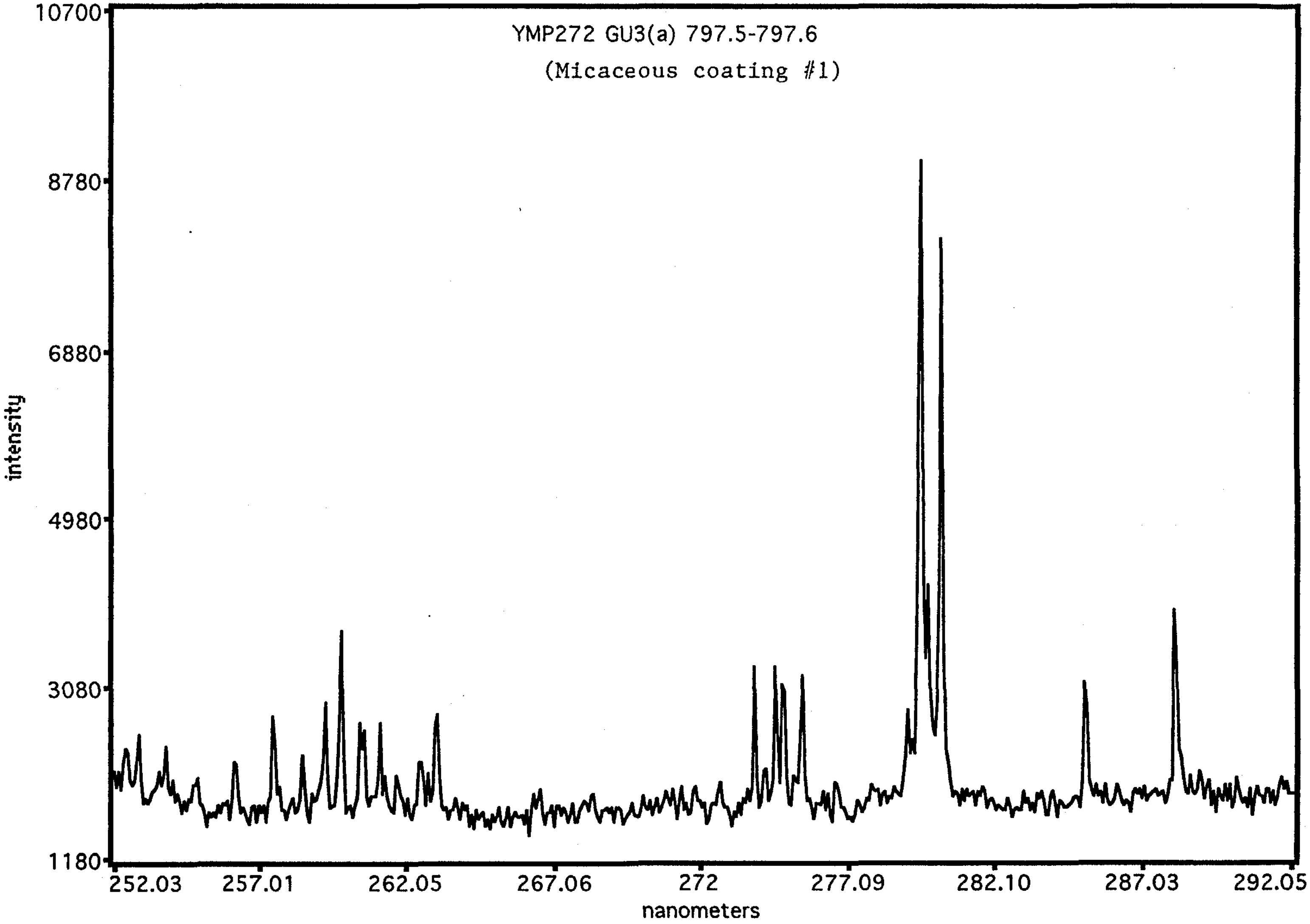
YMP272 GU3(a) 797.5-797.6
(Micaceous coating #1)
intensity
10700
8780
6880
4980
3080
1180
252.03
257.01
262.05
267.06
272
277.09
282.10
287.03
292.05
nanometers

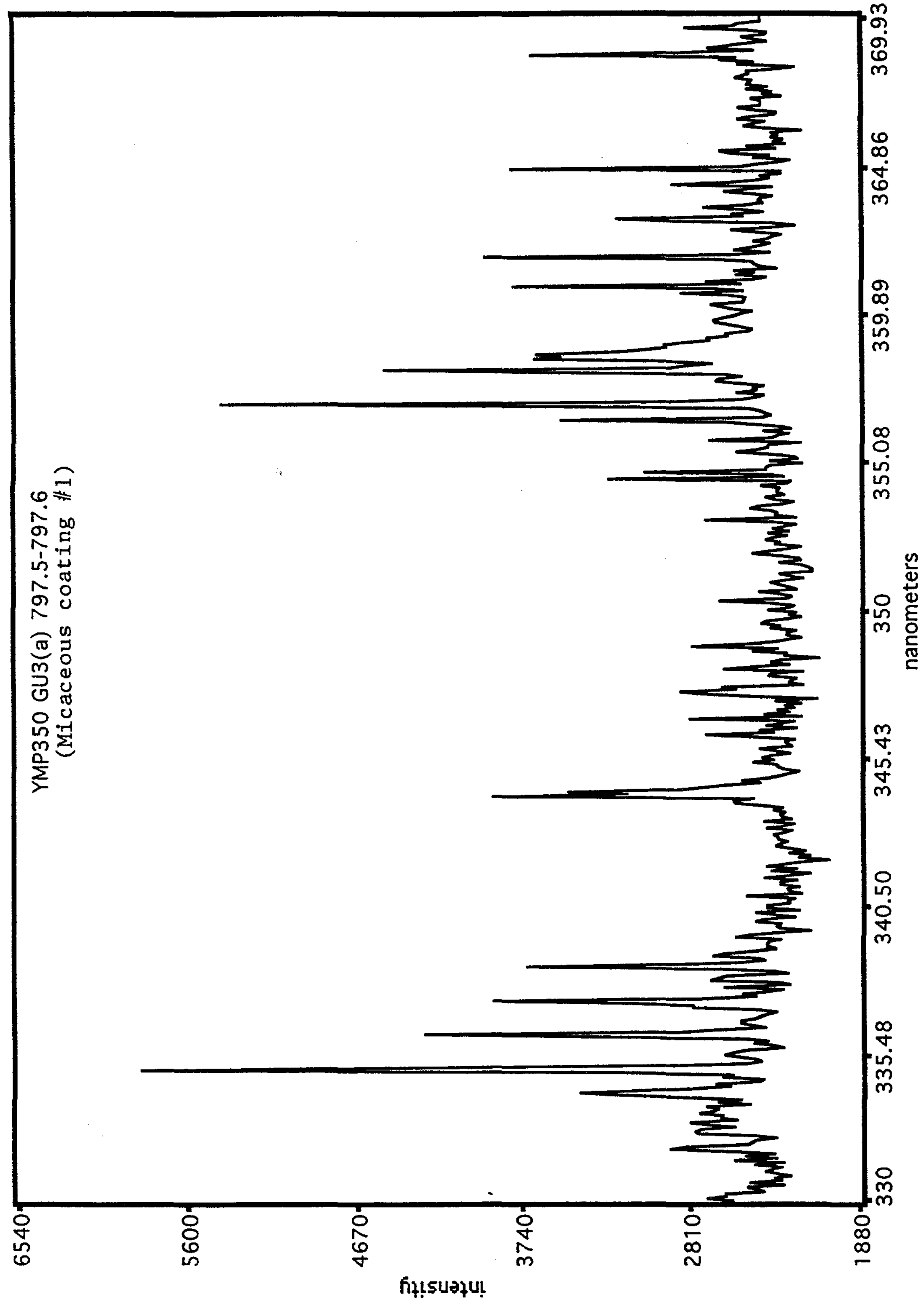
YMP350 GU3(a) 797.5-797.6
(Micaceous coating #1)
intensity
6540
5600
4670
3740
2810
1880
330
335.48
340.50
345.43
350
355.08
359.89
364.86
369.93
nanometers

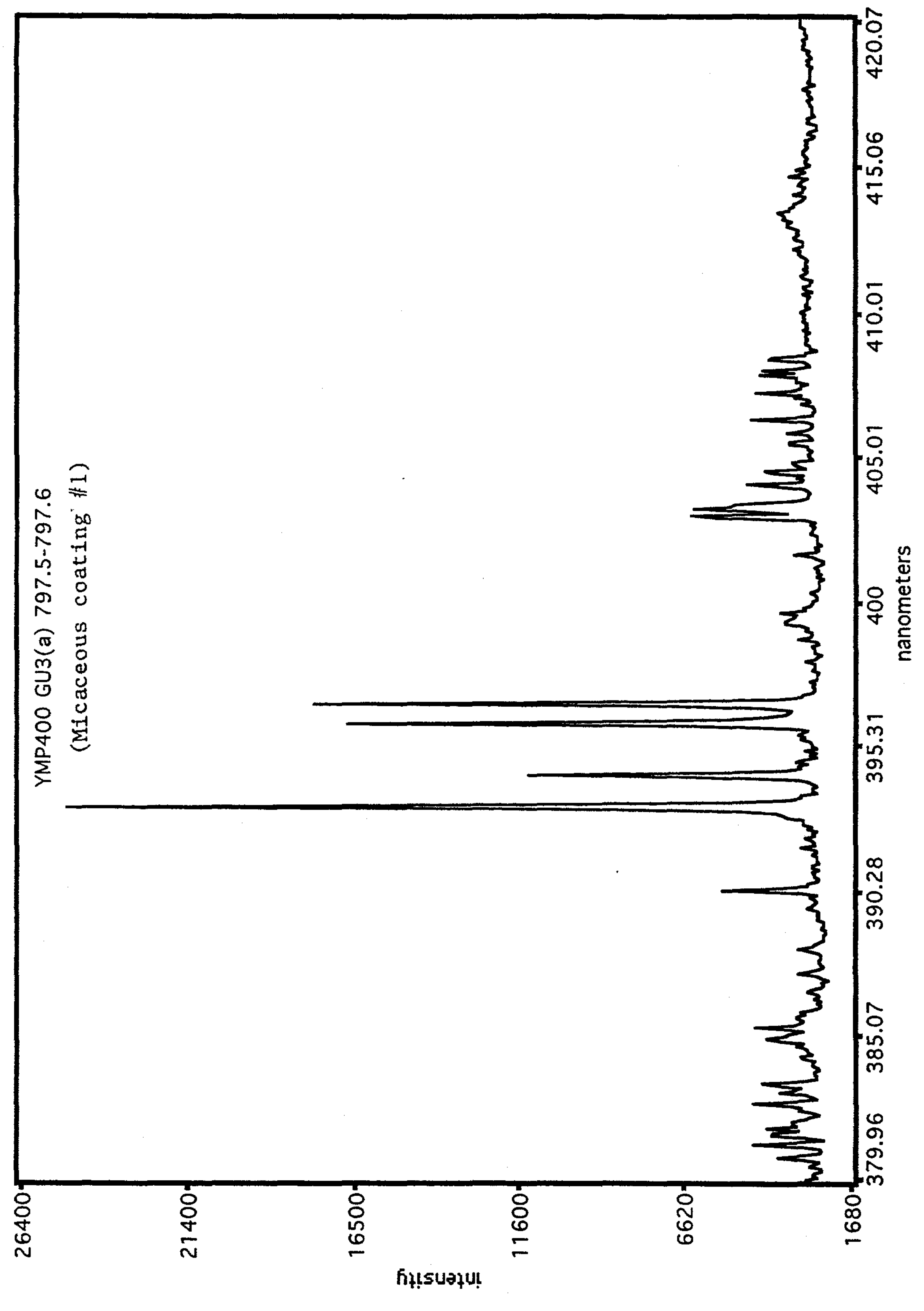

YMP400 GU3(a) 797.5-797.6

(Micaceous coating #1)

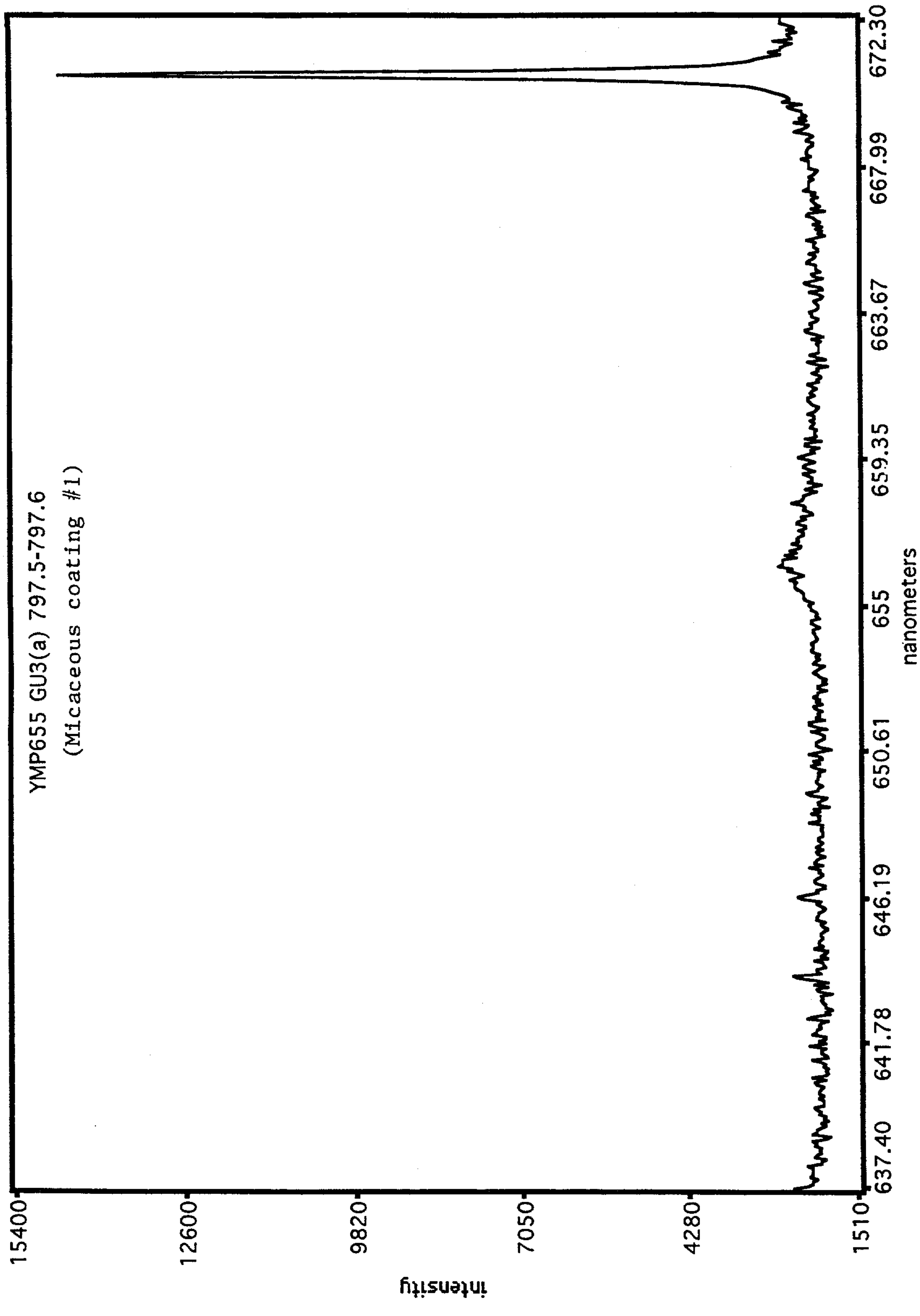
YMP655 GU3(a) 797.5-797.6
(Micaceous coating #1)
intensity
15400
12600
9820
7050
4280
1510
nanometers
637.40
641.78
646.19
650.61
655
659.35
663.67
667.99
672.30

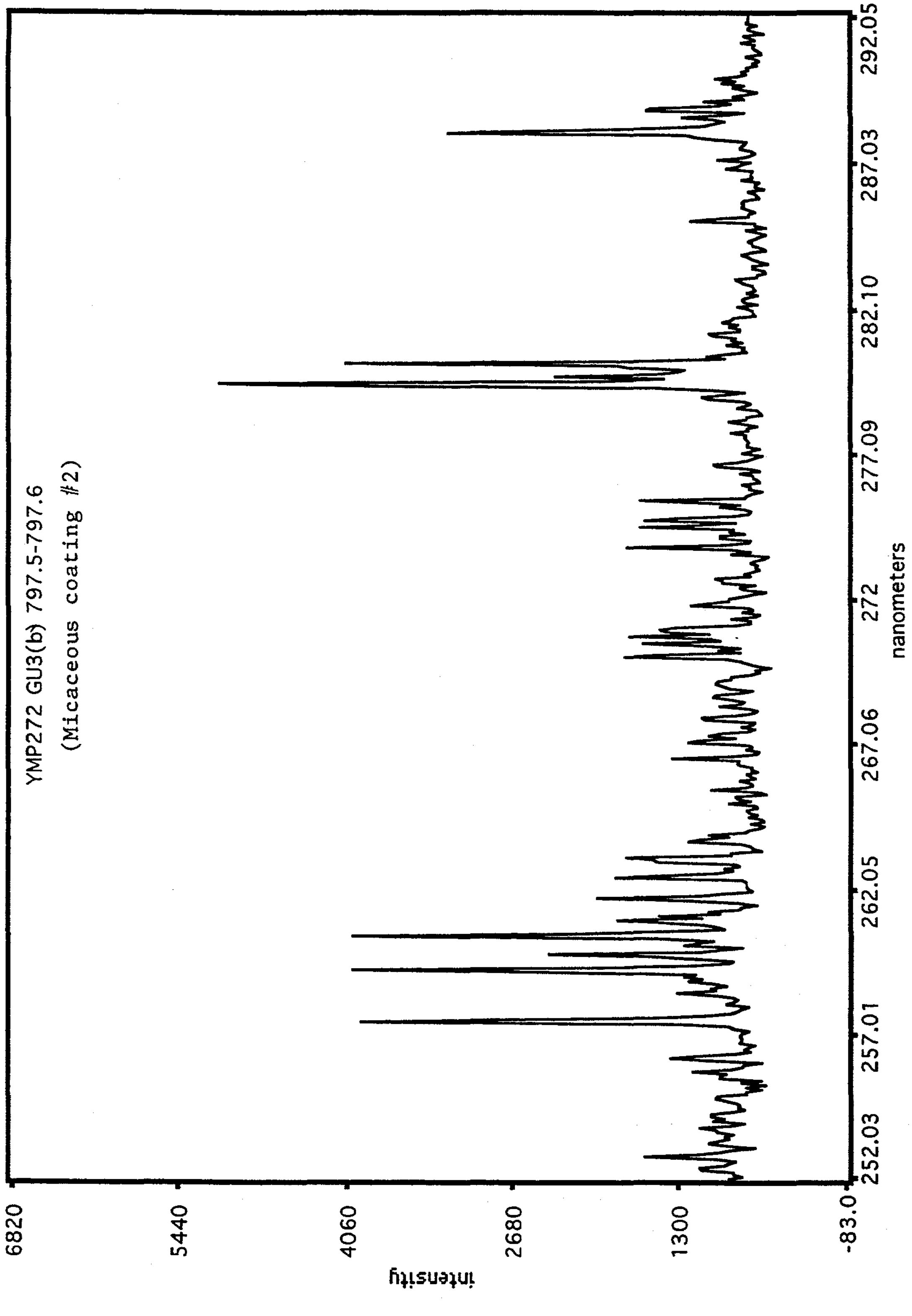
YMP272 GU3(b) 797.5-797.6
(Micaceous coating #2)
intensity
6820
5440
4060
2680
1300
-83.0
252.03
257.01
262.05
267.06
272
277.09
282.10
287.03
292.05
nanometers

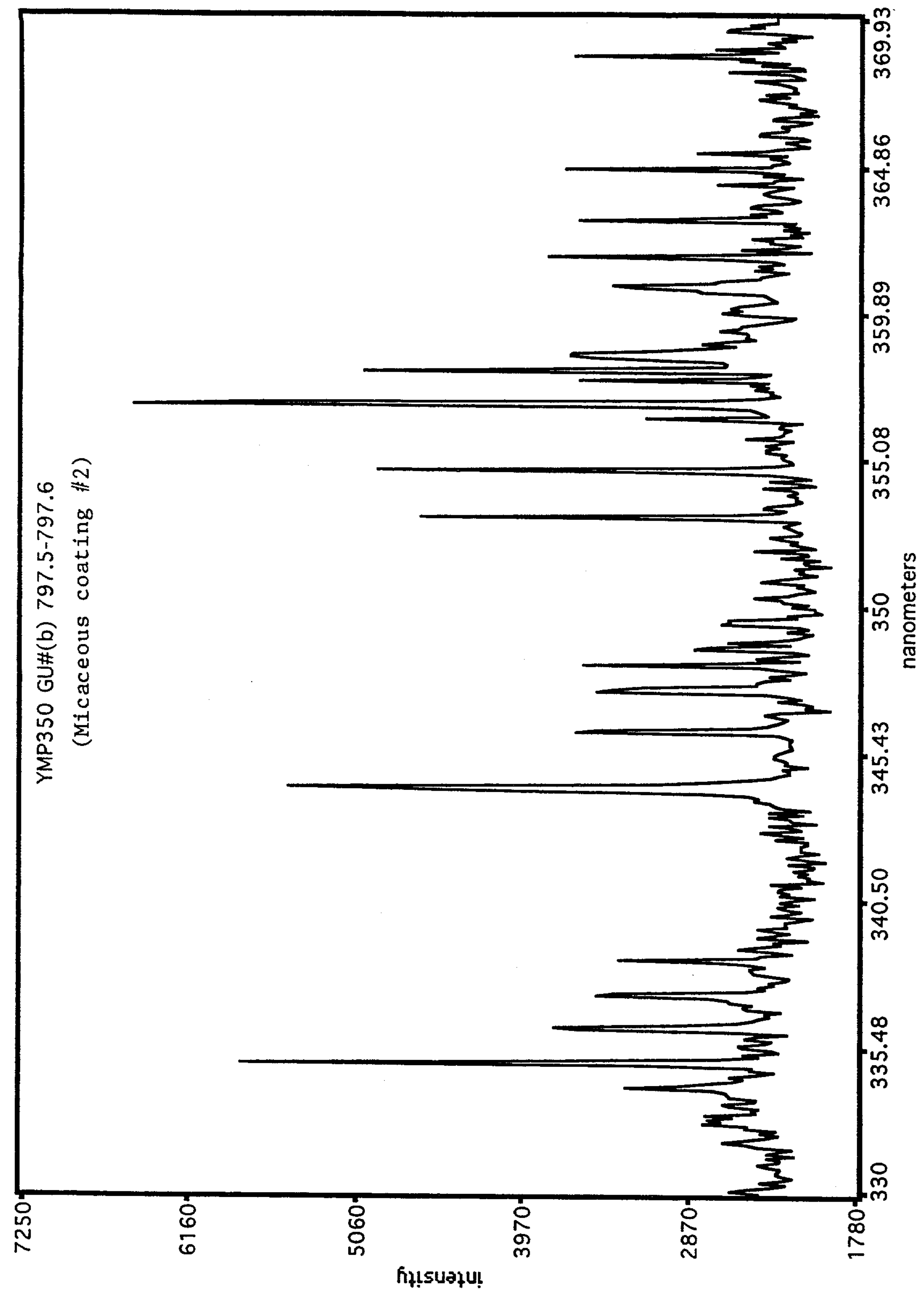
YMP350 GU#(b) 797.5-797.6
(Micaceous coating #2)
intensity
7250
6160
5060
3970
2870
1780
nanometers
330
335.48
340.50
345.43
350
355.08
359.89
364.86
369.93

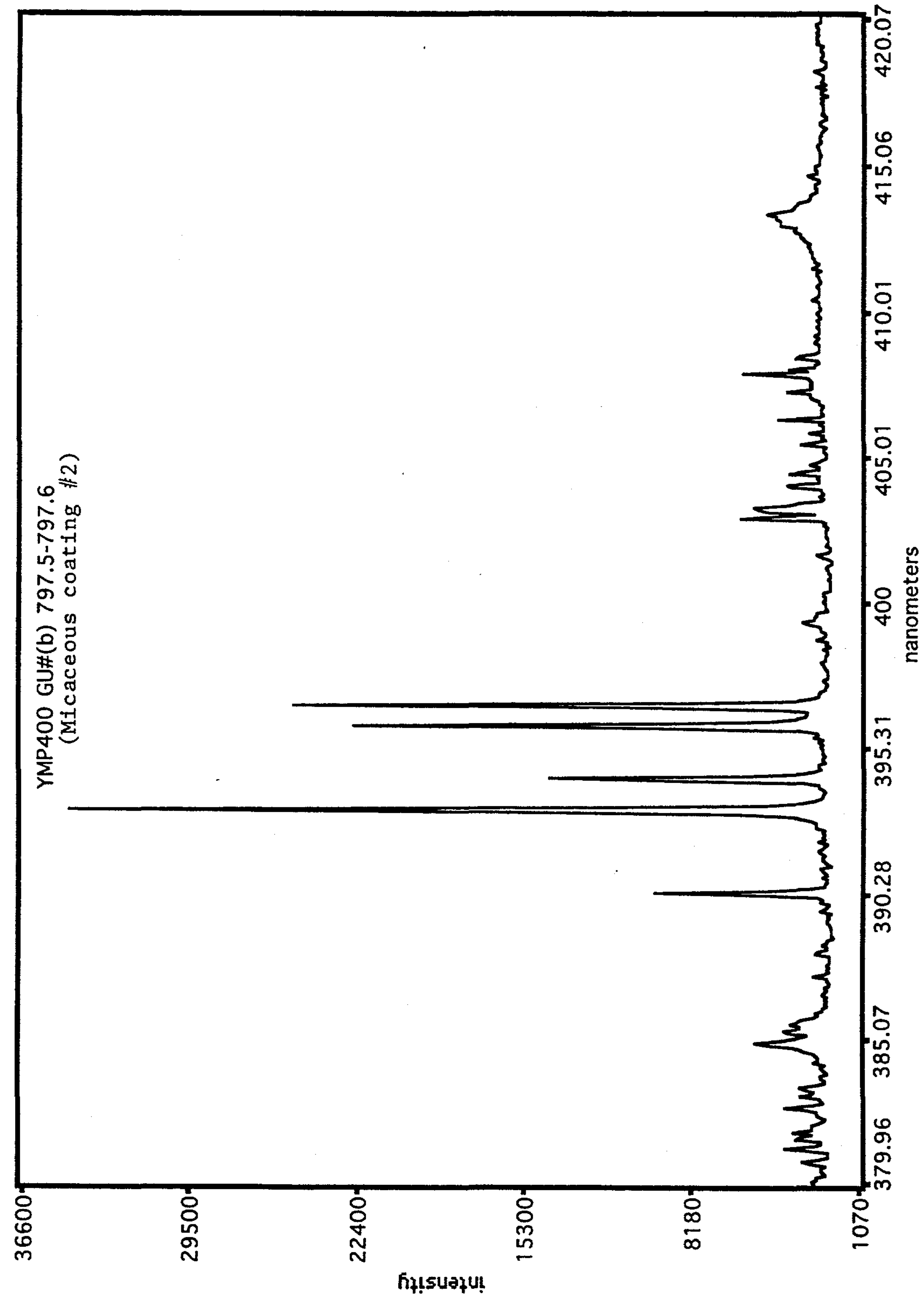
YMP400 GU#(b) 797.5-797.6
(Micaceous coating #2)
intensity
36600
29500
22400
15300
8180
1070
379.96
385.07
390.28
395.31
400
405.01
410.01
415.06
420.07
nanometers

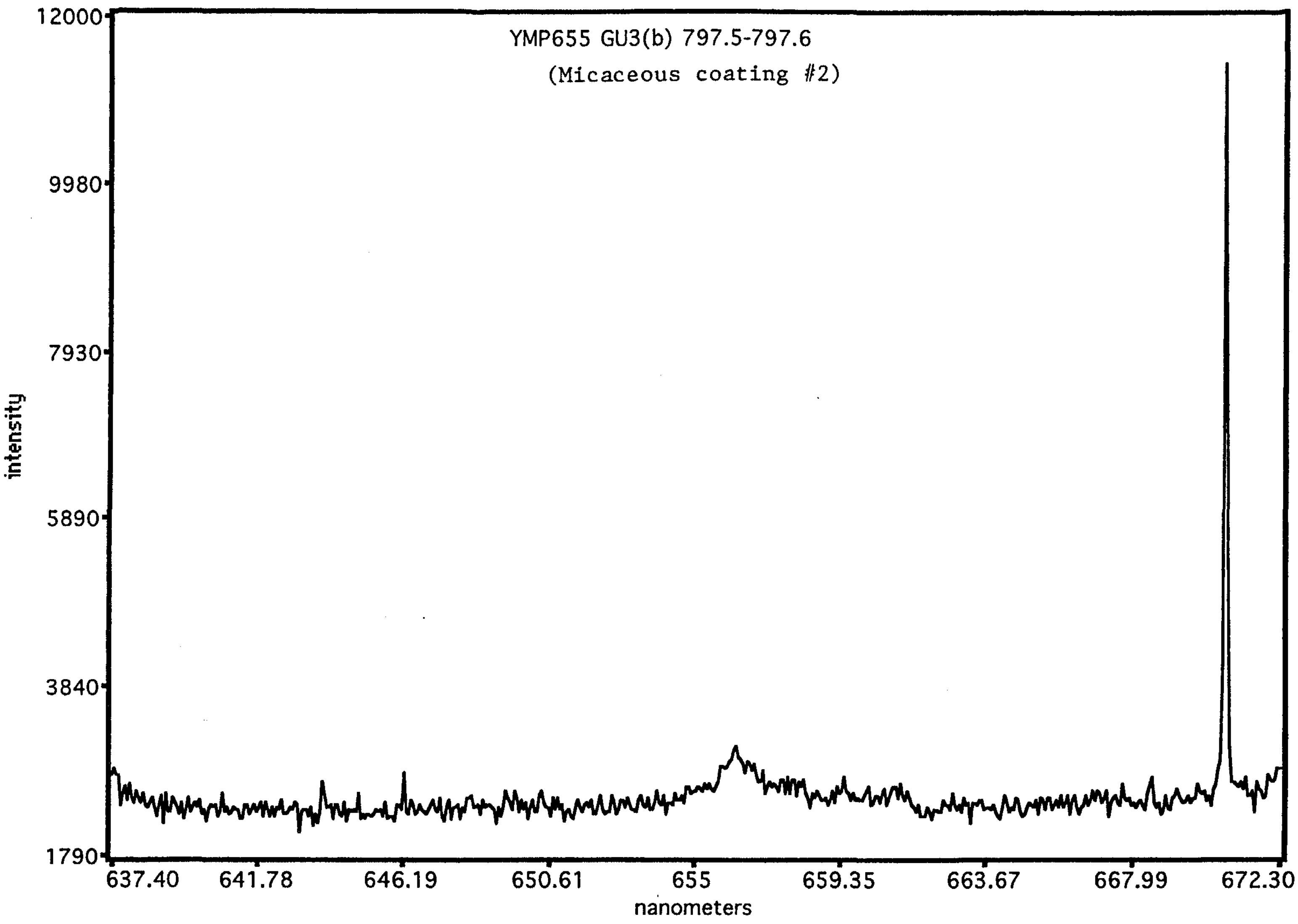
YMP655 GU3(b) 797.5-797.6
(Micaceous coating #2)
12000
9980
7930
5890
3840
1790
intensity
637.40
641.78
646.19
650.61
655
659.35
663.67
667.99
672.30
nanometers

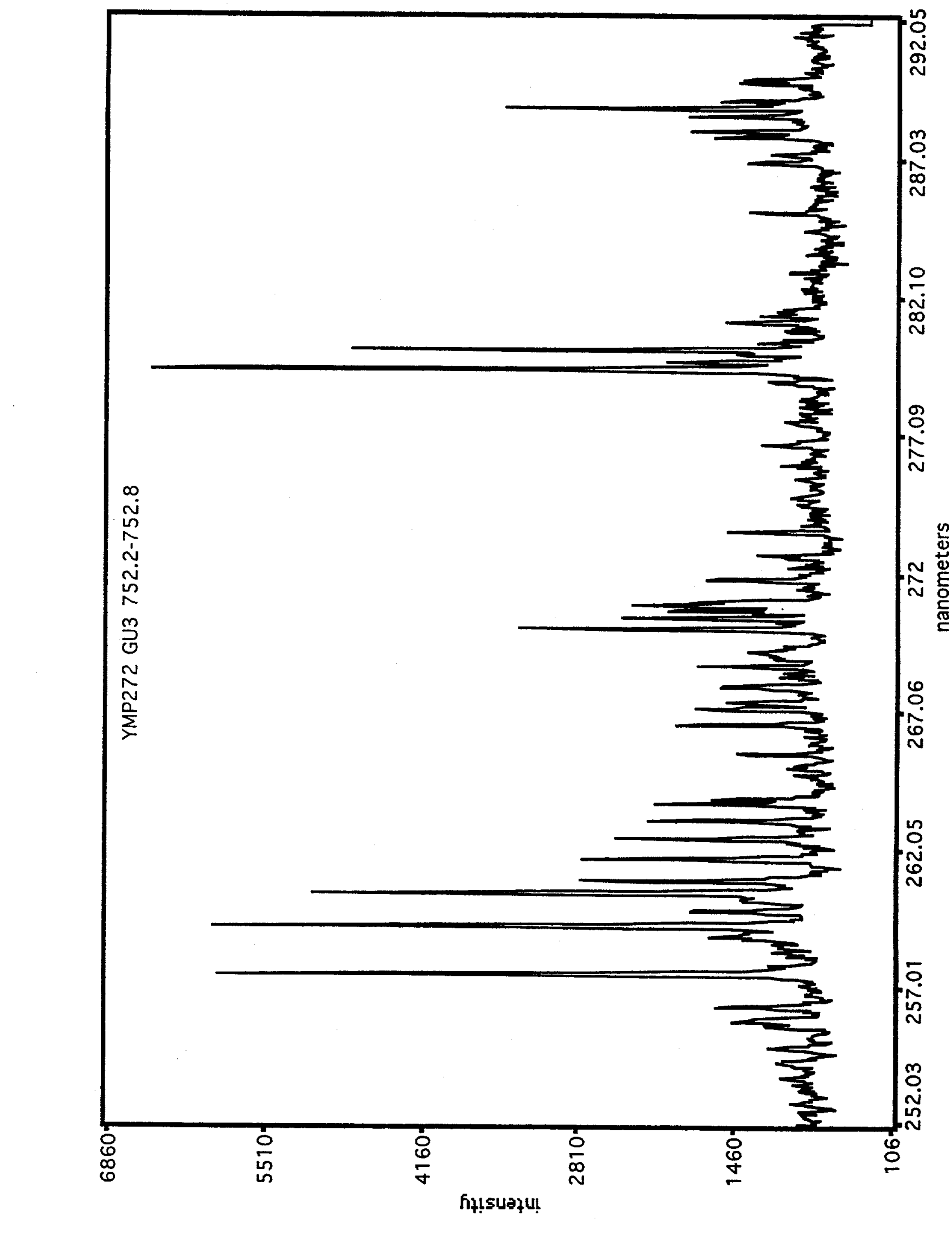
YMP272 GU3 752.2-752.8
intensity
6860
5510
4160
2810
1460
106
nanometers
252.03
257.01
262.05
267.06
272
277.09
282.10
287.03
292.05

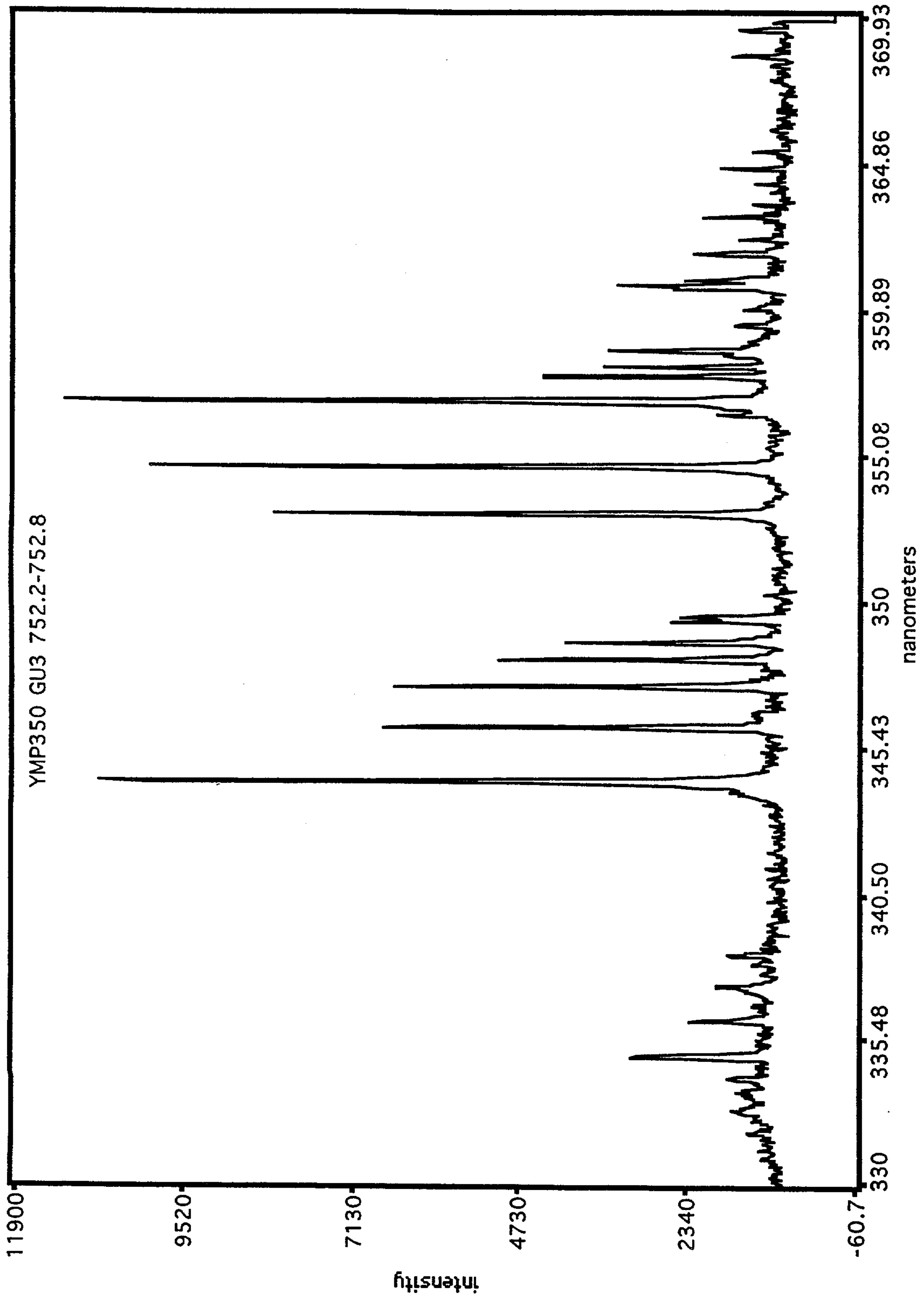
YMP350 GU3 752.2-752.8
intensity
11900
9520
7130
4730
2340
-60.7
nanometers
330
335.48
340.50
345.43
350
355.08
359.89
364.86
369.93

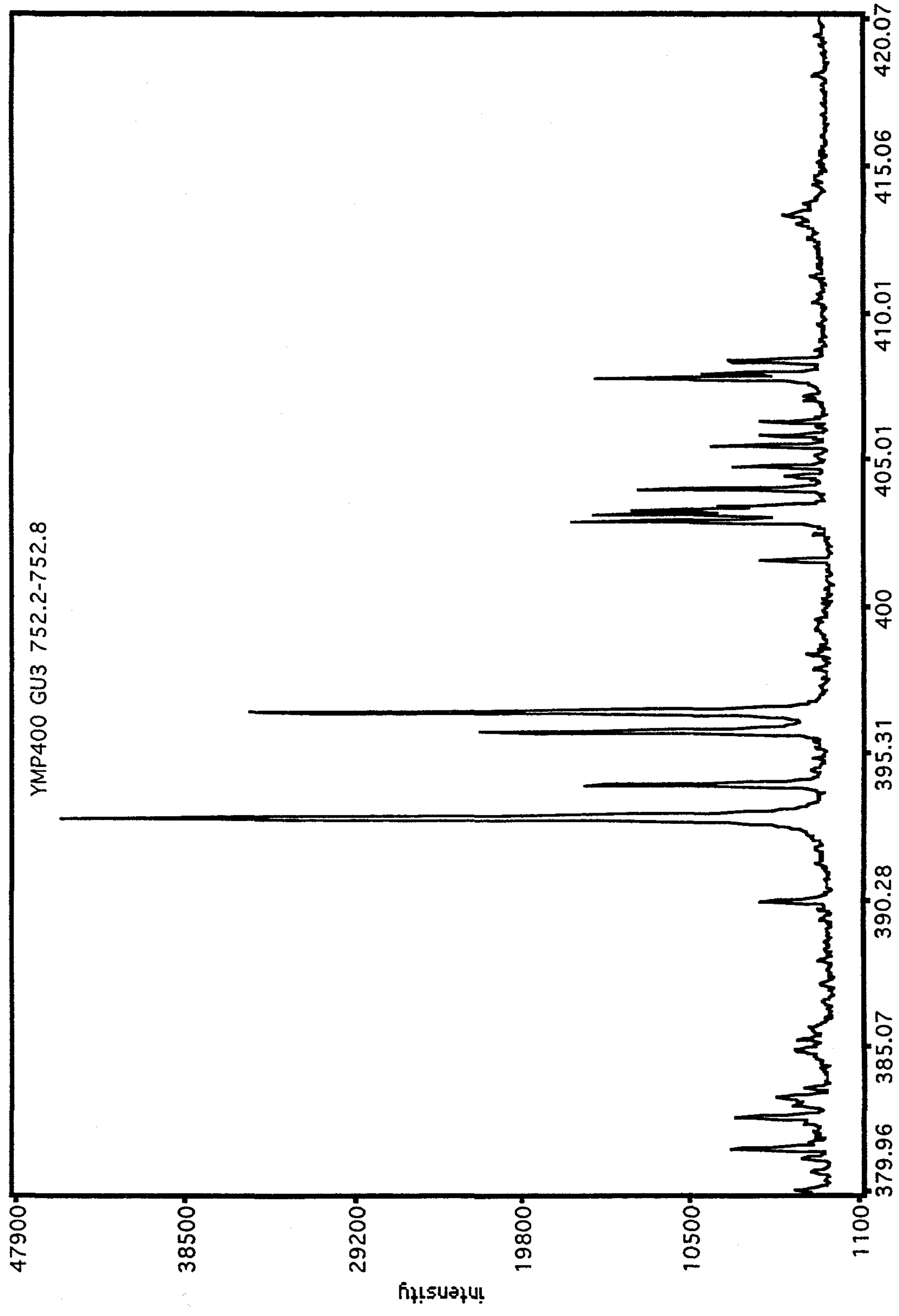
YMP400 GU3 752.2-752.8
intensity
47900
38500
29200
19800
10500
1100
nanometers
379.96
385.07
390.28
395.31
400
405.01
410.01
415.06
420.07

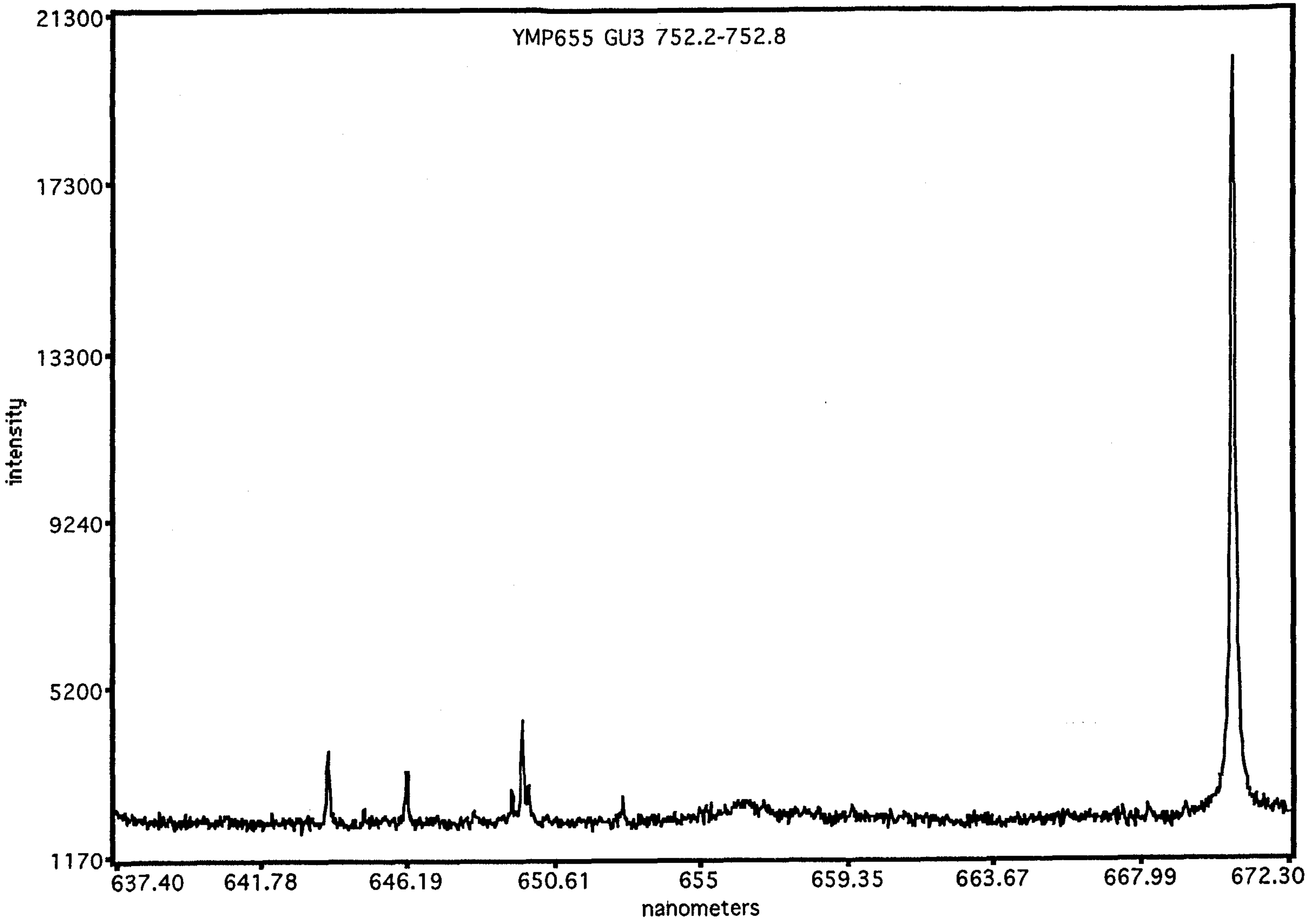
YMP655 GU3 752.2-752.8
intensity
21300
17300
13300
9240
5200
1170
637.40
641.78
646.19
650.61
655
659.35
663.67
667.99
672.30
nanometers

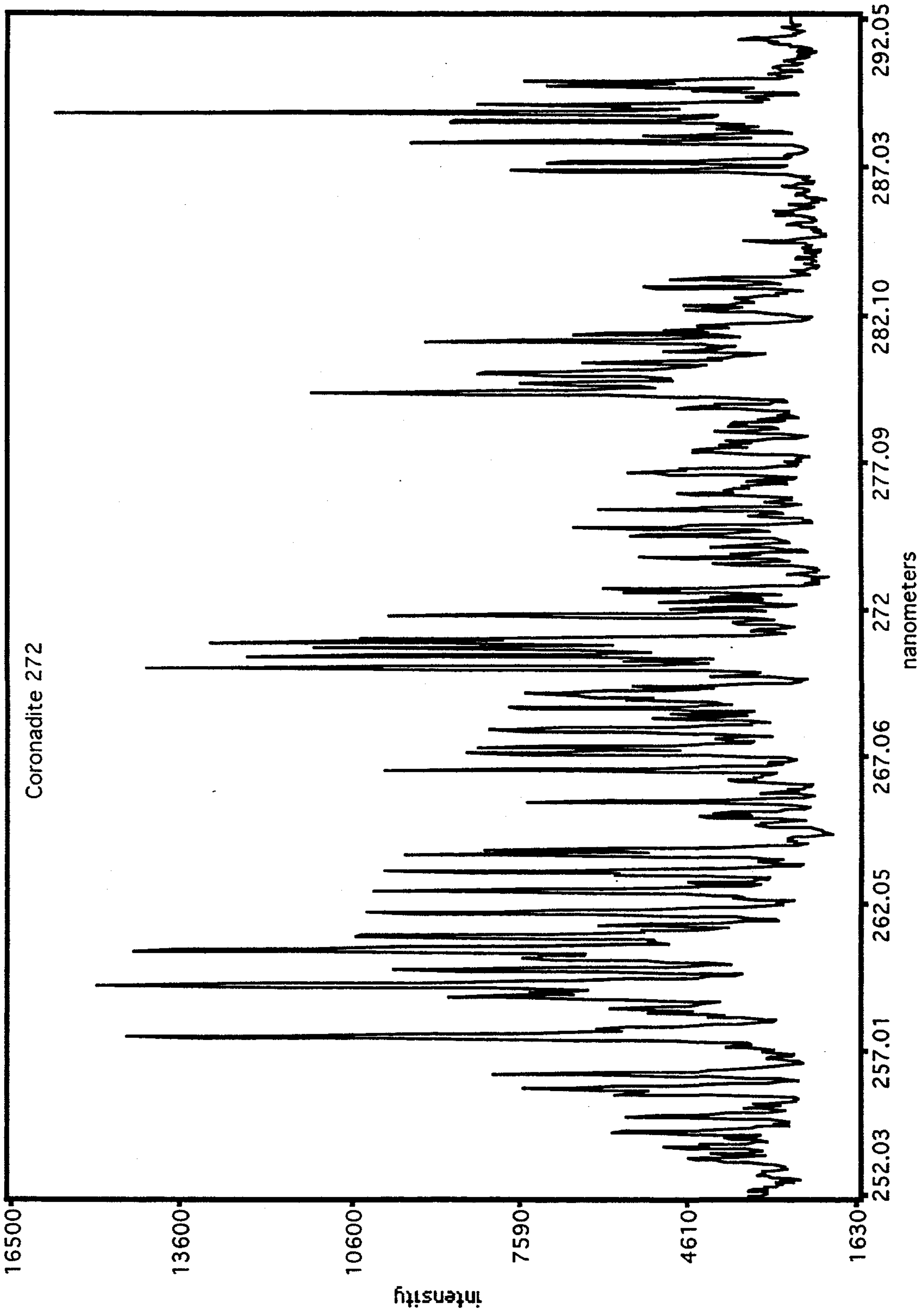
Coronadite 272
intensity
16500
13600
10600
7590
4610
1630
252.03
257.01
262.05
267.06
272
277.09
282.10
287.03
292.05
nanometers

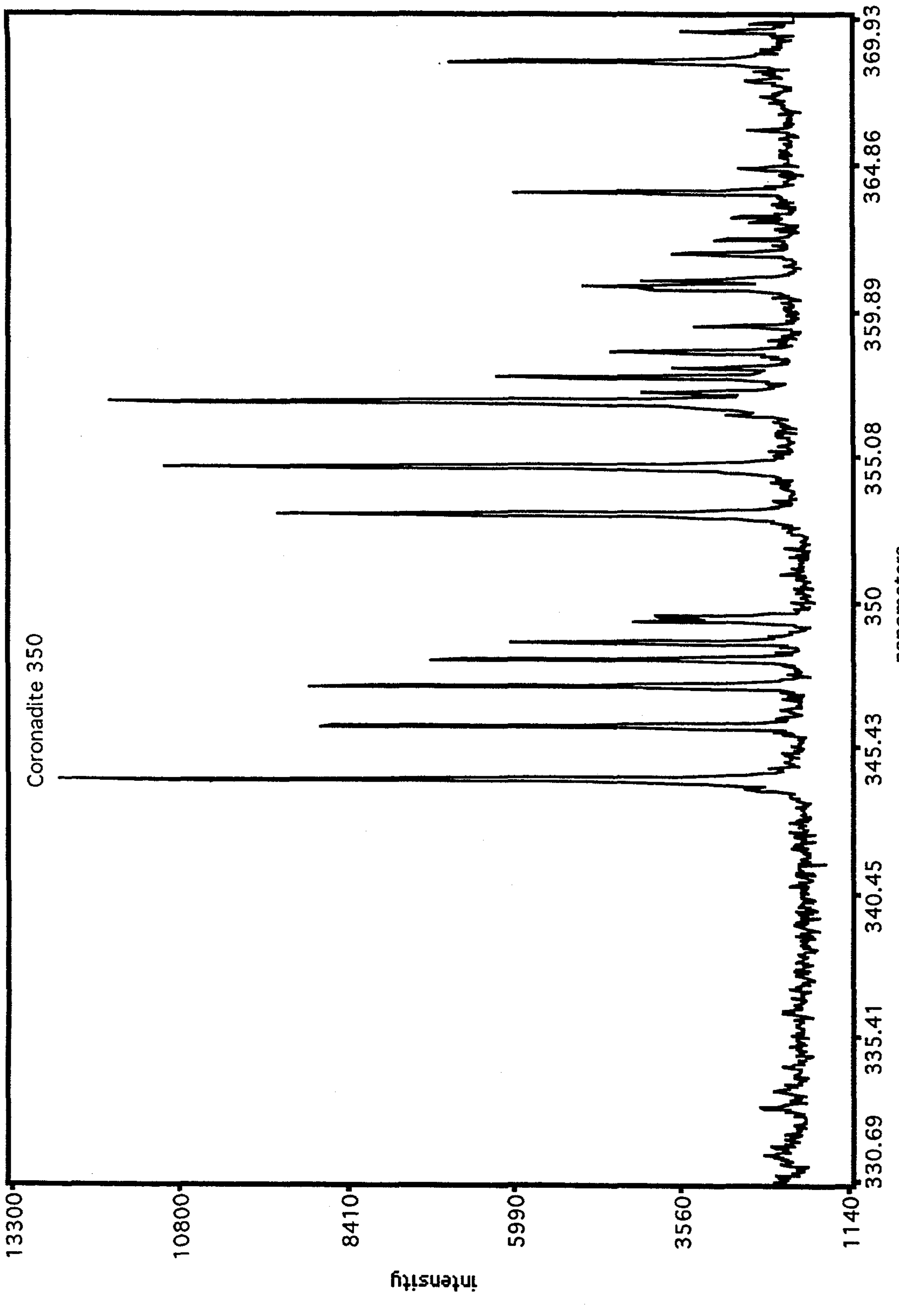
Coronadite 350
intensity
13300
10800
8410
5990
3560
1140
nanometers
330.69
335.41
340.45
345.43
350
355.08
359.89
364.86
369.93

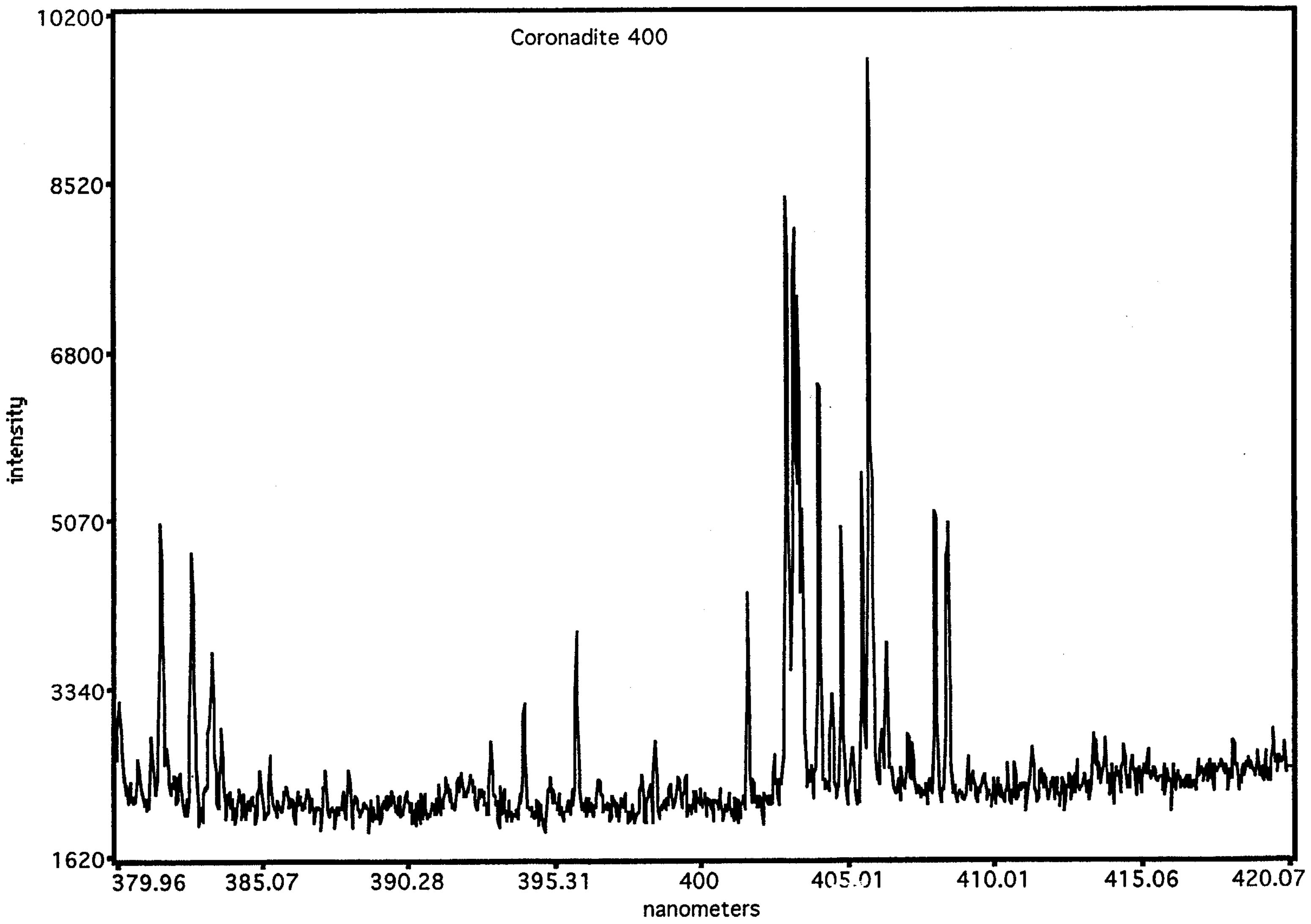
Coronadite 400
intensity
10200
8520
6800
5070
3340
1620
379.96
385.07
390.28
395.31
400
405.01
410.01
415.06
420.07
nanometers

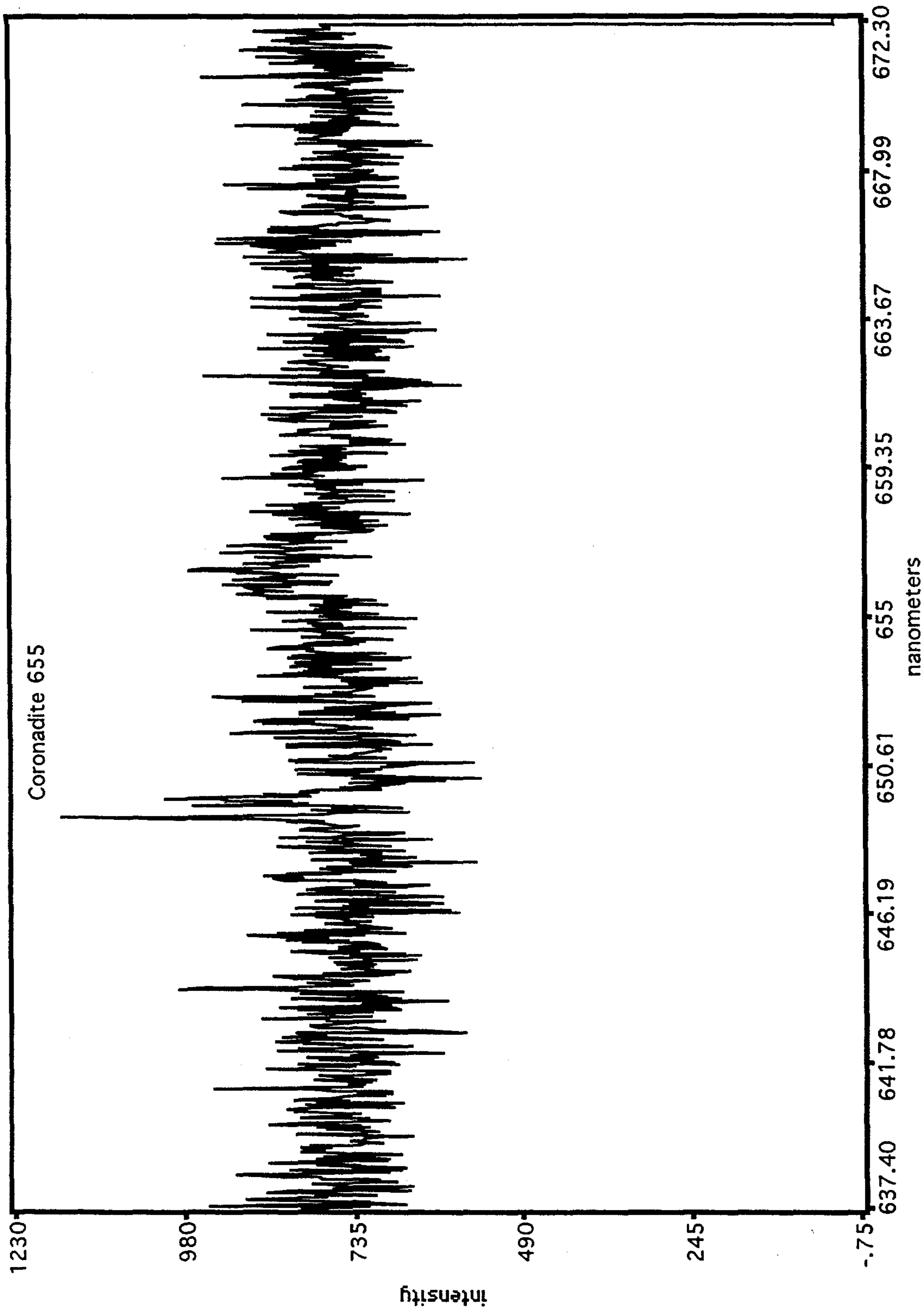
Coronadite 655
intensity
1230
980
735
490
245
-.75
nanometers
637.40
641.78
646.19
650.61
655
659.35
663.67
667.99
672.30

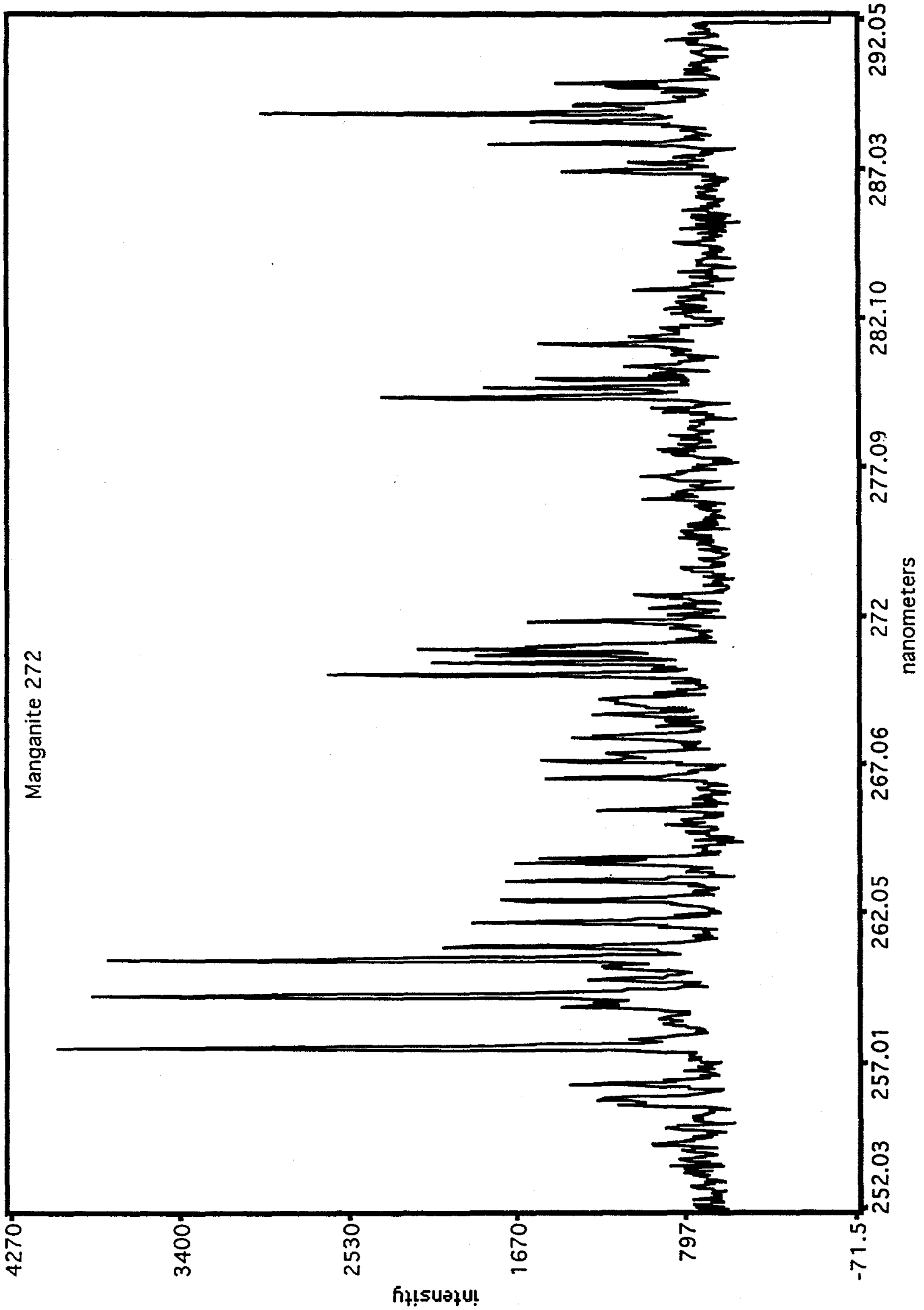
Manganite 272
intensity
4270
3400
2530
1670
797
-71.5
nanometers
252.03
257.01
262.05
267.06
272
277.09
282.10
287.03
292.05

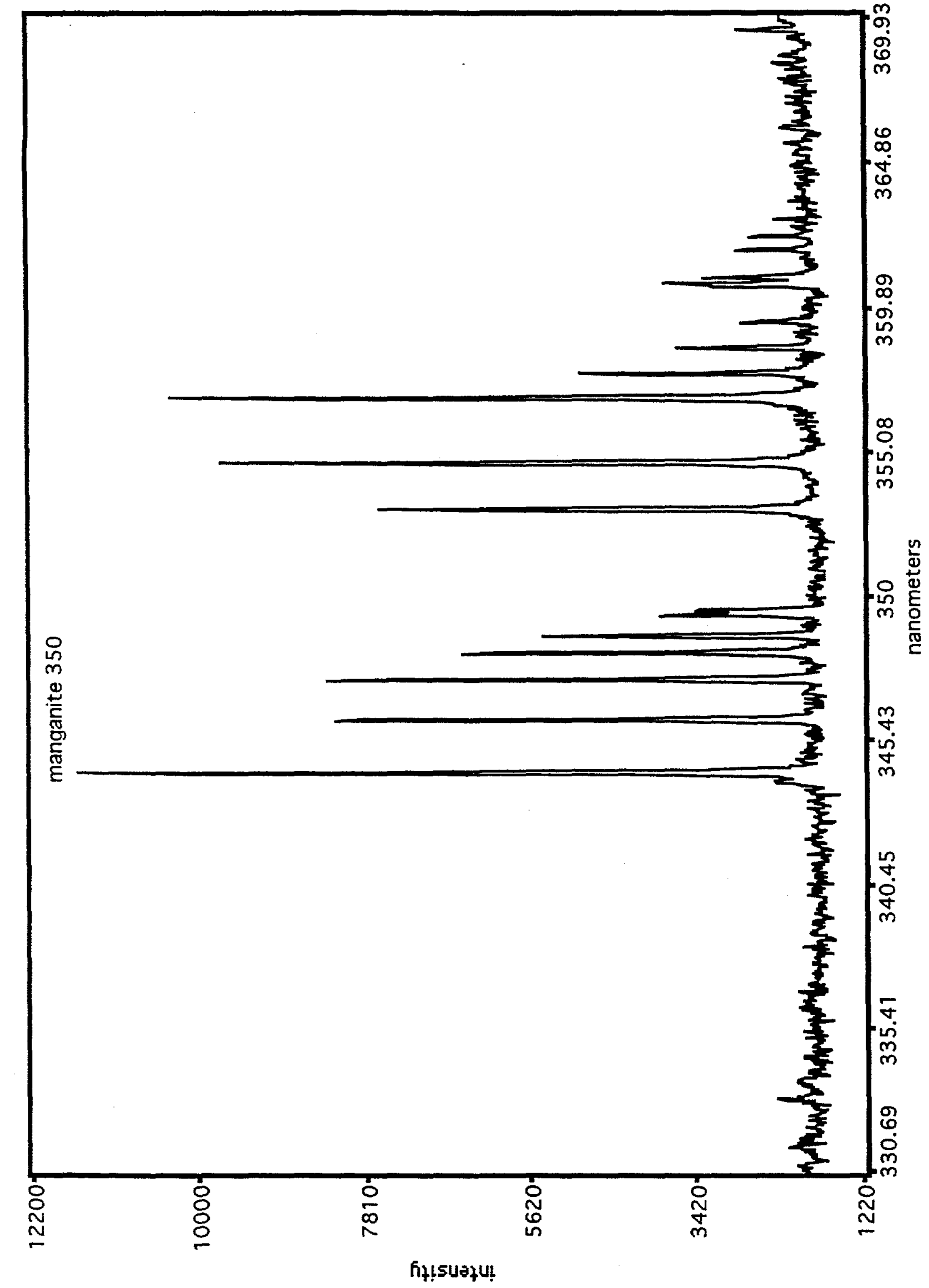
manganite 350
intensity
12200
10000
7810
5620
3420
1220
nanometers
330.69
335.41
340.45
345.43
350
355.08
359.89
364.86
369.93

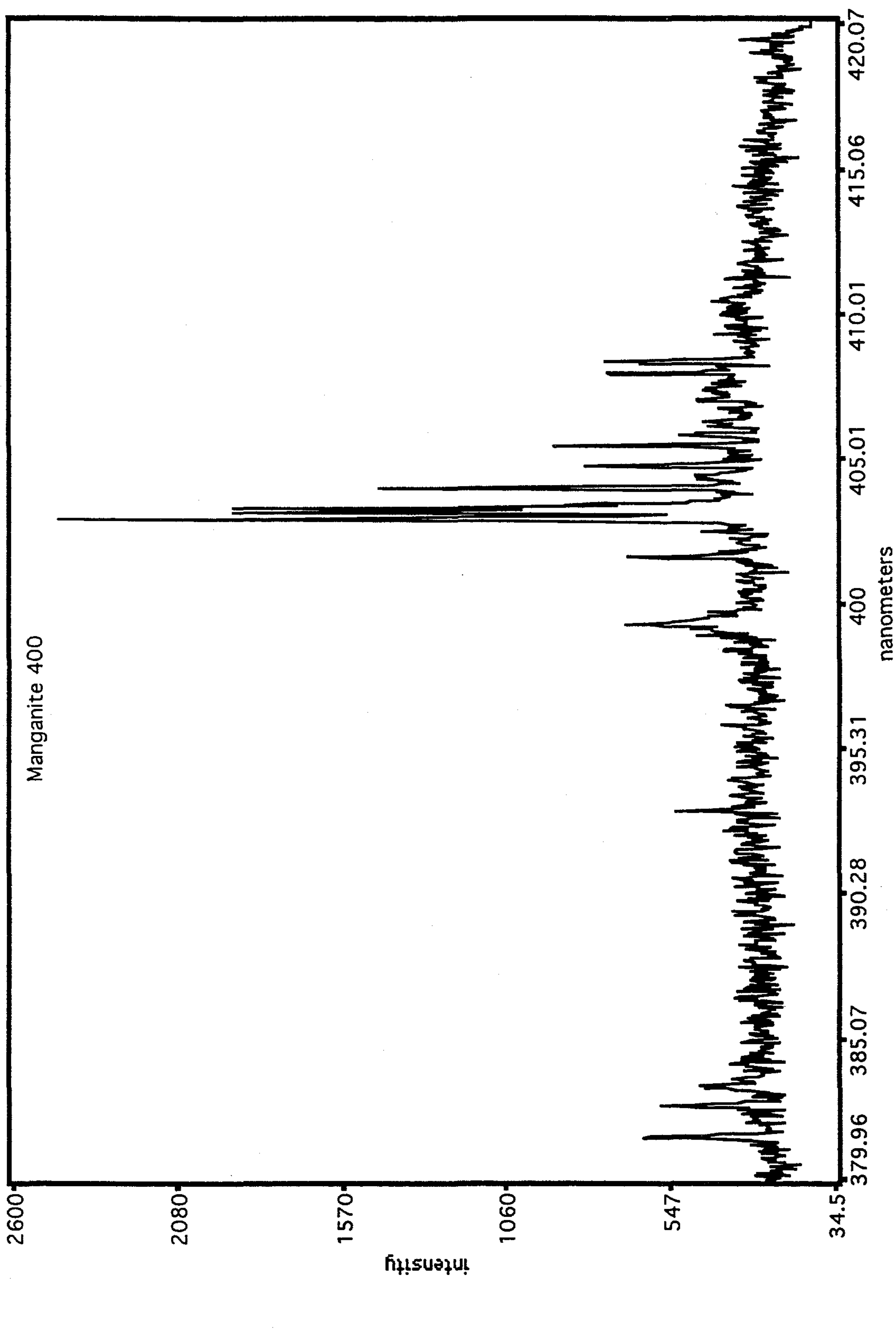
Manganite 400
intensity
2600
2080
1570
1060
547
34.5
nanometers
379.96
385.07
390.28
395.31
400
405.01
410.01
415.06
420.07

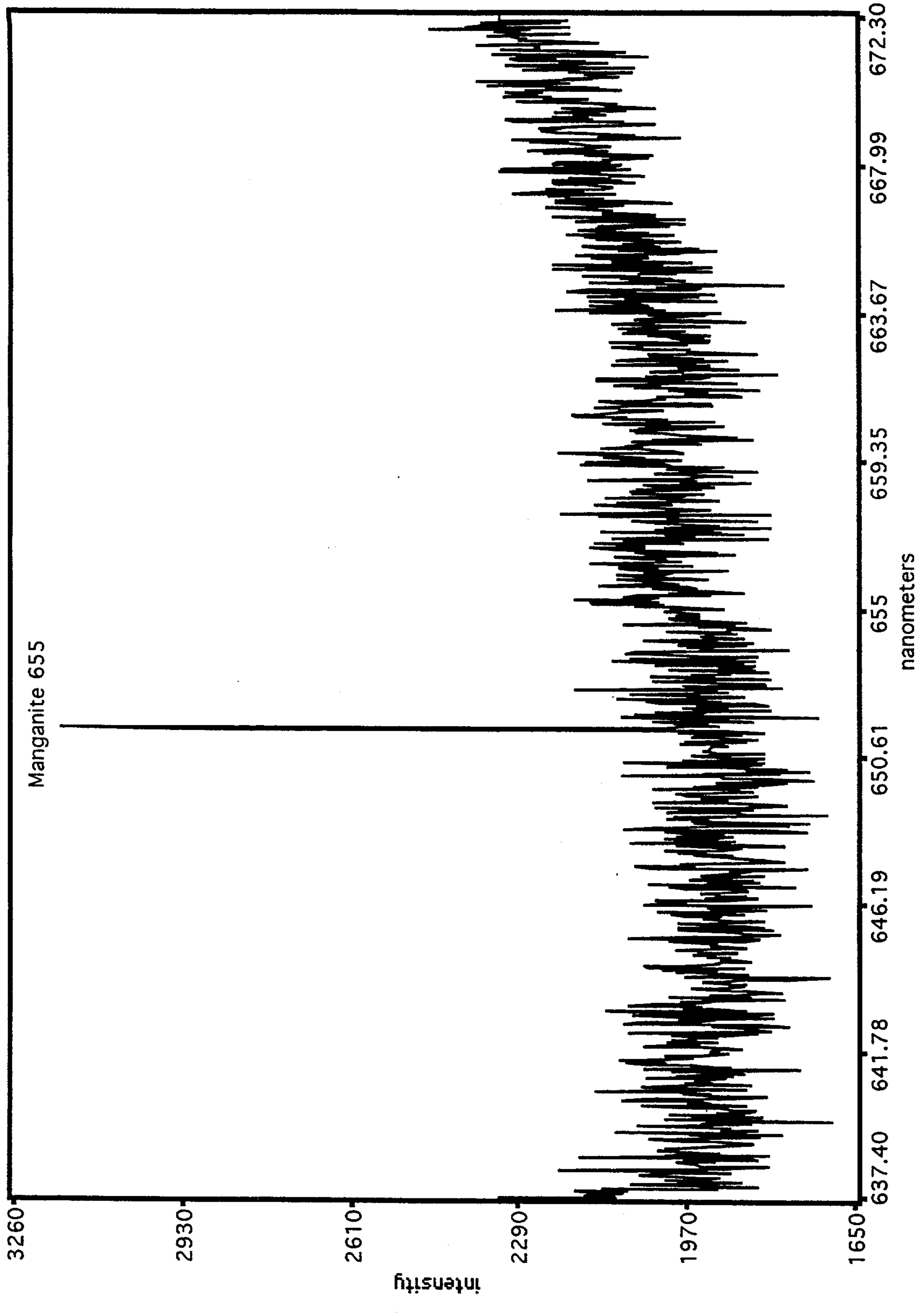
Manganite 655
intensity
3260
2930
2610
2290
1970
1650
nanometers
637.40
641.78
646.19
650.61
655
659.35
663.67
667.99
672.30

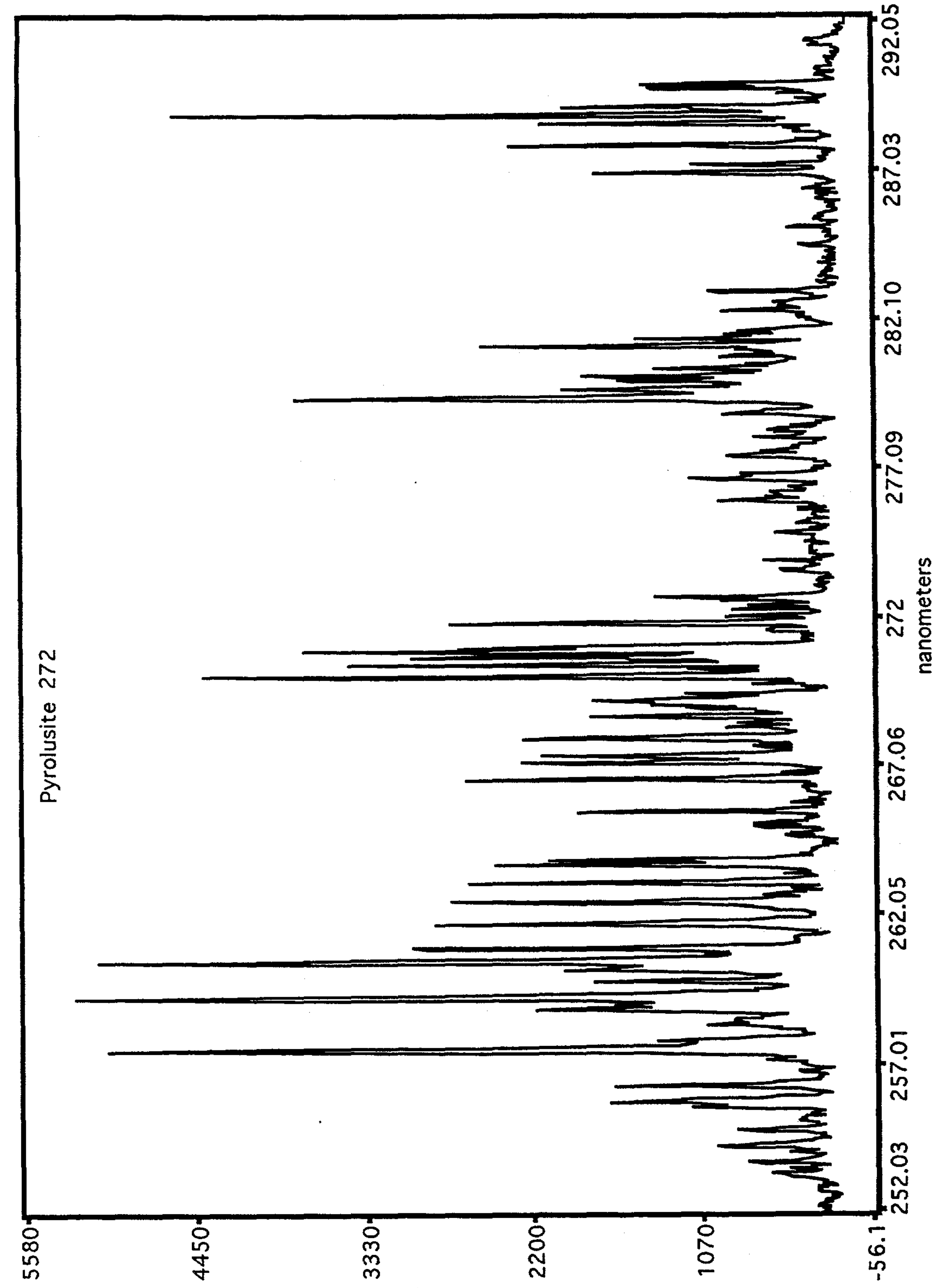
Pyrolusite 272
intensity
5580
4450
3330
2200
1070
-56.1
252.03
257.01
262.05
267.06
272
277.09
282.10
287.03
292.05
nanometers

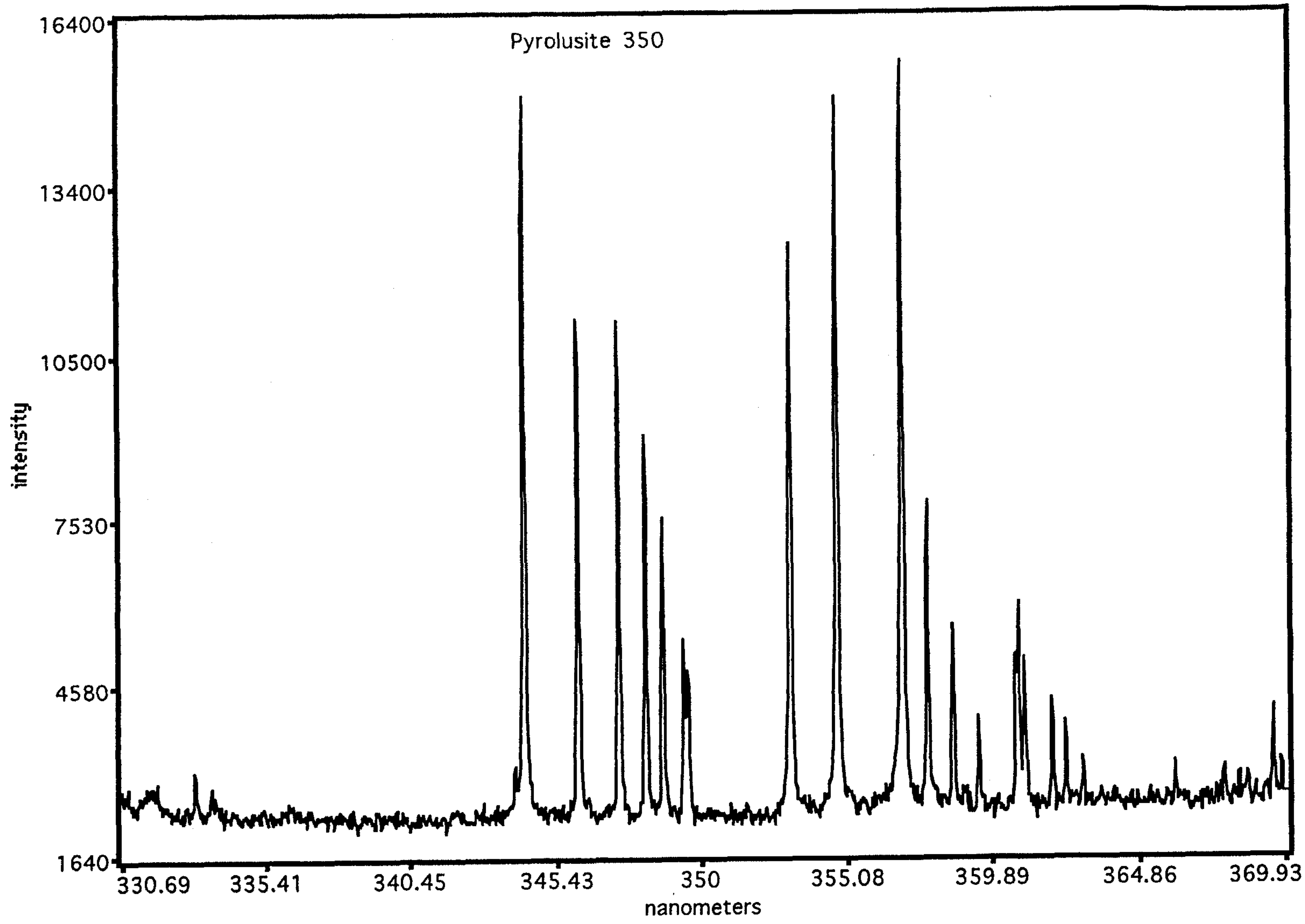
Pyrolusite 350
intensity
16400
13400
10500
7530
4580
1640
330.69
335.41
340.45
345.43
350
355.08
359.89
364.86
369.93
nanometers

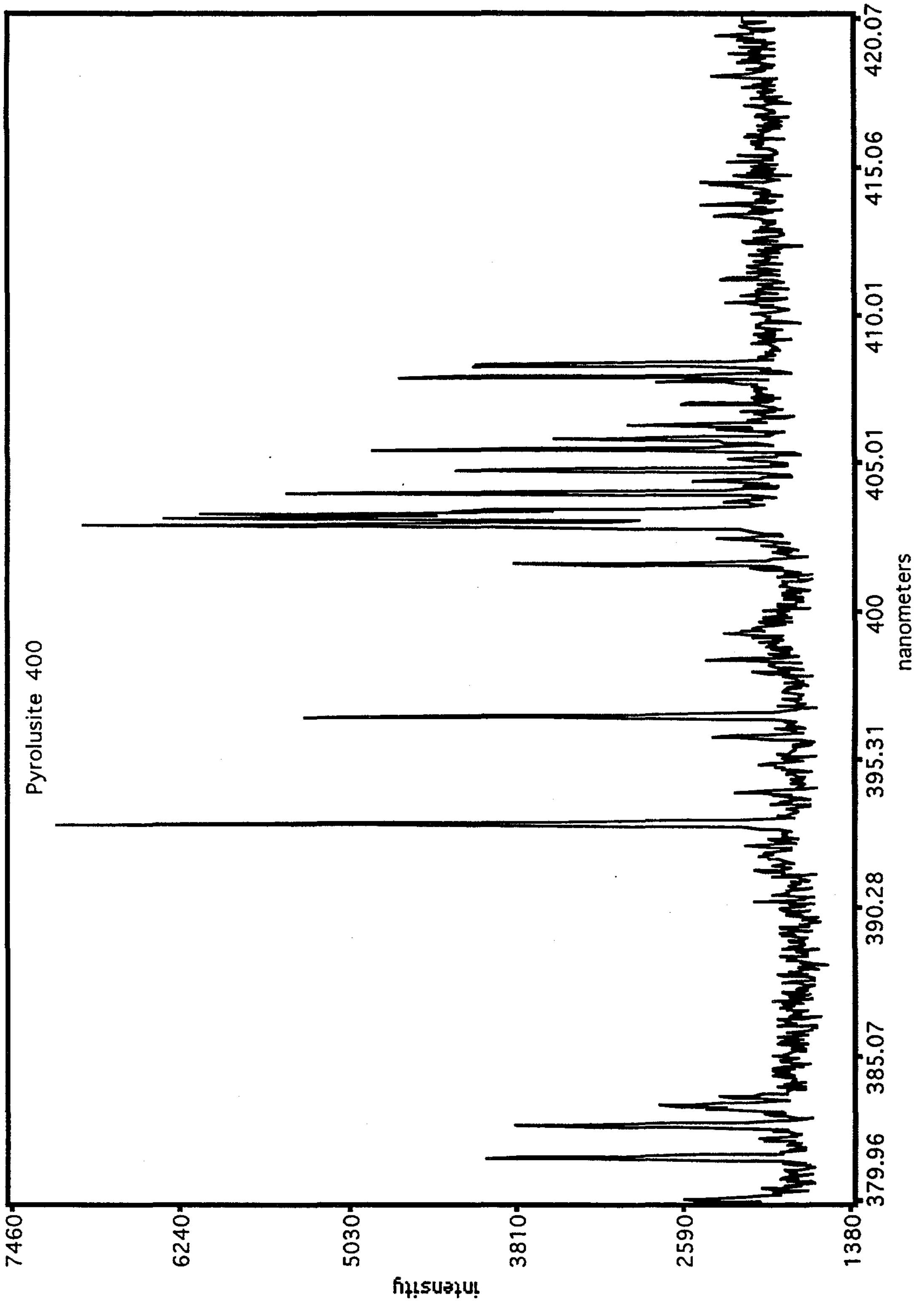
Pyrolusite 400
intensity
7460
6240
5030
3810
2590
1380
nanometers
379.96
385.07
390.28
395.31
400
405.01
410.01
415.06
420.07

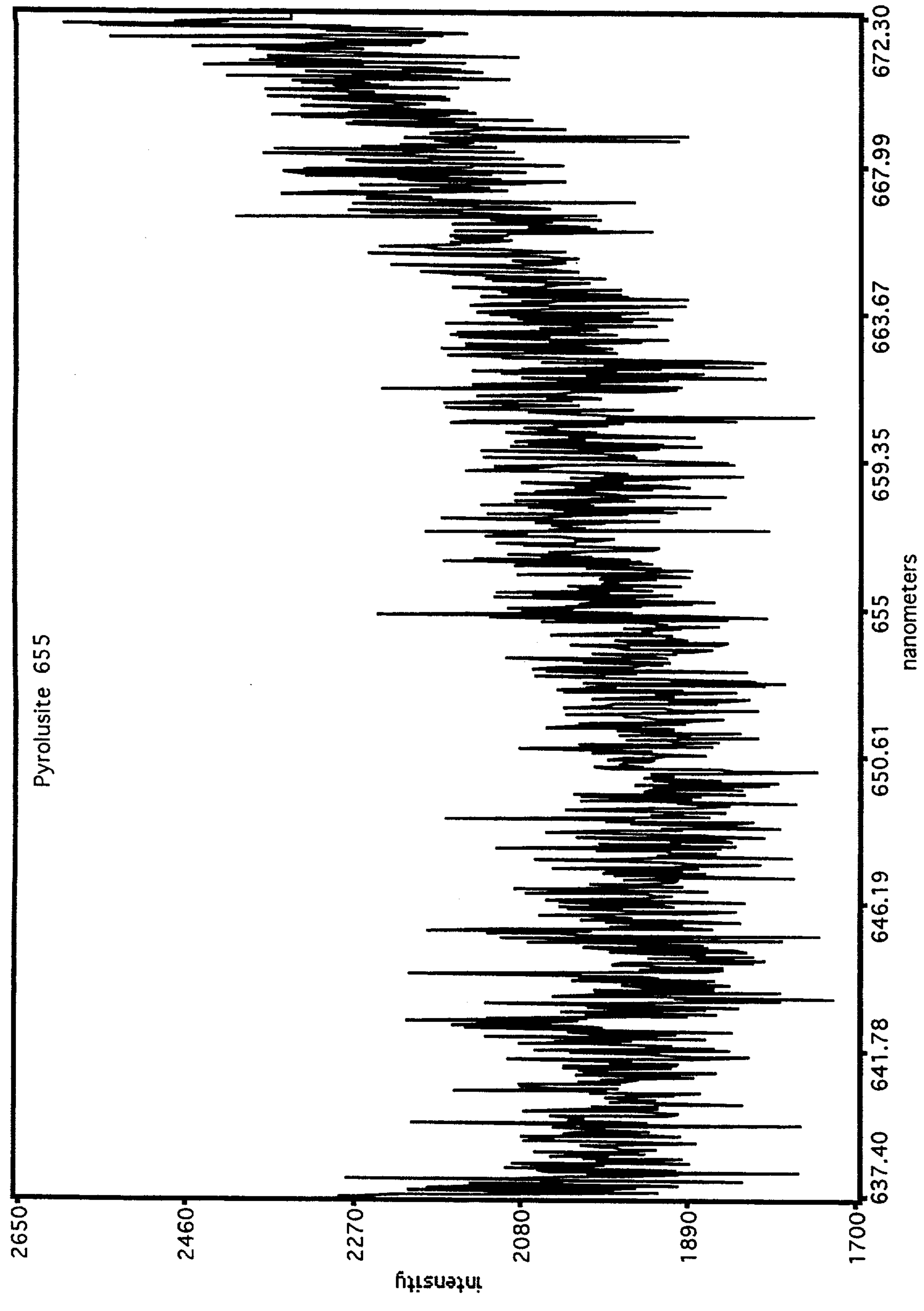
Pyrolusite 655
intensity
2650
2460
2270
2080
1890
1700
nanometers
637.40
641.78
646.19
650.61
655
659.35
663.67
667.99
672.30

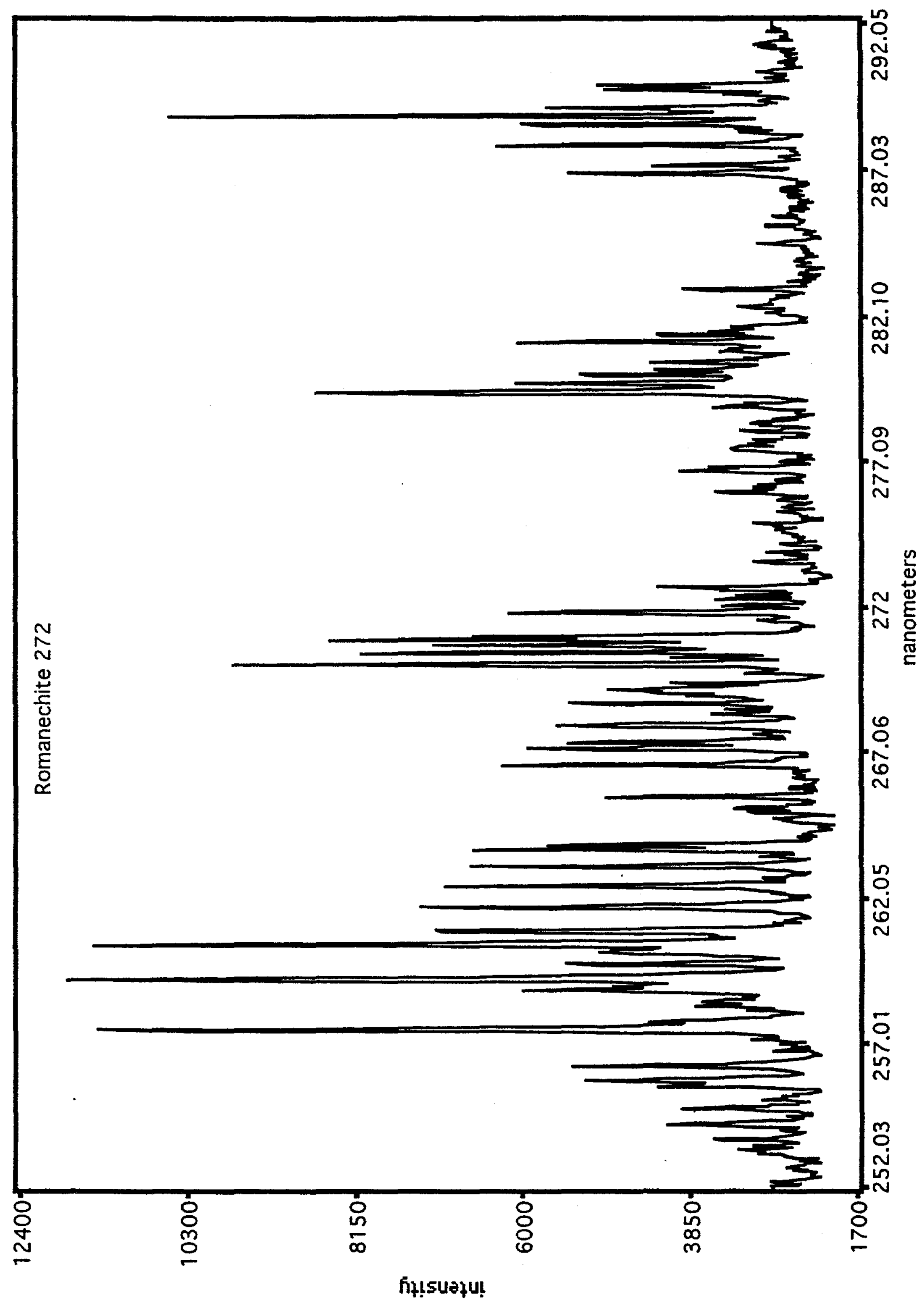
Romanechite 272
intensity
12400
10300
8150
6000
3850
1700
nanometers
252.03
257.01
262.05
267.06
272
277.09
282.10
287.03
292.05

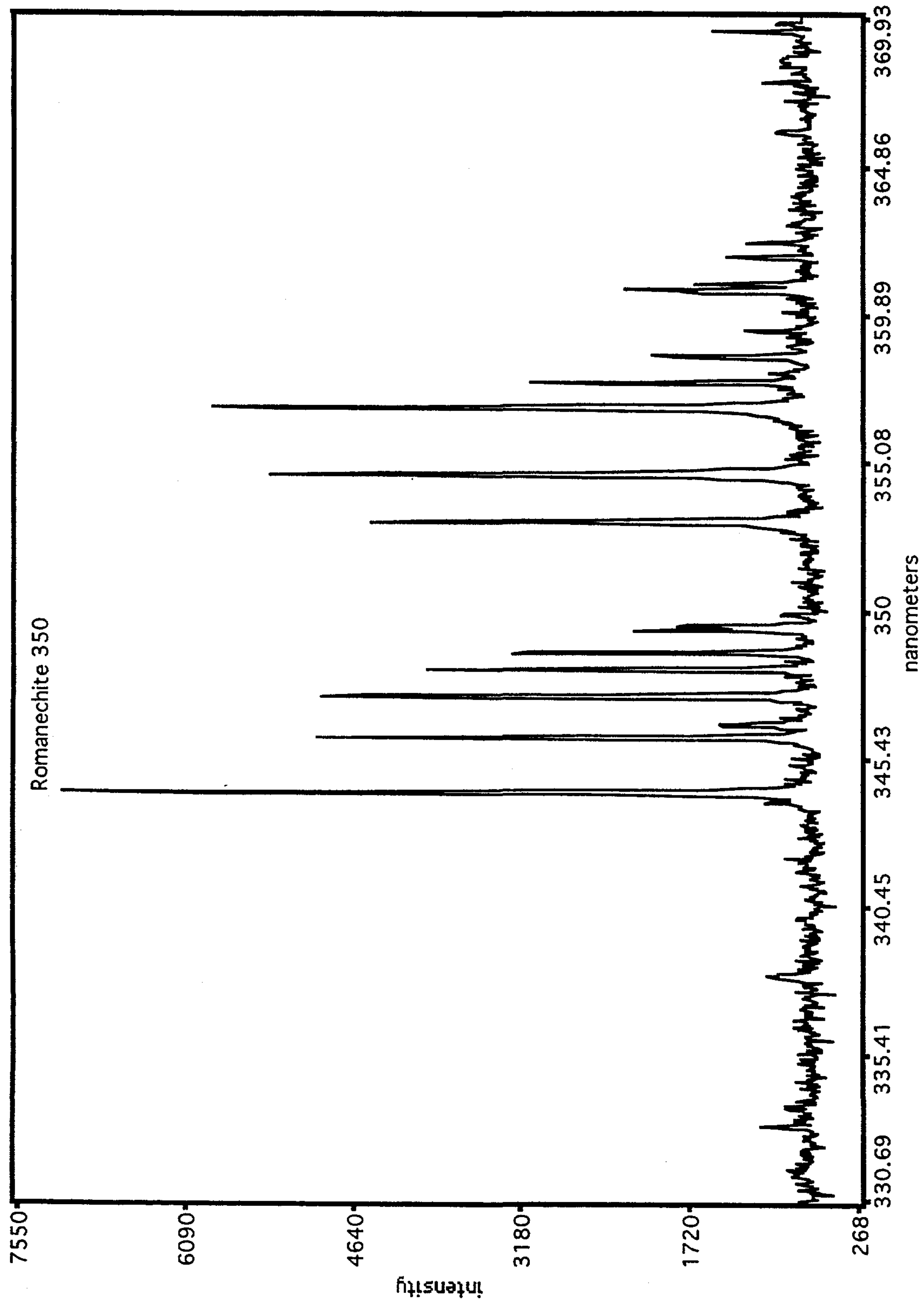
Romanechite 350
intensity
7550
6090
4640
3180
1720
268
330.69
335.41
340.45
345.43
350
355.08
359.89
364.86
369.93
nanometers

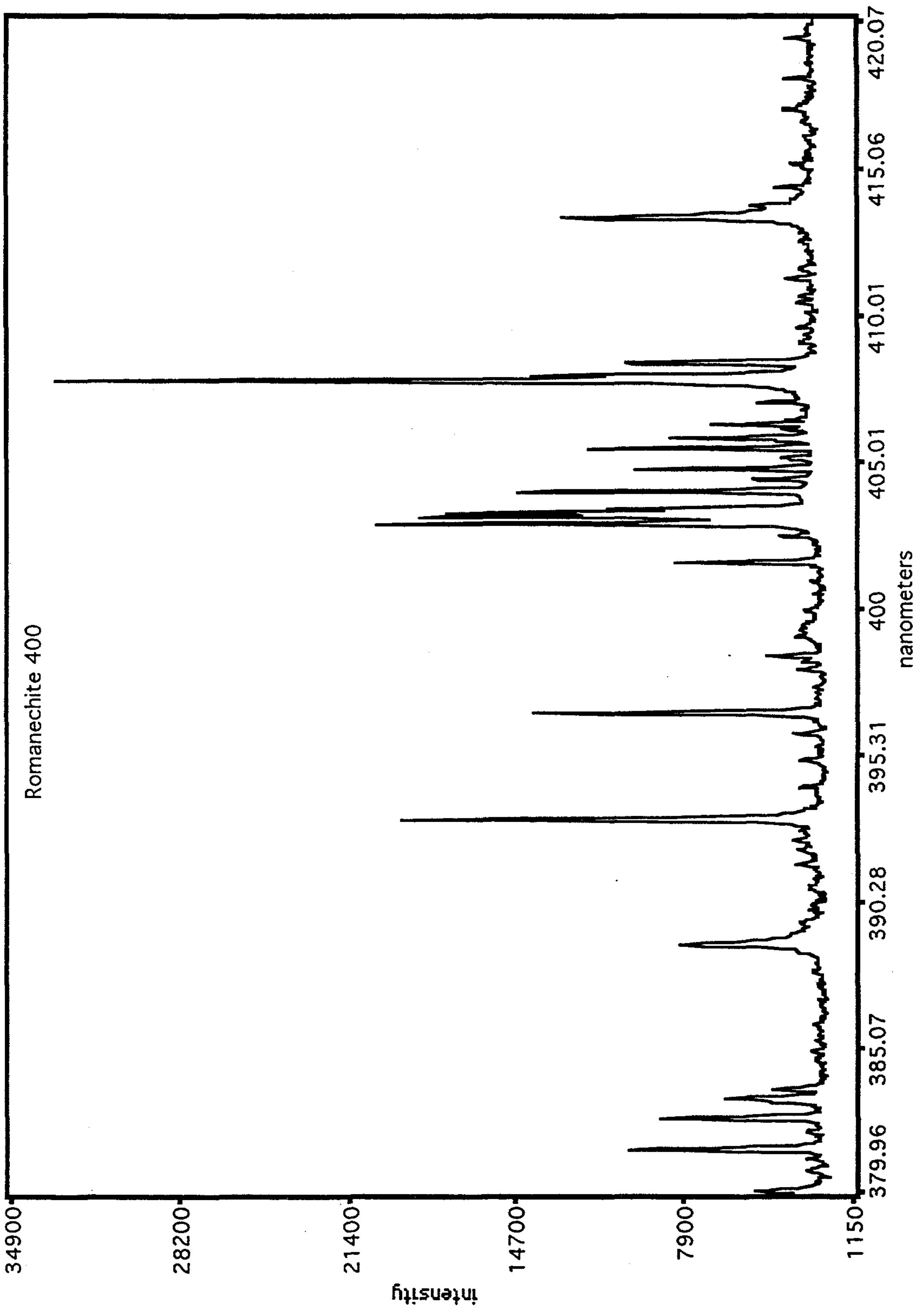
Romanechite 400
intensity
34900
28200
21400
14700
7900
1150
379.96
385.07
390.28
395.31
400
405.01
410.01
415.06
420.07
nanometers

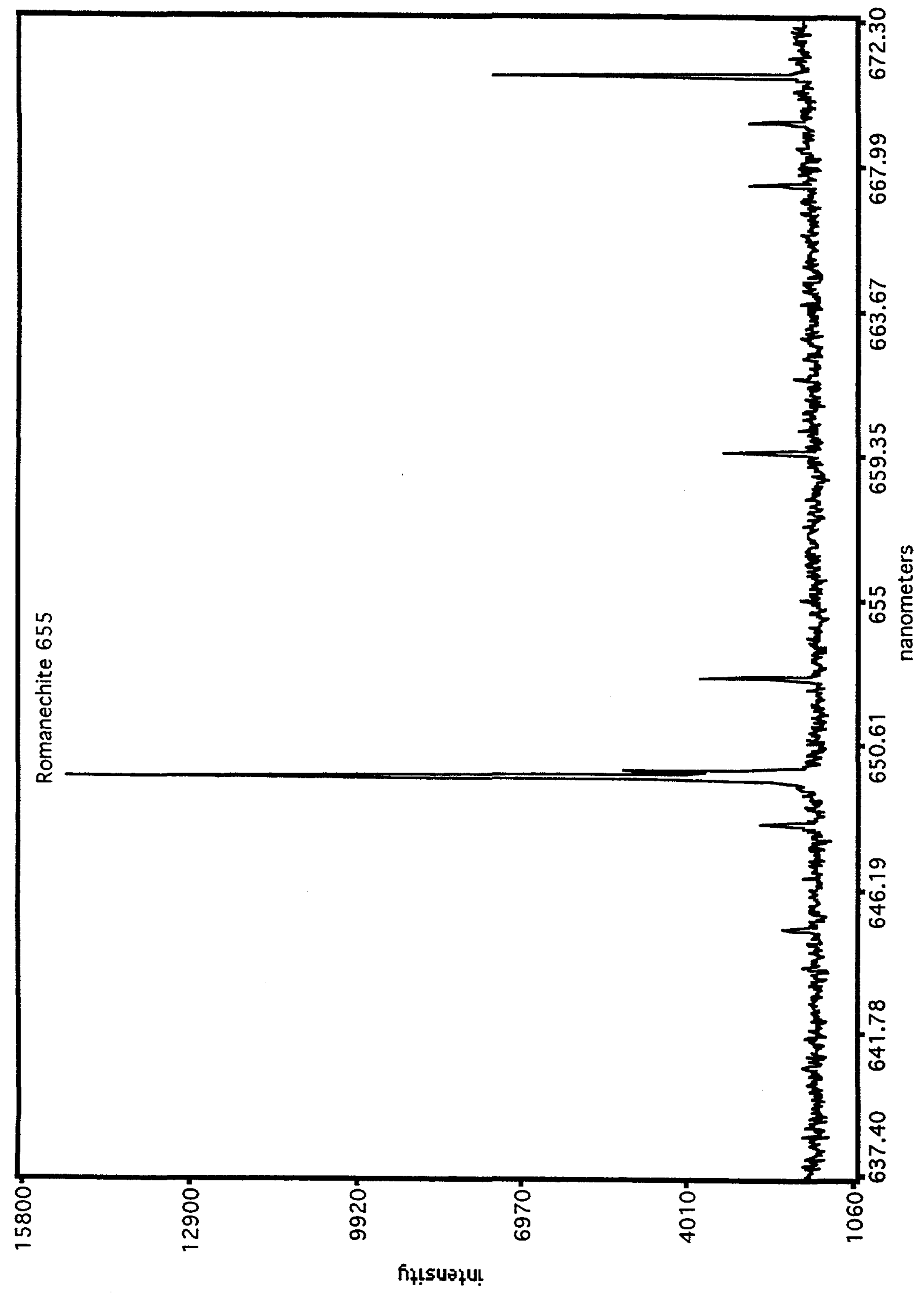
Romanechite 655
intensity
15800
12900
9920
6970
4010
1060
nanometers
637.40
641.78
646.19
650.61
655
659.35
663.67
667.99
672.30

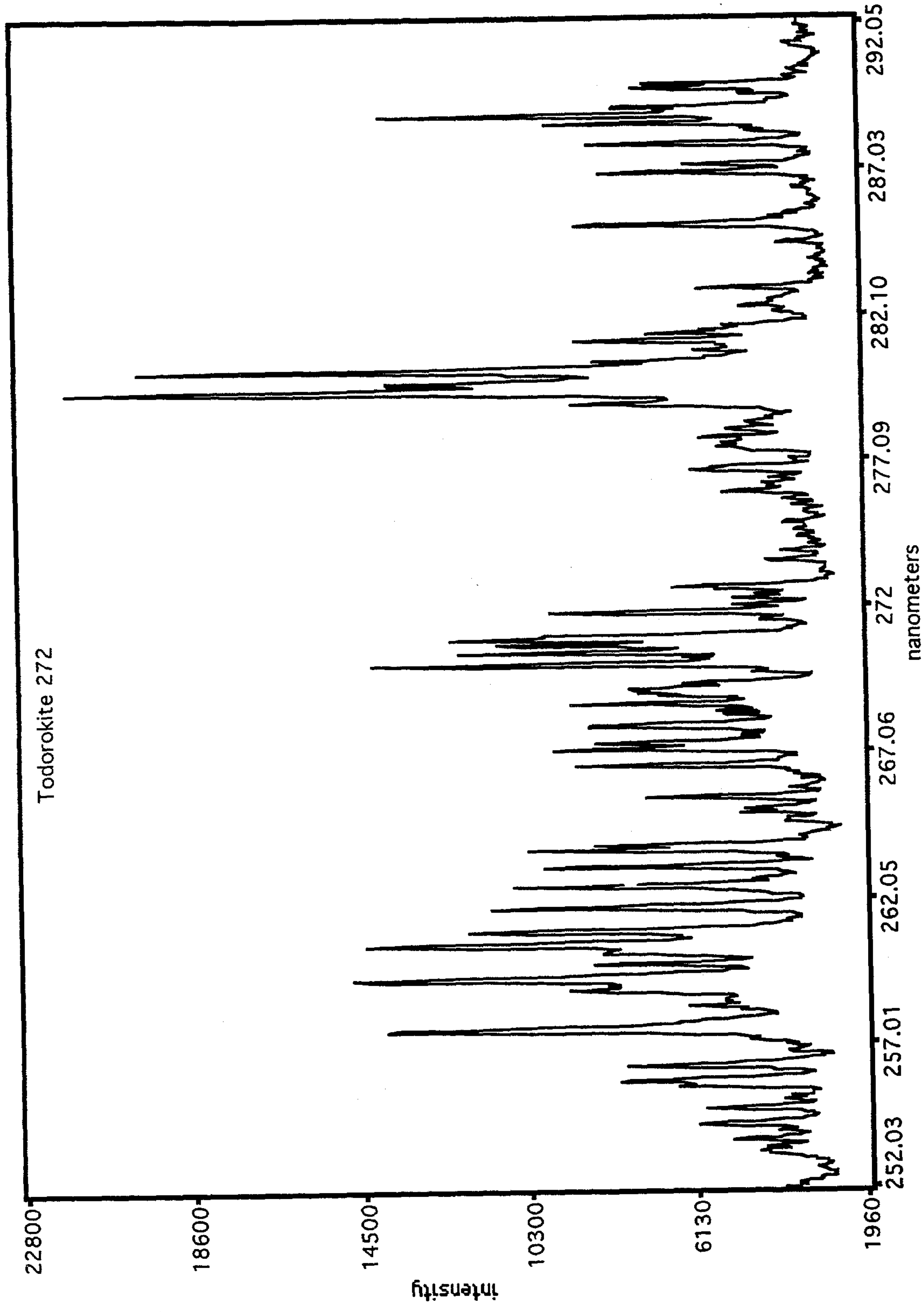
Todorokite 272
intensity
22800
18600
14500
10300
6130
1960
252.03
257.01
262.05
267.06
272
277.09
282.10
287.03
292.05
nanometers

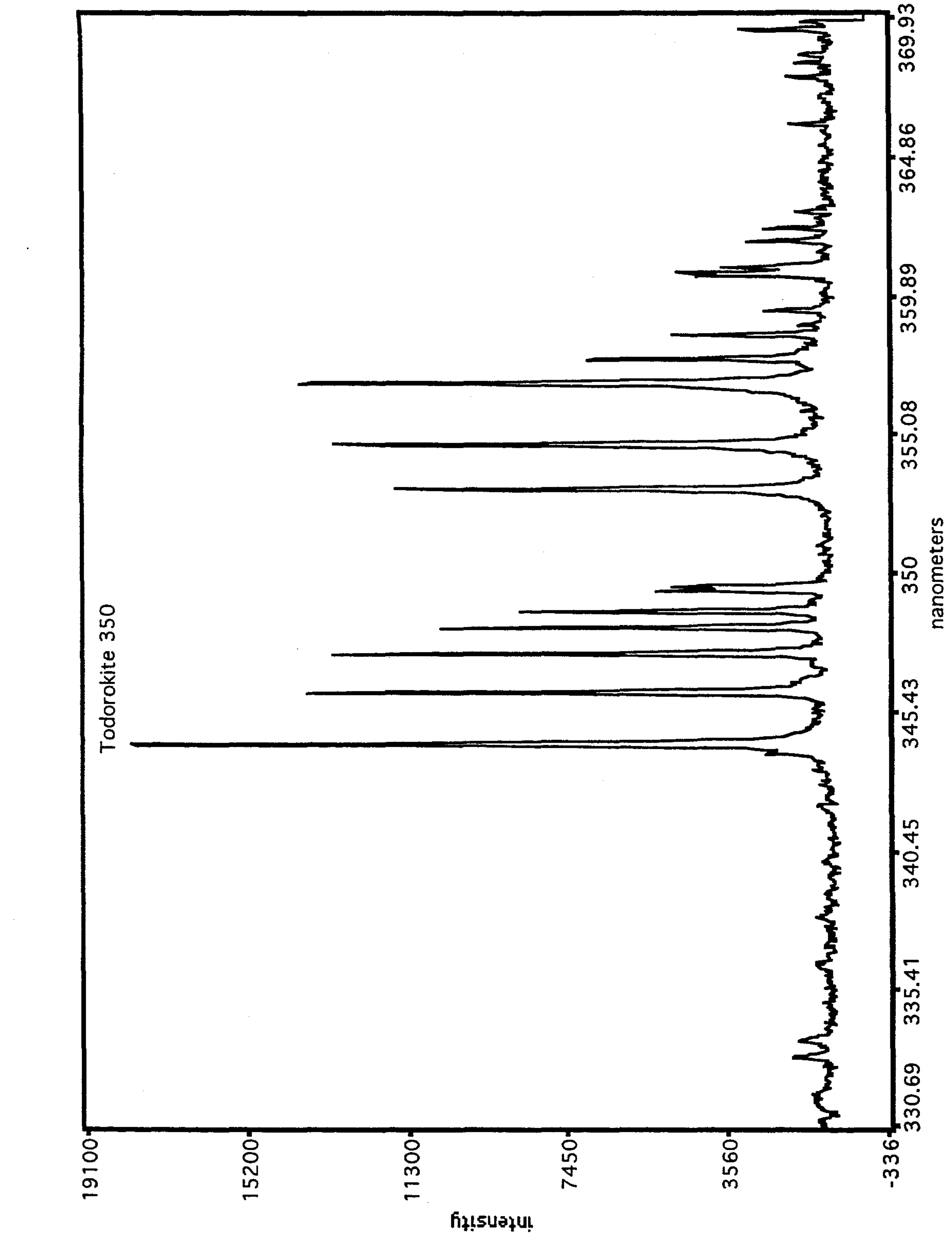
Todorokite 350
intensity
19100
15200
11300
7450
3560
-336
330.69
335.41
340.45
345.43
350
355.08
359.89
364.86
369.93
nanometers

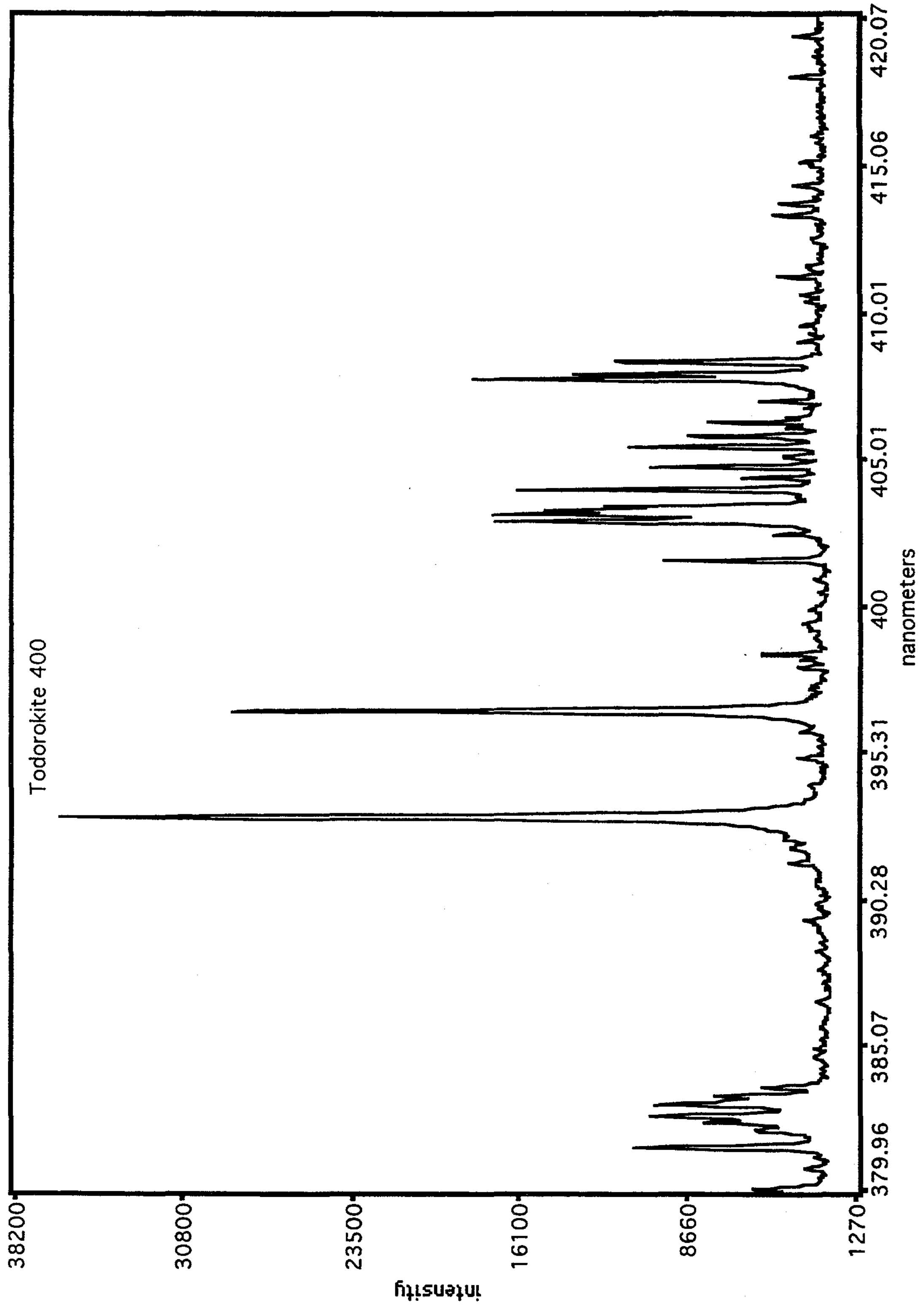
Todorokite 400
intensity
38200
30800
23500
16100
8660
1270
nanometers
379.96
385.07
390.28
395.31
400
405.01
410.01
415.06
420.07

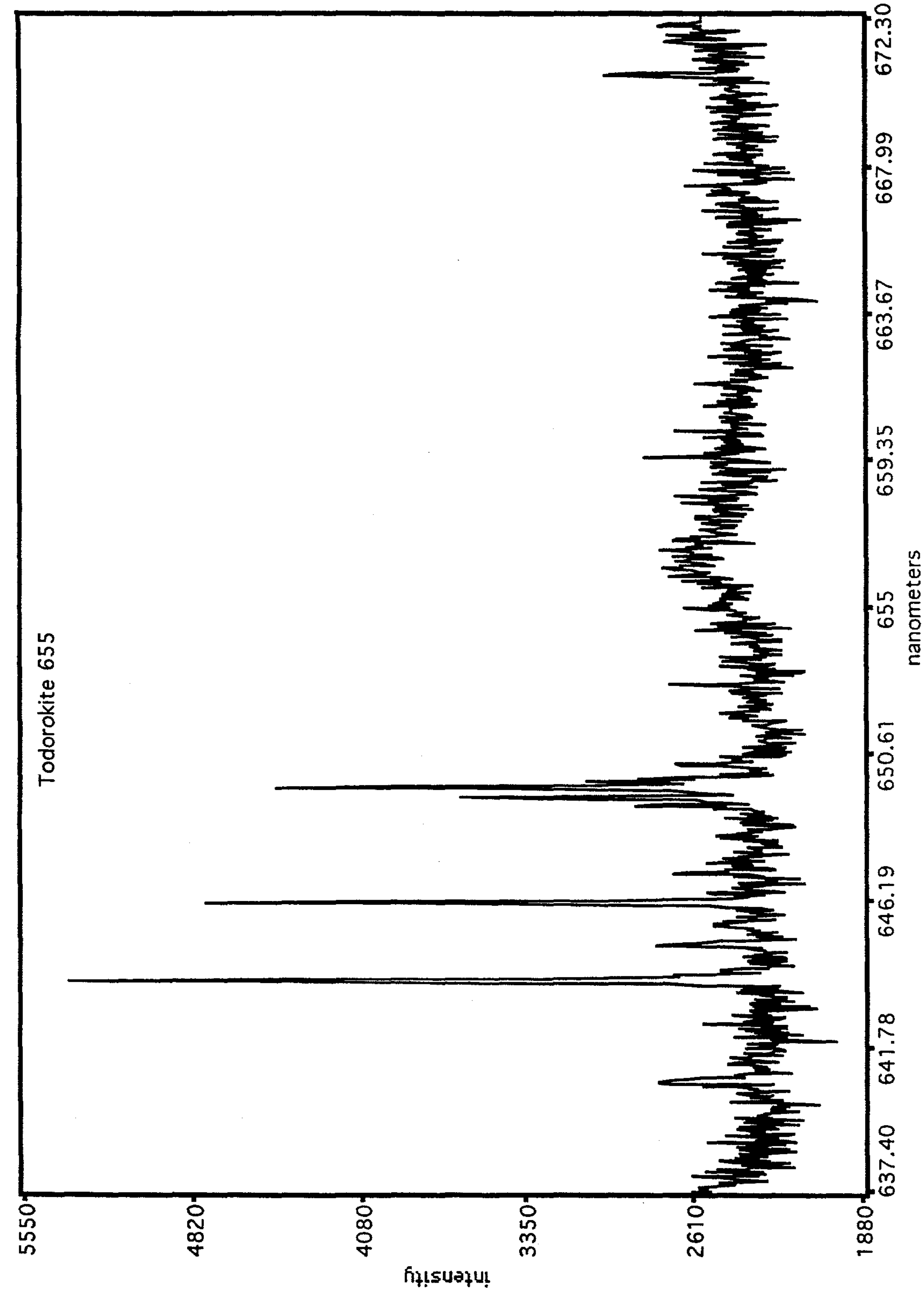
Todorokite 655
intensity
5550
4820
4080
3350
2610
1880
nanometers
637.40
641.78
646.19
650.61
655
659.35
663.67
667.99
672.30

APPENDIX II: EMISSION LINE INTENSITY RATIOS

This appendix contains emission line intensities for selected elements (see text for specific line wavelengths), normalized to manganese line intensity, for all mineral standards and Yucca Mountain samples analyzed.

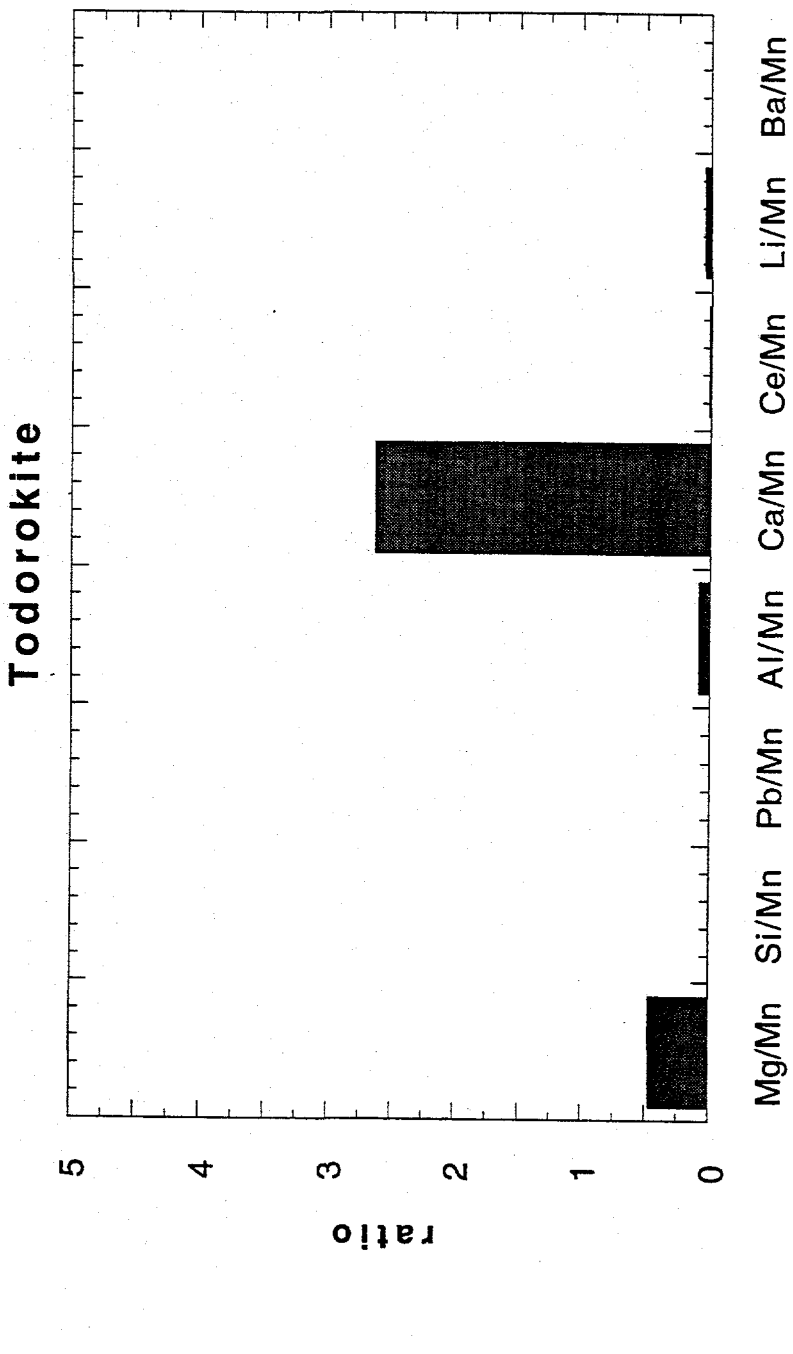
Todorokite
ratio
0
1
2
3
4
5
Mg/Mn
Si/Mn
Pb/Mn
Al/Mn
Ca/Mn
Ce/Mn
Li/Mn
Ba/Mn

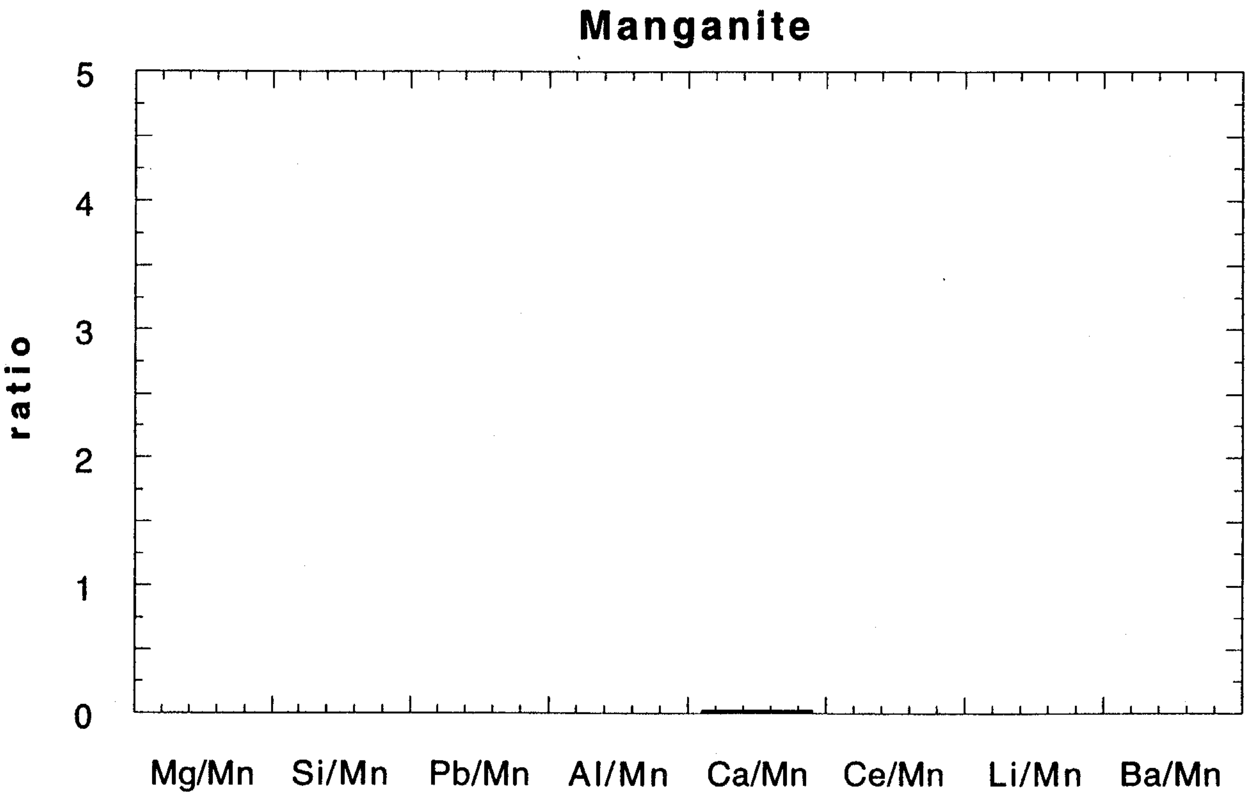
Manganite
ratio
5
4
3
2
1
0
Mg/Mn
Si/Mn
Pb/Mn
Al/Mn
Ca/Mn
Ce/Mn
Li/Mn
Ba/Mn

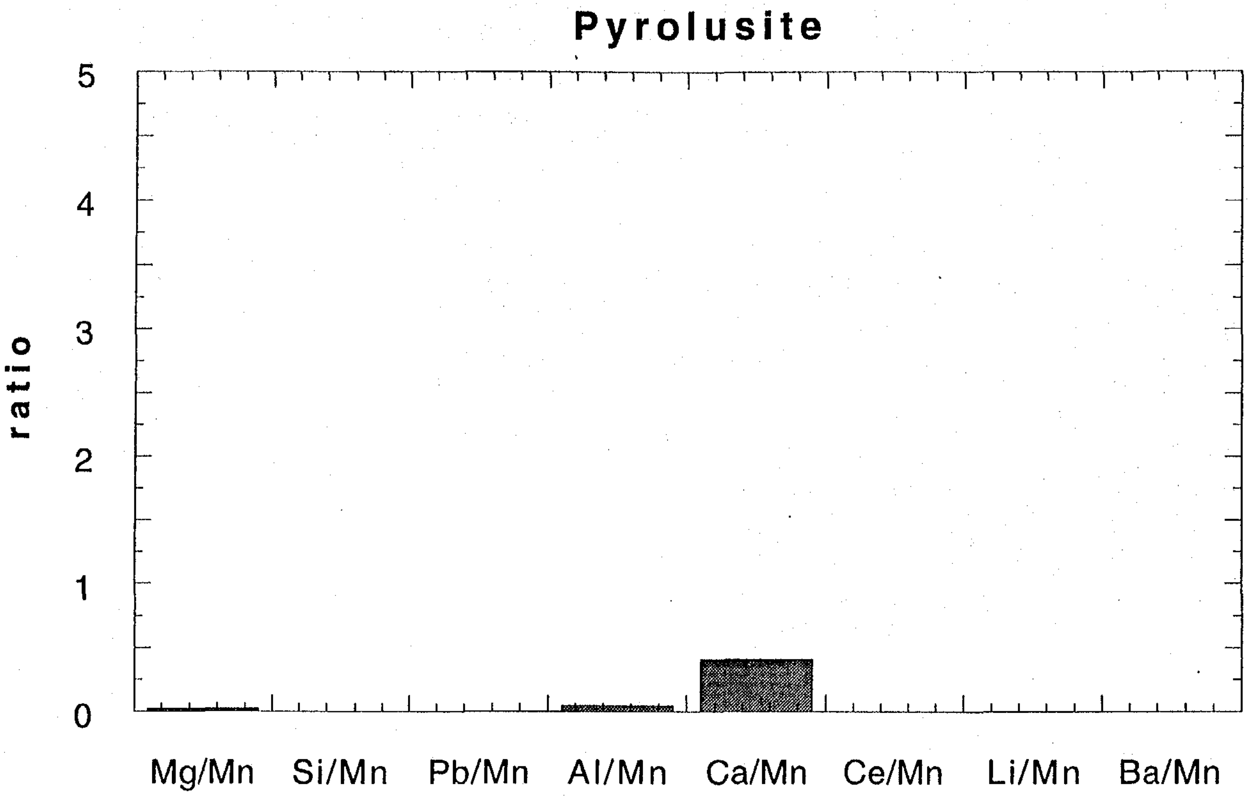
Pyrolusite
ratio
0
1
2
3
4
5
Mg/Mn
Si/Mn
Pb/Mn
Al/Mn
Ca/Mn
Ce/Mn
Li/Mn
Ba/Mn

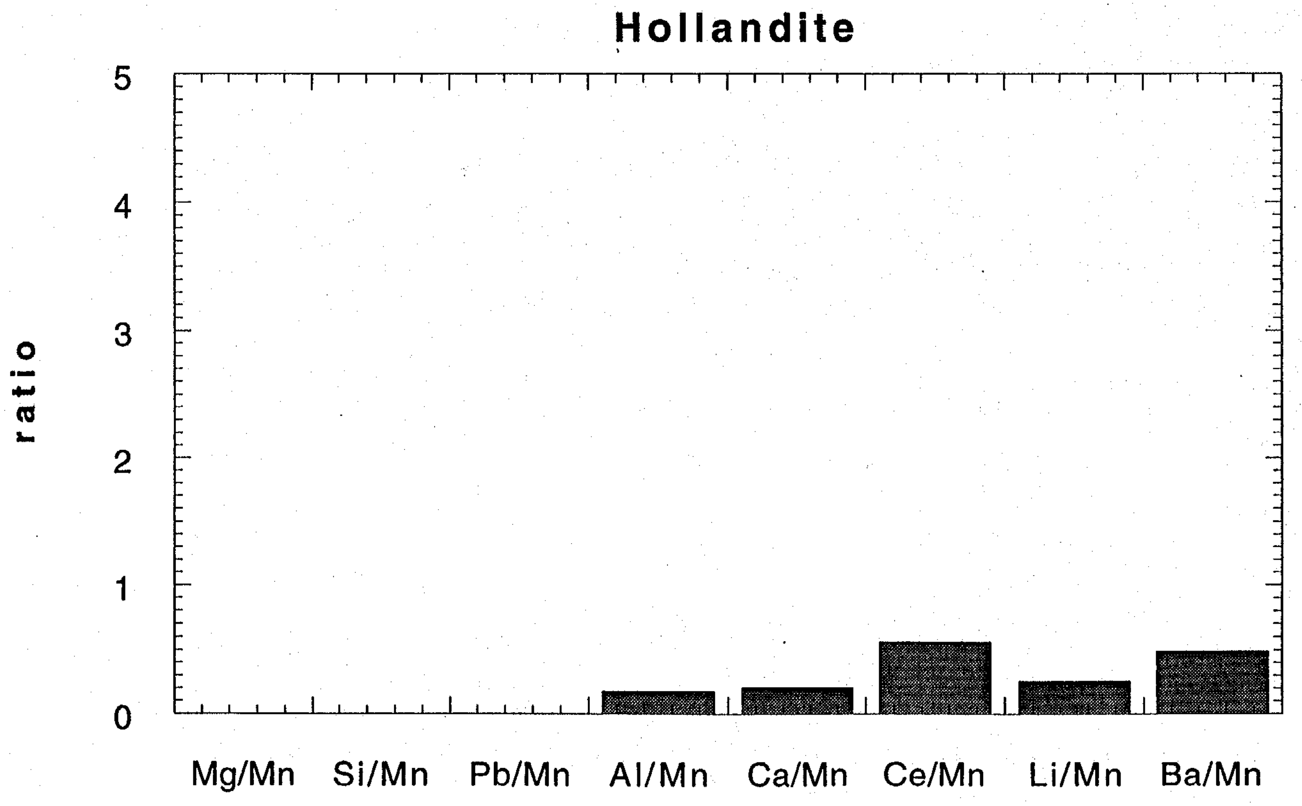
Hollandite
ratio
5
4
3
2
1
0
Mg/Mn
Si/Mn
Pb/Mn
Al/Mn
Ca/Mn
Ce/Mn
Li/Mn
Ba/Mn

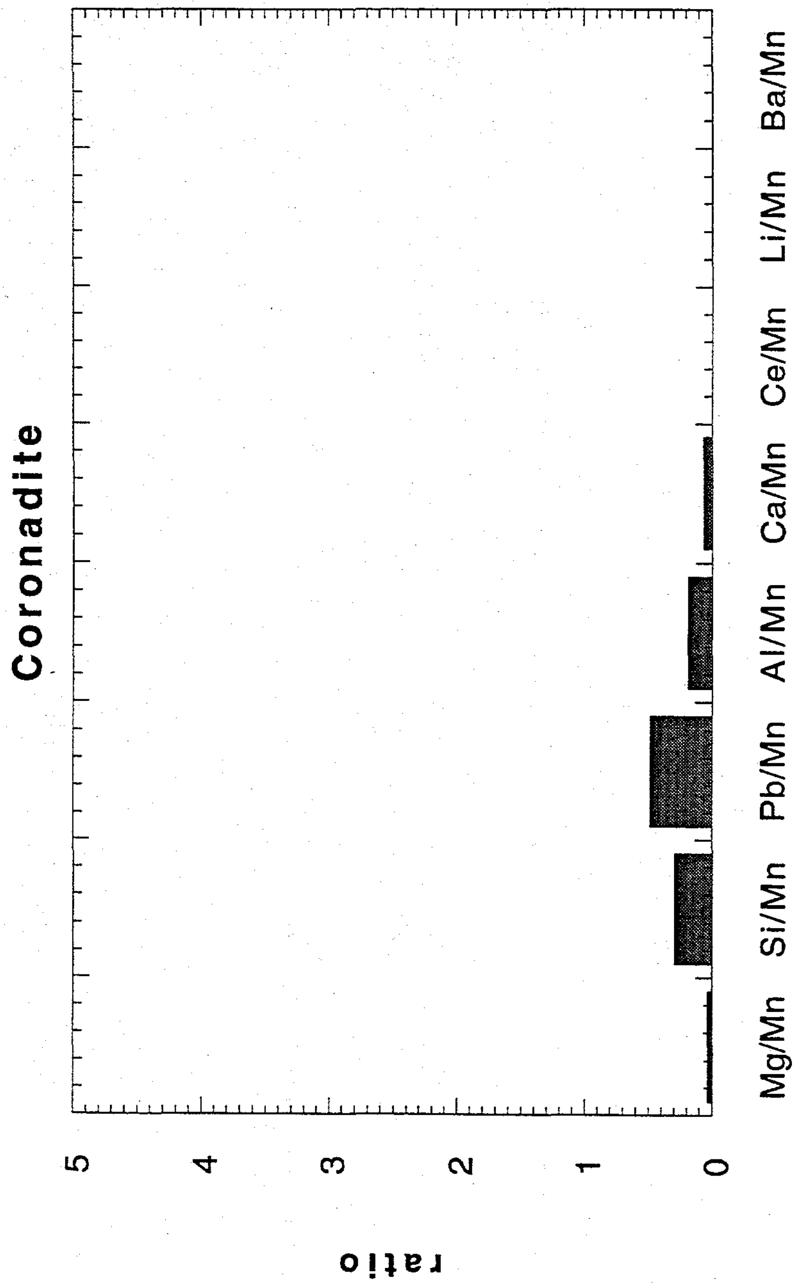
Coronadite
ratio
0
1
2
3
4
5
Mg/Mn
Si/Mn
Pb/Mn
Al/Mn
Ca/Mn
Ce/Mn
Li/Mn
Ba/Mn

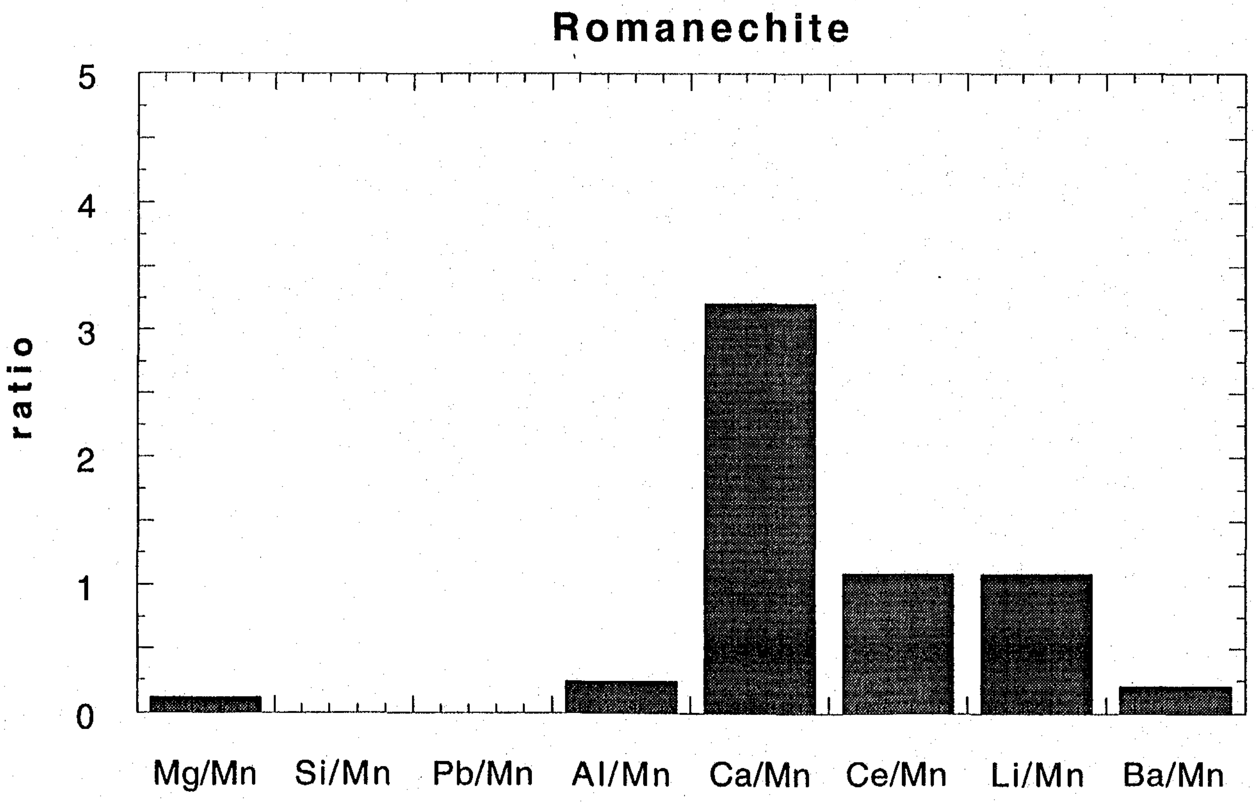
Romanechite
ratio
5
4
3
2
1
0
Mg/Mn
Si/Mn
Pb/Mn
Al/Mn
Ca/Mn
Ce/Mn
Li/Mn
Ba/Mn

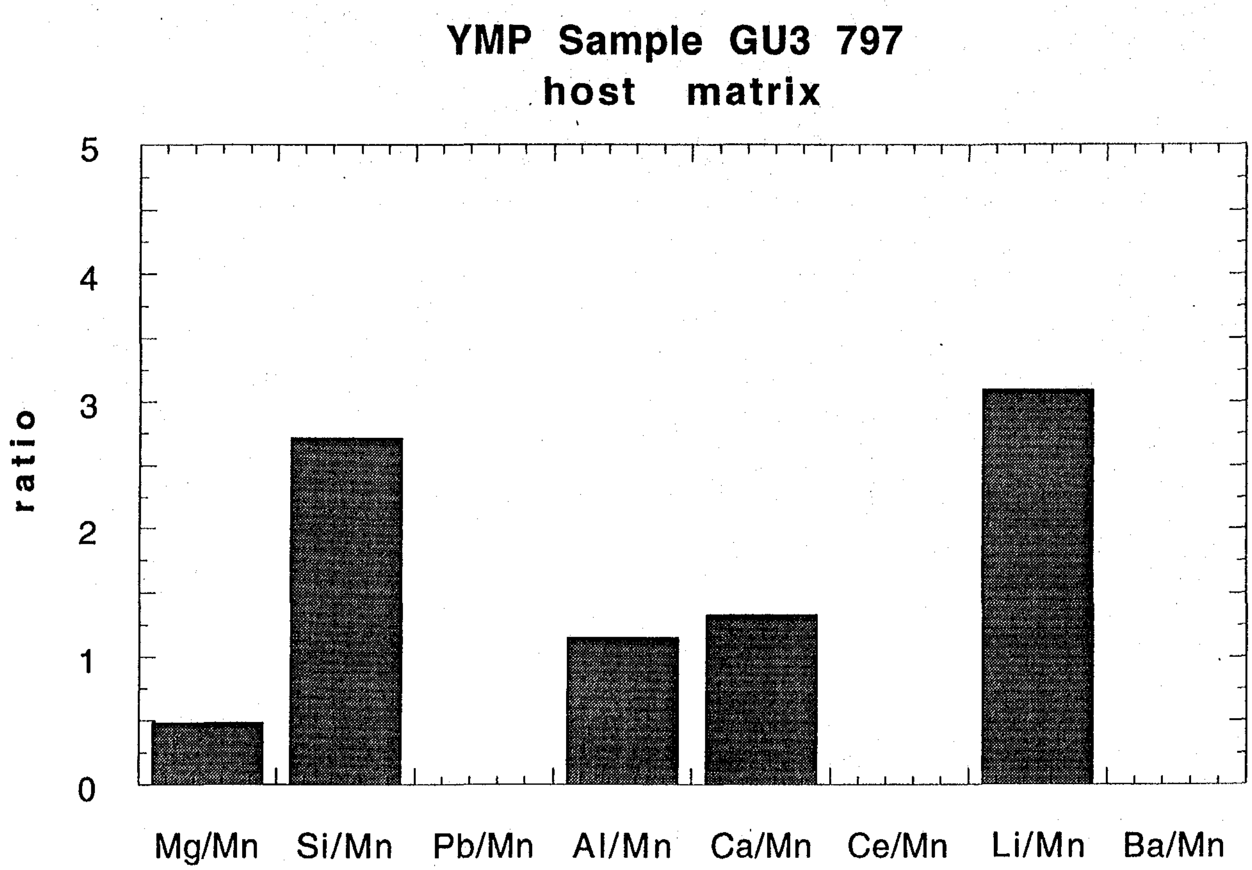

YMP Sample GU3 797
host matrix

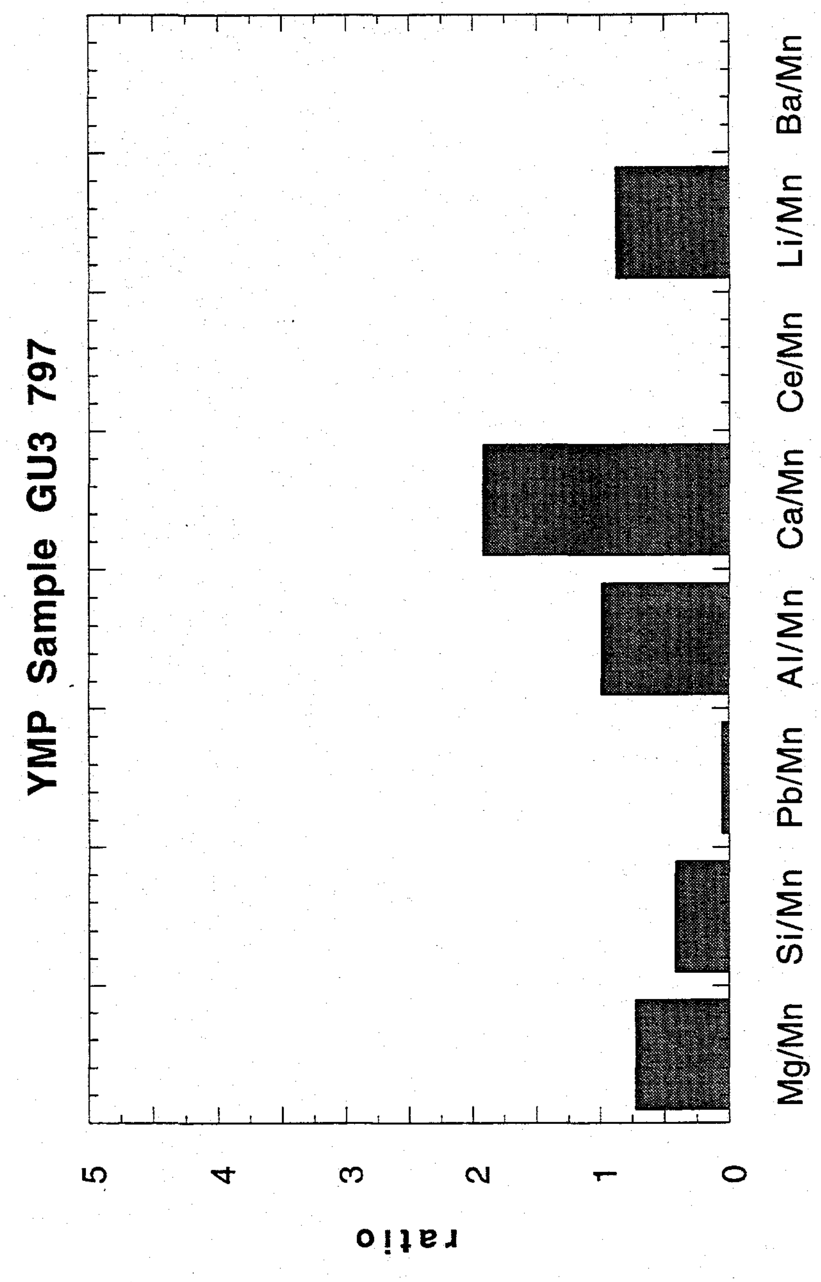
YMP Sample GU3 797
ratio
0
1
2
3
4
5
Mg/Mn
Si/Mn
Pb/Mn
Al/Mn
Ca/Mn
Ce/Mn
Li/Mn
Ba/Mn

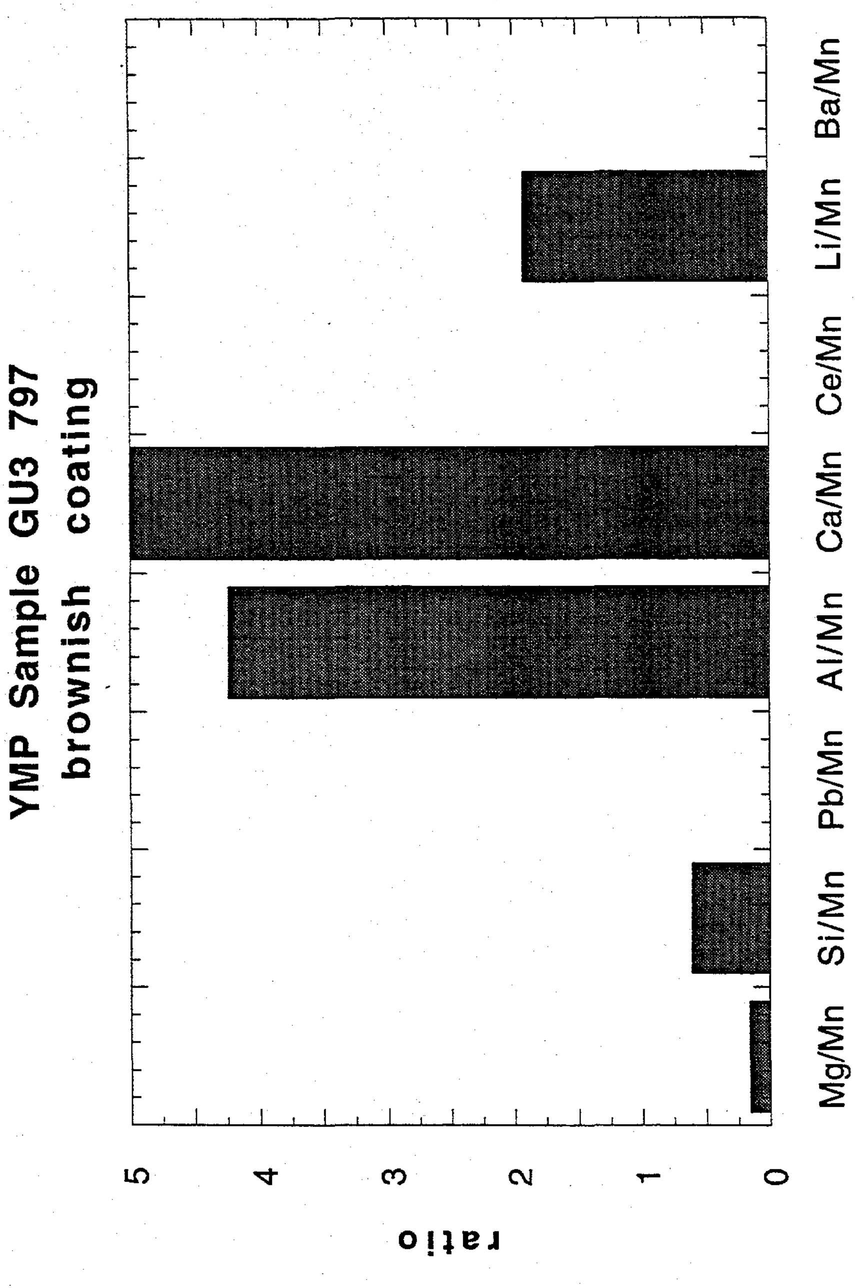
YMP Sample GU3 797
brownish coating
ratio
0
1
2
3
4
5
Mg/Mn
Si/Mn
Pb/Mn
Al/Mn
Ca/Mn
Ce/Mn
Li/Mn
Ba/Mn

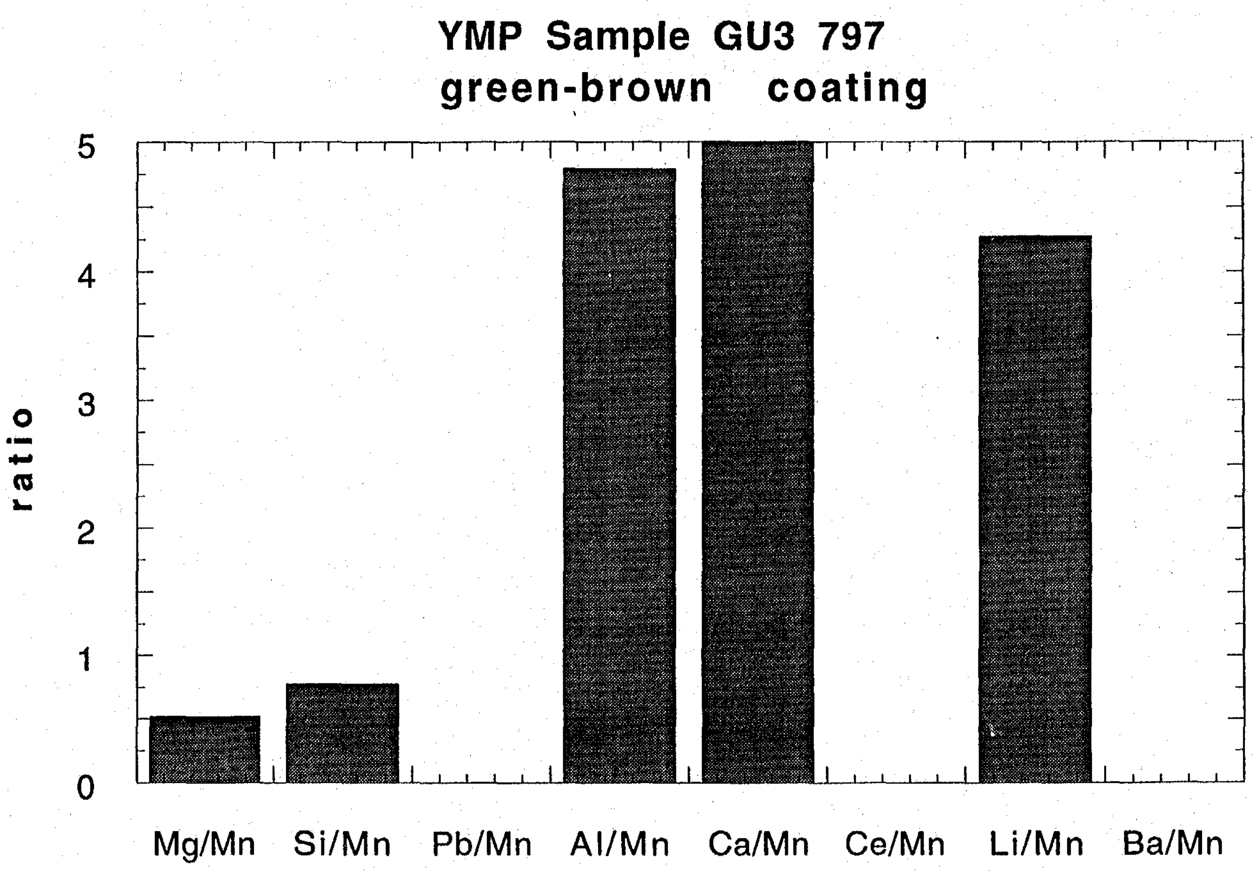
YMP Sample GU3 797
green-brown coating
ratio
0
1
2
3
4
5
Mg/Mn
Si/Mn
Pb/Mn
Al/Mn
Ca/Mn
Ce/Mn
Li/Mn
Ba/Mn

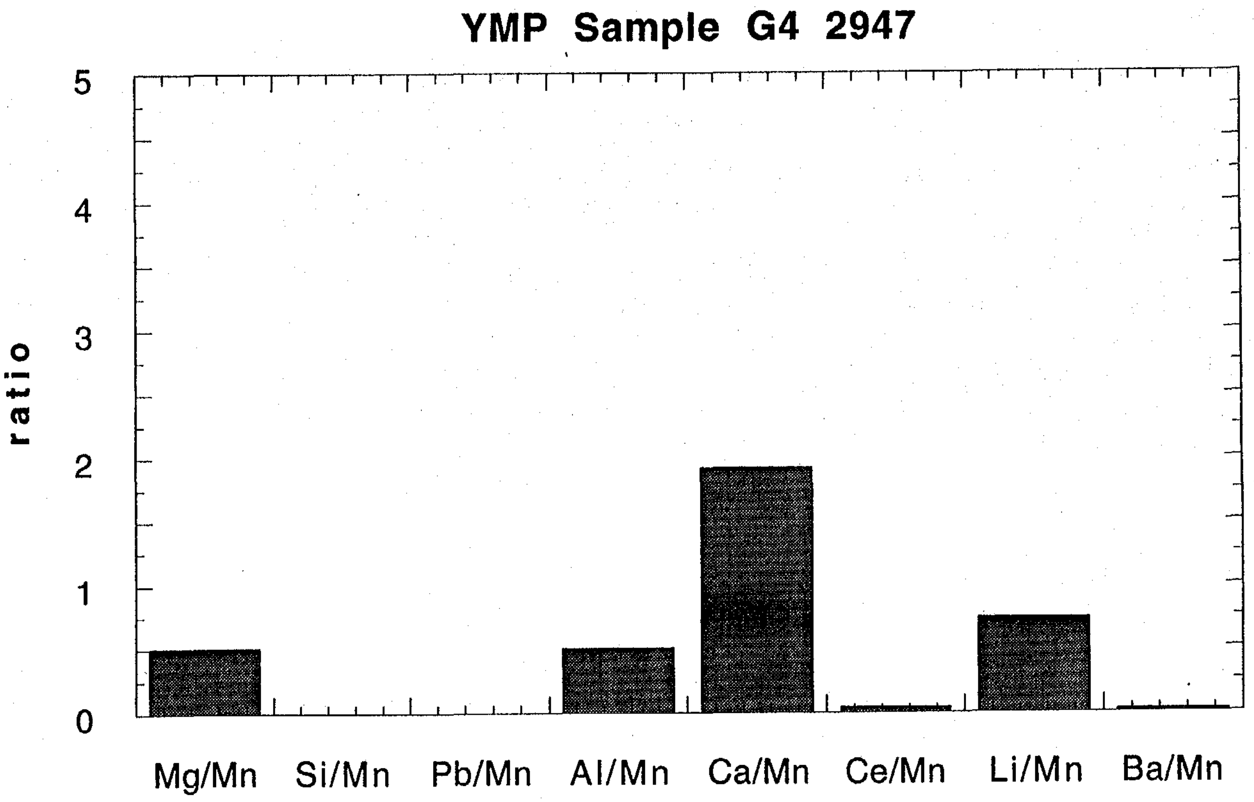
YMP Sample G4 2947
ratio
5
4
3
2
1
0
Mg/Mn
Si/Mn
Pb/Mn
Al/Mn
Ca/Mn
Ce/Mn
Li/Mn
Ba/Mn

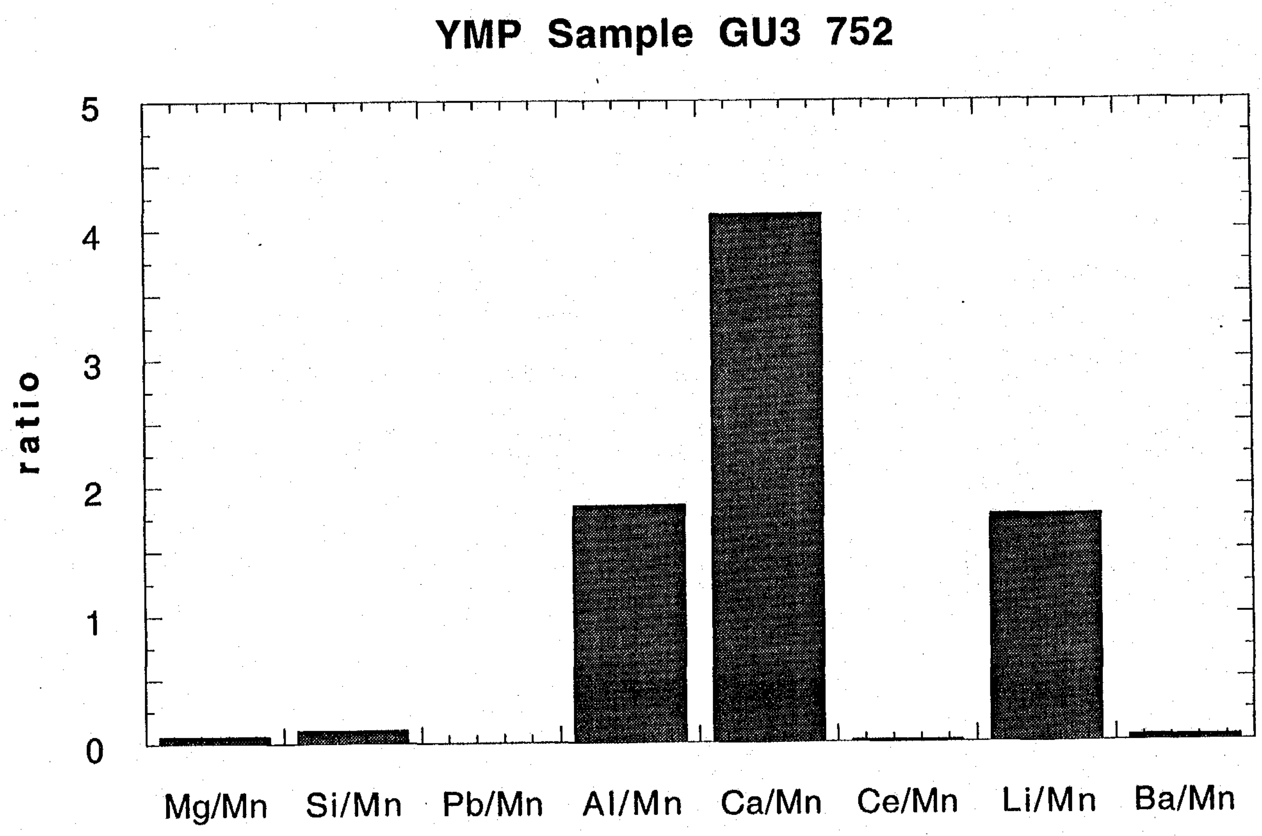
YMP Sample GU3 752